Modeling the influence of mussels and oysters on hydrodynamics and sediment transport

Niels Alferink

April 2016

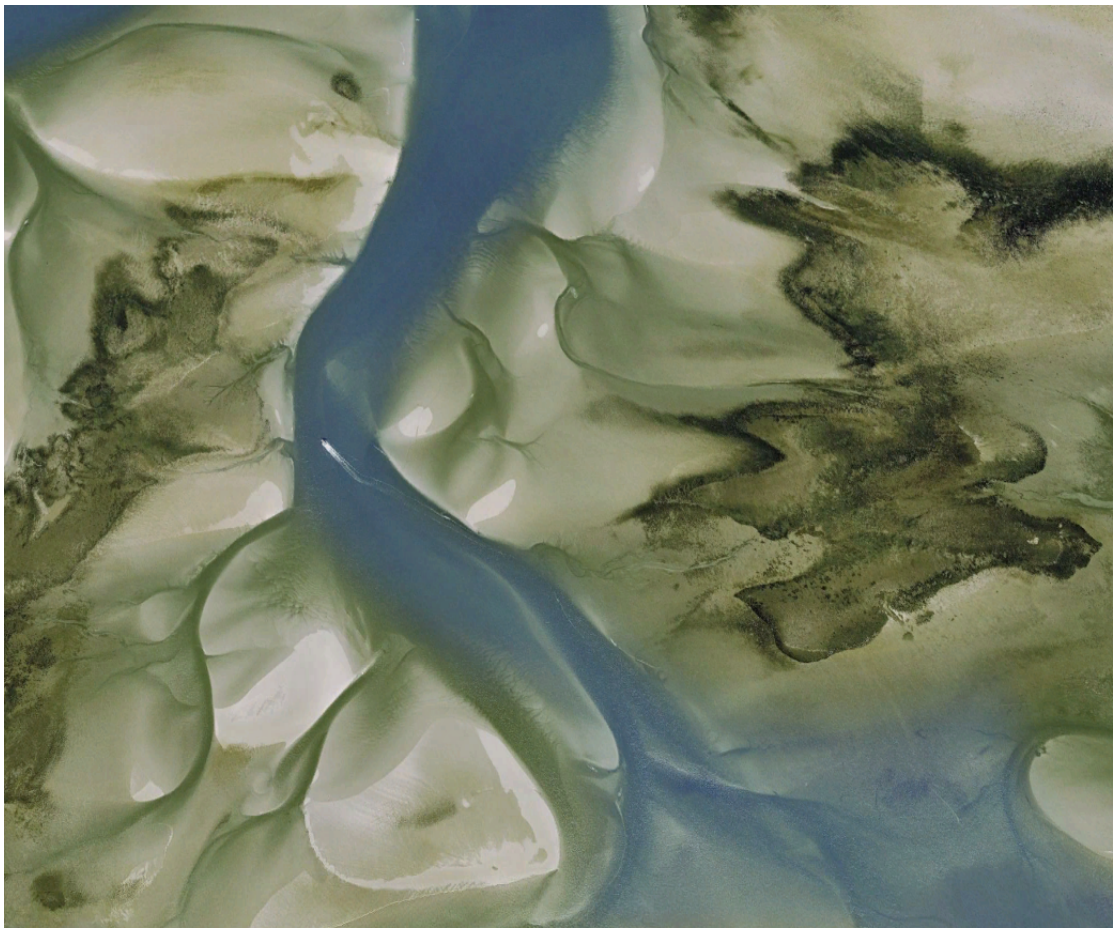

UNIVERSITY OF TWENTE.

Deltares
Enabling Delta Life

Master Thesis

Modeling the influence of mussels and oysters on hydrodynamics and sediment transport

---

Niels Alferink

Supervisors:
Prof. Dr. S.J.M.H. Hulscher
Dr. Ir. B.W. Borsje
Drs. M.B. de Vries

April 2016

Image cover: Mussel beds at the Engelsmanplaat in the Wadden Sea.

Preface

This document is the last part of my study Civil Engineering & Management with the track Water Engineering & Management at the University of Twente. This modeling study describes the influence of mussels and oysters on the hydrodynamics and sediment transport. The research was performed at the Deltares, which is an independent institute for applied research in the field of water and subsurface.

The recovery of subtidal and intertidal mussel and oyster beds is a hot topic at this moment. Mussels and oysters have a positive influence on other biota and are important for the biodiversity in marine systems. The findings in this work can hopefully contribute to further projects, for example the recovery of mussels and oysters in the Wadden Sea and North Sea.

I would like to thank the people of my graduation committee: Suzanne Hulscher for her suggestions and focus on the positive results and Bas Borsje for his guidance, support and suggestions during this study. I thank Mindert de Vries for his enthusiastic supervision and his original ideas regarding this subject. Moreover, I would like to thank Jasper Dijkstra for helping me with modeling issues and analysis of the results. Furthermore, I would like to thank Rob Uittenbogaard for helping me with the modeling problems regarding the flume measurements. Further people that I would like to thanks for sharing their knowledge are: Luca van Duren, Herman Kernkamp, Theo van der Kaaij and Jan van Kester. Lastly, I would like to thank: my fellow students and colleagues at Deltares for all the lunches, coffee breaks and conversations, my parents, brother and friends for their support.

Niels Alferink

Delft, April 2016

Abstract

Mussels and oysters are known as ecosystem engineers; consequently, they have an influence on the hydrodynamics and sediment transport. At this moment, it is unknown to what extent these bivalves influence the hydro- and sediment-dynamics on a patch scale. By applying the process-based model Delft3D with the rigid 3D vegetation module, the influences of mussels and oysters on the hydrodynamics and sediment transport are determined on a tidal flat scale.

Mussels and oysters are modeled as solid cylinders that affect the drag and turbulence; thereby these bivalves affect the local sediment dynamics. An essential parameter for the implementation of a bivalve bed in Delft3D is a variable bivalve shell height. A variable shell height is needed to simulate the flow velocity above the bivalve patch correctly, especially above oysters. Moreover, a variable shell height reduces the turbulence above the canopy of the bivalve bed and these turbulence levels corresponds with the two data sets. In contrast to oysters, mussels have an increased sediment flux towards the bed due to the production of heavy faeces. This process is implemented in Delft3D by adapting the transport equation; the settling velocity above the mussel bed is increased with an additional term, the filtration rate. The influence of mussels and oysters on the sediment dynamics have been tested on a current dominated tidal flat.

The resistance forces of mussels and oysters result in strongly reduced near-bed flow velocities and a turbulent kinetic energy (TKE) peak at the top of the canopy. These model predictions showed good agreement with the velocity profiles of two flume experiments, while the TKE patterns above the bivalve beds correspond reasonably well with these data sets. The high resistance forces of mussels and oysters have also an effect on the sediment transport above and around the patch. The low near-bed flow velocities leads to high accumulation of sediment in the bivalve beds. Besides, the production of heavy faeces by mussels leads also to an increase of sediment deposition. The modeled net biodeposition is approximately 30% of the total deposition in a mussel patch in a cohesive environment and corresponds with field measurements. The physical structure of mussels and oysters also induces flow routing; the flow accelerate at the left and right side of the patch, relative to the flow direction, resulting in erosion; while calmer conditions occur at the lee side, relative to the flow direction, of the patch resulting in sedimentation. The effects of mussels and oysters reach beyond their patches and they might be helpful reducing hydrodynamic forces on the coast. Based on the sensitivity analysis, the bed shear stress is always lower than the critical bed shear stress. Consequently, forces induced by currents cannot erode the sediment between mussel or oyster shells and it appears that there is missing process. This process is probably waves; waves can presumably induce larger bed shear stresses than currents. The present models identify the need for more knowledge about bio-physical interaction, both from experiments as well as from models.

Contents

List of Figures

List of Tables

List of Symbols

c	$[kg\ m^{-3}]$	suspended sediment concentration
D	$[kg\ m^{-3}\ s^{-1}]$	deposition
D_{bio}	$[kg\ m^{-3}\ s^{-1}]$	biodeposition
E	$[kg\ m^{-3}\ s^{-1}]$	erosion
F	$[m\ s^{-2}]$	horizontal Reynold's stresses
fr	$[m\ s^{-1}]$	filtration rate
H	$[m]$	total water depth
h_{bed}	$[m]$	bivalve bed height (base)
h_{mus}	$[m]$	mussel shell height
h_{oys}	$[m]$	oyster shell height
k_s	$[m]$	Nikuradse roughness height
l_{shell}	$[m]$	length bivalve shell
n	$[ind\ m^{-2}]$	density
P	$[N\ m^{-2}]$	pressure gradient
Q	$[\mathrm{m}^3\ s^{-1}]$	discharge
TKE	$[m^2\ s^{-2}]$	turbulent kinetic energy
$\bar{U}$	$[m\ s^{-1}]$	average flow velocity
u, v, w	$[m\ s^{-1}]$	velocity components in the x, y and z direction, respectively
w_s	$[m\ s^{-1}]$	settling velocity
z	$[m]$	height above bed
τ_{bed}	$[N\ m^{-2}]$	bed shear stress on the sediment
τ_{biv}	$[N\ m^{-2}]$	bed shear stress on the bivalve (shell)

1 Introduction

Estuaries are important systems from an economical, ecological and flood safety perspective. Ecosystem engineering species can have a positive contribution to flood safety in the coastal zone by modifying their environment (Jones et al., 1994). Ecosystem engineering species can be implemented to fulfill civil-engineering objectives, consequently ecological and engineering aims can be achieved. Mussels and oysters are examples of ecosystem engineering species.

1.1 Problem definition

Mytilus edulis (Blue mussel) and *Crassostrea gigas* (Pacific oyster) are important species in the Dutch coastal zone, because they populate large parts of Dutch estuaries, such as the Wadden Sea and the Eastern Scheldt. Mussels and oysters modify their environment by increasing the roughness of the bed, reducing the sediment resuspension (Jones et al., 1994). Another important influence of these ecosystem engineers is the production of (pseudo) faeces. Mussels and oysters filter material from the water column, and combine it into aggregates and eject it as (pseudo)faeces (Haven and Morales-Alamo, 1966). The surface area of mussel beds are been strongly diminished in the last decades, while they are important for the biodiversity in a marine system (Dankers and Fey-Hofstede, 2015). This report focuses on the Blue mussel and the Pacific oyster. For the sake of conciseness, 'Blue mussels' and 'Pacific oysters' are referred to 'mussels' and 'oysters', respectively, unless specified otherwise in the context.

Mussel and oyster beds can provide suitable habitats for other species. For example, eelgrass (*Zostera marina*) survives better in a mussel bed than outside a mussel bed (Bos and Van Katwijk, 2007). Moreover, mussel beds and oyster beds are acknowledged to attenuate waves and stabilize sediments. Consequently, mussels and oysters could be used to lower the wave impact on dikes and prevent erosion of the shoreline. These bivalves could take over the role of groins and revetments on a local scale. Besides, mussel and oyster beds may keep up with the sea level rise and provide a long-term suitable protection (Borsje, 2014).

Up to now, much research is executed on biogeomorphology of mussels and oysters in the field and in laboratory flumes, like the influence of mussels on mudflats in the Wadden Sea (Donker et al., 2013; Drost, 2013; Flemming and Delafontaine, 1994) and the influence of mussels and oysters on the hydrodynamics in a laboratory flume (De Vries et al., 2012; Folkard and Gascoigne, 2009; Van Duren et al., 2006). The interaction between a mussel patch and large scale sediment dynamics has been investigated in a depth-averaged model by Van Leeuwen et al. (2010). Walles et al. (2014) analyzed the interaction between oyster reefs and the tidal flat. All these studies have shown that mussels and oysters have a significant influence on hydrodynamics and sediment transport. However, at this moment it is not known how the hydrodynamics, such as the vertical velocity profile and turbulent kinetic energy, above a bivalve patch can be simulated in a model. Moreover, the influence of mussels and oyster patches on the hydrodynamics and sediment transport on a tidal flat is not known. The patch scale is defined as a uniform covered bed with

mussels or oysters and the order of magnitude of the length and width of this patch is tens of meters. The 'Mosselwad program' and the World Wide Fund for Nature tries to recover mussel and oyster beds in the Dutch marine system (Tubantia, 2016; Mosselwad, 2016). Research is needed to increase the knowledge of these ecosystems; consequently, the recovery of stable mussel and oyster beds can be more successful. 3D model including the effect of mussels and oysters on the local hydrodynamics and sediment transport can help to understand these bivalve ecosystems and help to recover mussel and oyster beds by indicating suitable locations for bivalve beds.

1.2 Methodology

To determine the influence of mussel beds and oyster beds on the local hydrodynamics and sediment transport, these bivalves will be implemented in a 3D model. Currently, there is no sufficient data of the influence of mussels and oysters on the tidal flats to calibrate and validate a flow and wave model. However, there is sufficient data to calibrate the hydrodynamics above a mussel or oyster bed for laboratory flume conditions. Therefore, a model is applied to simulate the flow characteristics above a mussel or oyster bed for laboratory flume conditions. After this calibration of the hydrodynamics, the model is validated against other flow rates to determine the performance at other flow velocities. After this calibration and validation, the model is extended to represent a mussel or oyster bed on a tidal flat. The model is imposed by a tidal current and the hydro- and sediment-dynamics around these bivalve patches are determined.

1.3 Research objective

Based on the problem definition the main objective of this research can be formulated:

Determine the different influences of mussels and oysters on hydrodynamics and sediment transport on a patch scale, by implementing the phenotypes of these bivalves in the process-based model Delft3D.

Based on this objective, the following research questions are addressed in this research:

1. How can mussel beds and oyster beds be implemented in the process-based model Delft3D?
2. What is the influence of mussels and oysters on the hydrodynamics?
3. What is the influence of mussel and oyster beds on sediment dynamics on a tidal flat?

1.4 Report outline

The structure of this report is as follows: firstly, the main characteristics of a mussel and oyster bed is presented, the focus is hereby on characteristics that have an influence on the hydro- and sediment dynamics. The implementation of a mussel and oyster bed in Delft3D is presented in Chapter 3. Hereafter, the model set-up of the models representing the flume studies and the tidal flat is given. Next, the influences of mussels and oysters on the hydro- and sediment dynamics are discussed (Chapter 4). This chapter is followed by a discussion, conclusions and recommendations for future research.

2 Mussels, oysters and sediments

Mussels and oysters are ecosystem engineers (Jones et al., 1994), they have therefore an influence on the hydrodynamics and sediment transport. Ecosystem engineering species have the ability to modify the local physical environment by their structures or activities. Mussels and oysters can trap and stabilize sediment and can change the properties of the sediment with the production of (pseudo)faeces (Borsje et al., 2011). Firstly, a short introduction into mussels and oysters is presented. Hereafter, the hydrodynamics over and around a bivalve patch is presented. Thirdly, important biological effects of mussels and oysters on sediment dynamics are given in Section 2.3. Finally, Section 2.4 explains the influence of mussels and oysters on the sediment dynamics.

2.1 Mussels and oysters

This section presents the biological processes that influence the dynamics in a marine system; firstly, the characteristics of mussels and oysters are described (Section 2.1). Secondly, the effect of mussels and oyster on the hydrodynamics is explained in Section 2.2. The biological components which can influence the sediment transport are given in Section 2.3. Finally, an introduction to sediment dynamics on a tidal flat is presented in Section 2.4.

2.1.1 Mussels

A mussel is a bivalve species and they filter suspended particles form the water column for food. Mussels open their shells, to inhale and exhale water, the exhaled water is called a jet or (exhaled) siphon. A schematisation of a filter feeding mussel and a picture of a clump of Blue mussels are presented in Figure 2.1 (A and B). Mussels live most of the time in large colonies, and a colony of mussels is called a mussel patch (or mussel bed). Figure 2.1C presents a mussel bed in the Wadden Sea.

The shell of a mussel is smooth and in equilateral. Despite their smooth shells, the influence of individual mussels (and an entire mussel bed) on the hydrodynamic forces can be large. Mussels prefer not too course and neither too silty sediment for their settling, because mussel larvae prefer hard and course surfaces for settlement, while adult mussels prefer silty surfaces for settlement (Mcgrorty et al., 1993). There are many types of mussels; however, an important mussel in the Netherlands is the blue mussel (*Mytilus edulis*) as a result of its high appearance in Dutch marine systems. The average shell length of a blue mussel is 30-100 mm. Blue mussels are well acclimated to a temperature range of 5–20 °C, however they are able to withstand freezing conditions for several months. The blue mussel is found in the high intertidal to shallow subtidal areas, and the depth varies from approximately 1 to 10 m (Zagata et al., 2008).

Deposition of sediment can occur in a mussel bed, mainly due to passive settling of sediment during slack tide and active filtration of suspended sediment. This latter is a consequence of the filtering feeding process of mussels. Mussels filter large amounts of suspended particles, algae and suspended sediment, from the water column; the indigestible particles are excreted

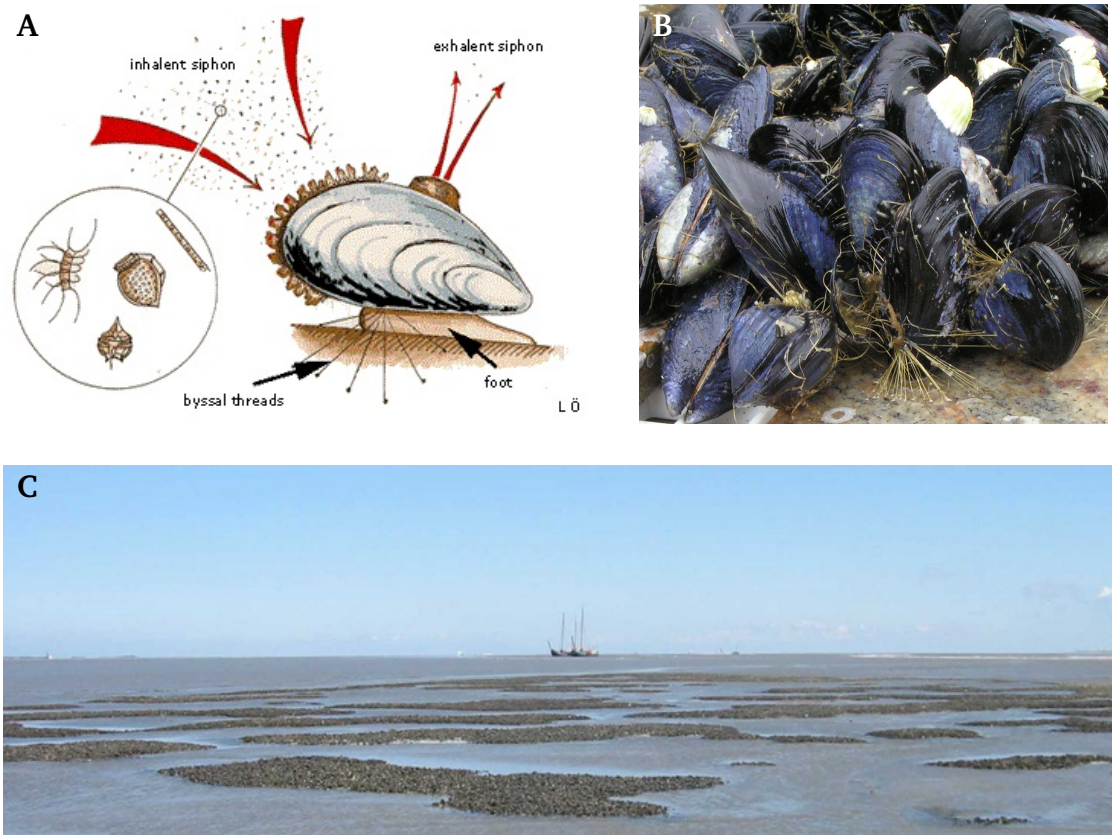

Fig. 2.1. (A) A schematic overview of an active Blue mussel, with the inhalent and exhalent siphons (Johannesson et al., 2000). (B) An example of a Blue mussel clump (Dybas and Carrington, 2013). (C) A Blue mussel bed (Van de Koppel, 2012).

as agglomerated particles. These particles deposit in the mussel bed, and the mussels climb upwards and cover this sediment. Especially, young mussels are highly mobile and they can protect large quantities of sediment. Consequently, the flow has less chance to erode the sediment between or on top of the mussels. The sediments that are trapped by mussels (by climbing on top of it) are called mussel mud. According to Dankers et al. (2004a), young mussels can rise 30-40 cm between August and November. Widdows et al. (2002) observed that mussels can migrate 6 cm upwards in sand in a day, while the substrate has settled between and below the mussels. However, a young mussel bed with accretion of sediment is unstable, and these beds are vulnerable for storms. 50% of the young mussel beds get eroded during the first winter and do not survive the first winter. The ability to move is gradually lost when mussels grow older; nonetheless the older mussels are more important for retaining the deposited sediment and provide stability (Van Leeuwen et al., 2010). The recruitment of new mussels is very important for the existence of a mussel bed, because mussels are vulnerable for predation and erosion (Dankers and Fey-Hofstede, 2015). Mussels organize themselves in several ways, namely in a dense (near homogeneous) mussel bed, in a patterned mussel bed and in an isolated clustered mussel bed (Figure 2.2). The formation of patterns depends on the environmental factors, for example the hydrodynamic conditions, the availability of food and the amount of sedimentation/erosion (Van de Koppel et al., 2008).

A mussel bed has several different sizes and mussel densities. The length and width of a mussel bed have a range of a few meters till several hundreds of meters (sometimes even thousand

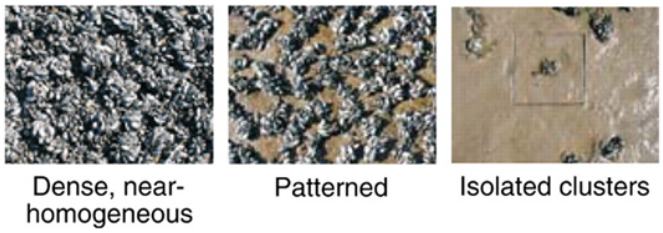

Fig. 2.2. Different mussel bed patterns, namely a dense (near homogeneous), a patterned and an isolated clusters of mussels (Van de Koppel et al., 2008).

meters). The height of a mussel bed can be tens of centimeters, while some older mussel beds can have heights up to 1 - 2 m (Dankers et al., 2004a; Widdows et al., 2002). Mussel beds have difficulty with survival when their height is above the mean sea level (Dankers and Fey-Hofstede, 2015; Mcgrorty et al., 1993). The length and height of four mussel beds is presented in Figure 2.3. Besides, there is a large variation in the density of mussel bed; the range of the density of a mussel bed can vary between 25 and more than 1000 mussels m^{-2} (Brinkman et al., 2003). Nehls et al. (2009) measured even a mussel density of 2000 mussels m^{-2} in the Danish Wadden Sea.

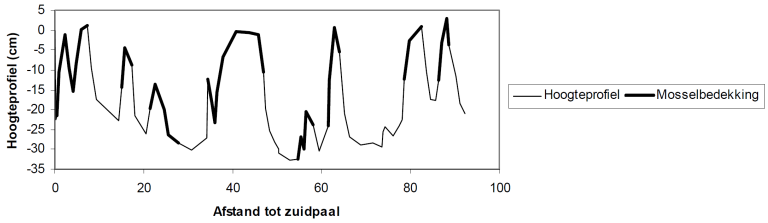

Fig. 2.3. The height in cm of a mussel bed at the 'Zuider Spruit Ameland' in the Wadden Sea (Mussel bed 529C) (Dankers et al., 2004a). The mussel covering is indicated with a thick solid line.

Mussel beds occur at locations which satisfy certain criteria, for example not too high flow velocity and low orbital motions. Brinkman et al. (2002) investigated areas that are most suitable for the natural establishment of mussel beds. They correlated the appearance of mussel beds at certain locations with the physical characteristics of these locations. The appearance of mussel beds was based on the locations where often mussel beds and mussel spatfall exist. The physical characteristics are: the maximum flow velocity, the maximum orbital velocity, the distance to the gully, the median grain size and the relative emersion time. The maximum flow velocity and orbital velocity are the velocities that occur during spring tide or storms. The correlations of suitable natural establishment of mussel beds with these physical characteristics are presented in Figure 2.4. The most important variable for suitable mussel habitats is the maximum orbital velocity according to Brinkman et al. (2002) and the preferred location of mussel beds has low orbital velocities.

2.1.2 Oysters

Oysters are, like mussels, a shell fish and they filter water for food. Oysters filter large amounts of suspended particles from the water column for food. This water, including the indigestible particles, is excreted into the water column. Figure 2.5 (A and B) presents a schematisation of a Pacific oyster and a clump of Pacific oysters. Oysters can form large reefs, and these reefs are

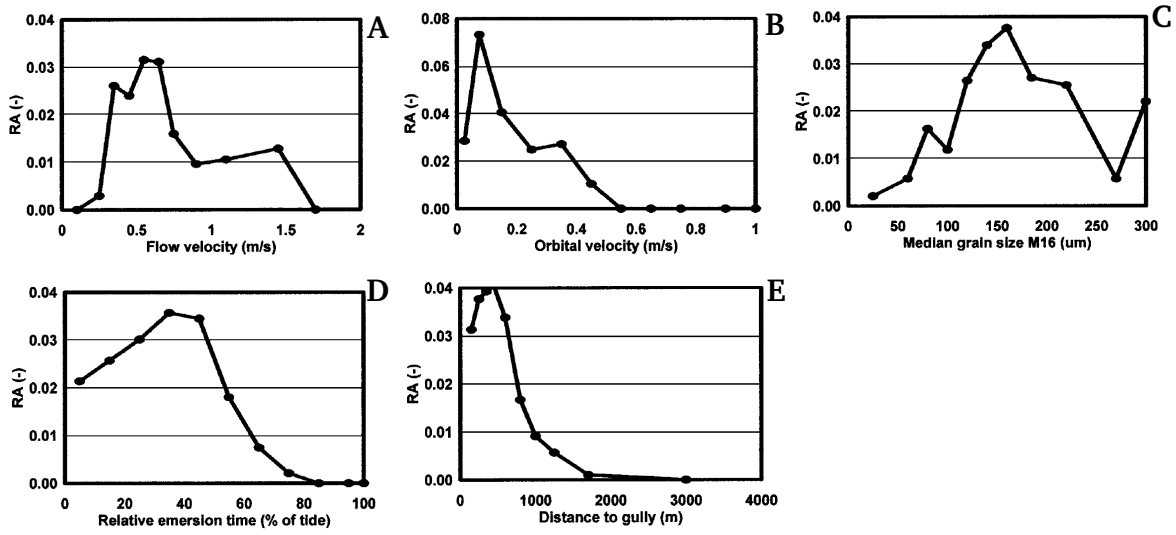

Fig. 2.4. Relative appearance (m^2 m^{-2}) of mussel beds on tidal flats related to five abiotic variables (Brinkman et al., 2002). (A) Maximum flow velocity, (B) Maximum orbital velocity, (C) Median grain size, (D) Relative emersion time, (E) Distance to gully

called oyster patches or oyster beds. An example of an oyster patch in the Eastern Scheldt is presented in Figure 2.5C.

The Pacific oyster (*Crassostrea gigas*) can have a shell length of 80-200 mm (Dowell, 2012; Xue et al., 2007). The Pacific oyster is important in the Netherlands, because of the successful marine invasion of this oyster. These oysters are primary found in areas with a temperature range of 5-25 °C. The shell of oysters is larger and rougher in comparison with mussels. Oysters attach to hard substrates in the area of shores and their habitat is in the low intertidal to shallow subtidal. According to Reise (1998), Pacific oysters prefer to settle on mussel beds. Consequently, the physical conditions of the Pacific oyster beds are similar to the physical conditions of the surrounding area of mussel beds. Oysters create strong reefs by settle on top of each other and cementing their shells together, consequently oysters are an immobile species (Troost, 2010). Consequently, an oyster reef can only increase their height by growth of the existing oysters or by new recruitment on top of the existing oysters. The immobility of oysters limits their survival, because sedimentation can have a negative impact on the survival of oysters. The vertical growth rate of an oyster reef must be higher than the sedimentation rate; consequently, the oyster is continuous growing ahead of the sediment accretion (De Vries et al., 2012). However, oysters can survive small burial depth for a short period of time. Dunnington (1968) concluded that oysters can survive burial depth of 13 mm or less, by clearing their shells of sediment by pumping water. According to Comeau (2014), oysters can survive burial depths of 20 mm, while they will die within 12 days if the burial depth was greater than 40 mm. Oysters grow around 20 – 50 mm in the first year /citepReise1998, Dankers2004a, so these oysters can survive sedimentation rates of 20 – 50 mm $year^{-1}$ or less.

An oyster shell is quite rough; it is therefore assumed that oysters require smaller patch sizes in order to maintain steep enough gradients and high enough turbulence. Oysters require steep gradients and high turbulence in order to balance the sedimentation with erosion; consequently, oysters protect themselves from being buried by sediment (De Vries et al., 2012). Walles et al. (2014) measured oyster reefs with a surface area of 2 till 1908 m^{-2}. The length and width of

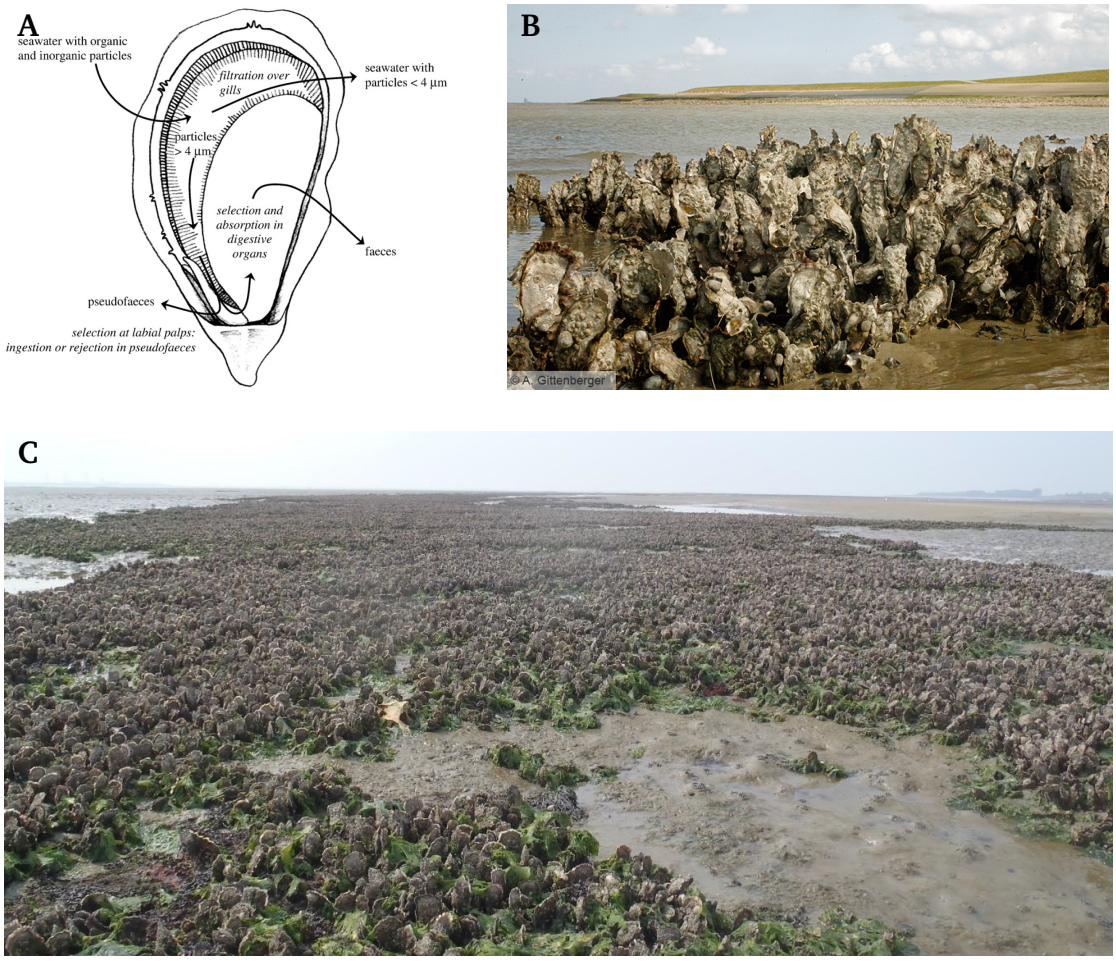

Fig. 2.5. (A) A schematic overview of an active Pacific oyster (Troost, 2010). (B) A close up of an Oyster patch (Gittenberger, 2000). (C) A Pacific oyster reef at the intertidal flat Viane in the Eastern Scheldt (Walles, 2015).

these oyster reefs varied between respectively 1 and 61 m and 1 and 45 m. The height of these reefs has a range of 0.2 to 1.08 m. Oyster beds have difficulty with survival when their height is above mean sea level (Walles, 2015). Figure 2.6 presents cross-sections of Pacific oyster reefs in the Eastern Scheldt. Fey et al. (2006) indicate the density of an oyster patch at several locations in the Wadden Sea, and this density varied between 10 and 500 oysters m^{-1}.

2.2 The effect of mussels and oysters on hydrodynamics

Hydrodynamic forces determine in a great extend the sediment dynamics. High flow velocities can result in erosion, while low flow velocities can result in deposition. Moreover, biology can change the increase or decrease the sediment transport. The mussel and oyster bed covering and the bed patterns have a significant influence on the hydro- and the sediment dynamics. These bivalves have an influence on the following hydrodynamic processes:

- High bed resistance due to the bed height and the roughness.
- High turbulence due to the high roughness and siphons/jets.
- Low near-bed velocities and near bed turbulence as a result of flow through mussels or oysters.

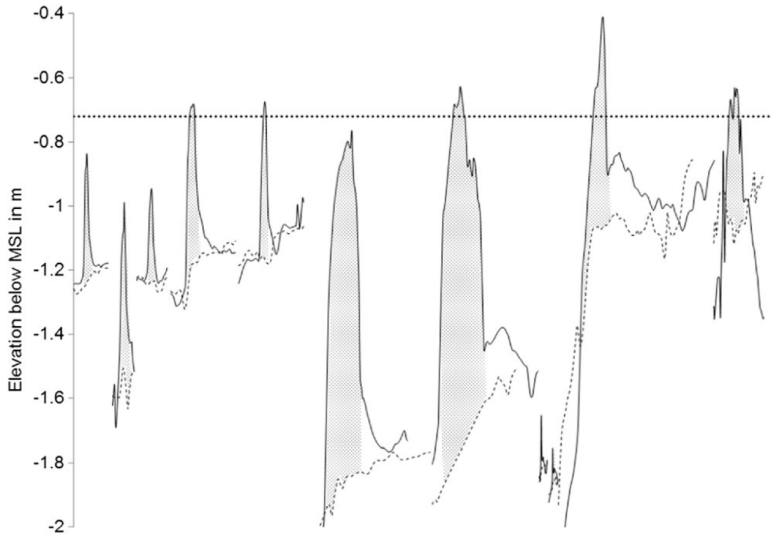

Fig. 2.6. Cross-sections of oyster reefs. The solid line indicates the top of the reefs and the dashed lane indicates the bare sediment level. The cross-sections are presented from the wave dominated side (left) towards the lee side (right). The grey shade indicates the reef. The black horizontal dotted line indicates the average reef height (0.72 below MSL) (Walles et al., 2014).

2.2.1 Roughness and bed height

Mussel and oyster beds have a larger roughness compared to the surrounding area. Water flows over and through the bivalve bed and the flow experience more stresses caused by the shells of the bivalves and the pattern of the bivalve bed. This roughness of the bivalve bed will result in lower velocities near the bed and will generate turbulence. This roughness is induced by the shells and by the patch patterns and this difference in roughness can be compared with the roughness induced by grains and the roughness induced by bed patterns. As a result of the larger roughness of a bivalve bed compared to the surrounding area, the near bed velocity will be lower and the amount of turbulence will be larger. The height of a bivalve bed (including with the higher roughness) forms a barrier which limits the through flow area. The flow must accelerate around or over the patch depending on the roughness of the patch and the water level (Donker, 2015).

2.2.2 Turbulence

Turbulence is caused by bottom friction and velocity differences between water layers. Turbulence, i.e. velocity fluctuations and vortices, is able to lift sediment grains from the bed and bring it to higher water levels, so the sediment is brought into suspension. Normally, only fine sand and silt/clay can be brought into suspension, because the turbulence lifting forces are large enough to overcome the counteracting gravity force. Turbulence distributes suspended sediment over the water column. Mussels and oysters are dependent on the horizontal advection and vertical turbulent mixing for the delivery of food (Folkard and Gascoigne, 2009). Turbulence will mix the algae content (bivalve food) over the water column, because turbulences mixes the lower layers, with low algae content, with the higher layers, with high algae content (Klausmeier and Litchman, 2001). Moreover, bivalves produce siphon currents during their filtering activity. Van Duren et al. (2006) discovered that the active mussels produce more turbulence than inactive mussels; this increased turbulence will result in more mixing of algae's over water column.

2.3 Biological components influencing the sediment dynamics

Biota can influence the sediment transport processes in several ways and four biological components can be distinguished, namely biodeposition, bio(re)suspension, bioturbation and biostability (Le Hir et al., 2007) and Lee and Swartz (1980).

2.3.1 Biodeposition

There are two types of biodeposition, namely direct and indirect biodeposition. Direct biodeposition is the settlement of faeces and pseudofaeces (faecal pellets) to the bottom. Sticky surfaces, such as biofilms, on the sea bed can also hold material which would otherwise stay in suspension. This effect is called indirect biodeposition (Graf and Rosenberg, 1997). Mussels and oysters do not produce sticky surfaces on the sea bed, therefore indirect biodeposition in ignored in the model. The characteristics of the biodeposition of mussels and oysters are described in this section.

2.3.1.1 Filtration rate

Mussels and oysters filter the water column for food and they deposit the inedible particles into the environment as (pseudo)faeces (Haven and Morales-Alamo, 1966). The filtration rate of bivalves is depended on the concentration of suspended particulate material (Figure 2.7A) (Widdows et al., 1979). Moreover, the filtration rate of mussels and oysters depends on the size of these bivalves, the temperature and the availability of food. The filtration rate for the Blue mussel has a range of 1.5–6.0 l h^{-1} $mussel^{-1}$ (Troost, 2010). The filtration rate (clearance rate) measured by Widdows et al. (1979) is presented in Figure 2.7B. The filtration rate of the Pacific oyster was between 1.2–12.5 l h^{-1} $oyster^{-1}$ (Bougrier et al., 1995; Gerdes, 1983; Troost, 2010).

2.3.1.2 Faeces and pseudofaeces

Faeces and pseudofaeces have different characteristics. Pseudofaeces are sediment particles, and these particles are excreted before they enter the intestines. Faeces are sediment particles which are excreted after ingestion. Figure 2.8 presents the shape of faecal and pseudofaecal pellets of the green-lipped mussel. The faeces (of mussels) sink easily to the sea bed as a result of the larger settling velocity. Faeces are heavier and more resistant to erosion than pseudofaeces. Moreover, the pseudofaeces are easily destroyed, so a pseudofaecal pellet will easily breakdown in energetic coastal environments (Giles and Pilditch, 2004). Besides the difference between faeces and pseudofaeces, there is also a difference between the faeces and pseudofaeces of oysters and mussels. The freshly deposited faeces of oysters (Eastern) consist of short green or brown segments; these segments are 1 to 5 mm long and are cylindrical with an approximate diameter of 1 mm (Haven and Morales-Alamo, 1966). These faecal pellets are very fluffy and have little stability (Dankers and Fey-Hofstede, 2015; De Vries et al., 2012). In contrast, the faeces of mussels are firmer, the length of the faeces is between 4 and 8 mm long (Carlsson et al., 2010).

The minimum and maximum sinking velocities of faecal pellets are 0.27 and 1.81 cm s^{-1} for Blue mussels ranging in size from 3 to 7 cm (Callier et al., 2006). (Chamberlain et al., 2001) measured a settling velocity for faecal and pseudofaecal pellets of 0.5 cm s^{-1} and 0.8 cm s^{-1}, respectively. However, the pseudofaeces are loose coils, they fall easily apart and (pseudo)

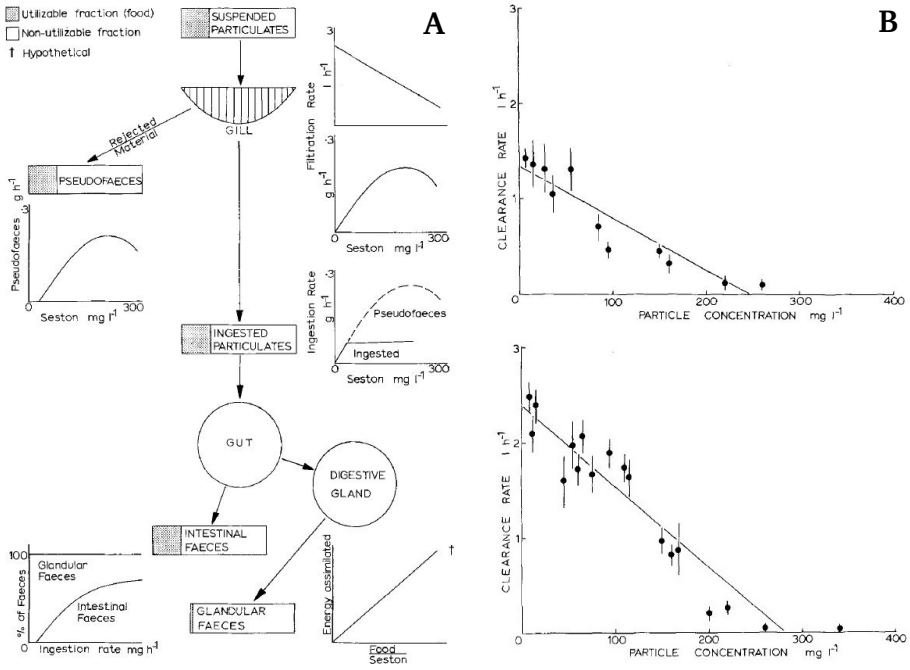

Fig. 2.7. (A) A schematic diagram representing the effect of suspended particulate concentration on feeding and digestive system (Widdows et al., 1979). (B) The filtration rate of the Blue mussel. The upper Figure presents the filtration rate of a 3 cm long mussel, while the lower Figure presents the filtration rate of a 5 cm long mussel (Widdows et al., 1979).

faeces are easily transported with the flow (Risk and Moffat, 1977). According to Widdows et al. (1979), the production of pseudofaeces (of the blue mussel) increases if the suspended sediment concentration increases as well, while the production of faeces is stable for an increase of the suspended sediment concentration (see Figure 2.7). The production of faeces is stable for a concentration smaller than 0.25 mg l^{-1}. The suspended sediment concentration in the Wadden Sea is 50 mg l^{-1} (Postma, 1981), so in the production of pseudofaeces is higher than the production of faeces in the Wadden Sea.

The mean sinking rate of faeces of the oyster was 0.45 cm s^{-1}. These results were measured in an aquarium (Nishikawa-Kinomura, 1978). However, it is hard to determine the influence of the (pseudo)faeces of oysters, because these faeces are fluffy and these faeces fall easily apart (Dankers et al., 2004b), consequently, the results of Nishikawa-Kinomura (1978) should be taken with caution.

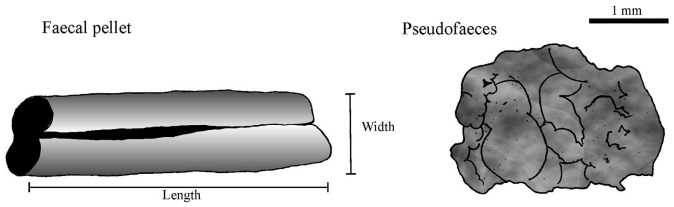

Fig. 2.8. The shape of faecal and pseudofaecal pellets of the green-lipped mussel *Perna canaliculus* (Giles and Pilditch, 2004).

2.3.1.3 Amount of biodeposition

The biodepositions of mussels and oysters are ± 100-200 g dry wt m^{-2} day^{-1} and ± 30-200 g dry wt m^{-2} day^{-1}, respectively (Ten Brinke et al., 1995; Dame and Dankers, 1988; Prins

et al., 1996; Flemming and Delafontaine, 1994; Mitchell, 2006; Haven and Morales-Alamo, 1966; Nishikawa-Kinomura, 1978). In contrast to the biodeposition of mussels is the biodeposition of oysters determined with laboratory experiments. All the (pseudo)faeces of oysters are collected with these experiments, while a large part of these faeces will normally be transported with the flow as a result of the light (pseudo)faeces (Dankers et al., 2004b).

Mussels filter large amounts of sediment out of the water column and eject these sediments into the environment as (pseudo)faeces. Large amounts of these faeces settle on the bottom due to a high settling velocity (Oost, 1995). The (pseudo)faeces contain a lot of inorganic materials, consequently, there is (often) a thick layer of mud in and around mussel beds (Hertweck and Liebezeit, 1996). Moreover, the influence of mussel beds on the hydrodynamics can result in the settling of larger materials, such as sand. Locally this can lead to high sand contents around mussel beds (Oost, 1995). In contrast, the (pseudo)faeces produced by oysters do not (or hardly settle) to the sea bottom, because these faeces are very light. These faeces are transported as fine suspended particles in the water column and the effect of (pseudo)faeces on the sediment dynamics in and around an oyster bed is small. Consequently, it can be argued that there is less mud in and around an oyster bed (compared to a mussel bed), because the faeces of oysters hardly settles to the bottom. This corresponds with many oyster beds in the Eastern Scheldt, because the Eastern Scheldt is a sandy environment (Walles, 2015). Notwithstanding, there are also mud concentrations in oyster beds and it is not known what the composition of these muds are (Dankers and Fey-Hofstede, 2015).

2.3.2 Bio(re)suspension, bioturbation and biostability

Graf and Rosenberg (1997) made also a distinction between direct and indirect bioresuspension. Direct bioresuspension are jets, containing sediment, produced by animals. The sediment is ejected several centimetres in the water column by these animals. Another indirect effect of bioresuspension is caused by construction activities, for instance pits and tubes, of animals.

Biota can destabilize the sediment through their burrowing and feeding activity, and this is called bioturbation (Widdows et al., 1998). Mussels and oysters do not destabilize the sediment with their activity, therefore bioturbation can be neglected.

Benthic species can stabilize sediment by physically covering it or by binding it by their byssal threads. Moreover, diatoms can excrete extracellular polymeric substances and cohere sediment (Paarlberg et al., 2005). Mussels and oysters are examples of species that can stabilize the sediment, because these bivalves protect the sediment by covering it with their shells.

2.4 Sediment dynamics on a tidal flat

A seasonal trend can be observed if the occurrence of accretion and erosion is investigated. There is an accretion period in the calmer summer period and an erosion period during the winter period. These accretion and erosion periods will result in a net annual sediment accretion or erosion (Flemming and Delafontaine, 1994). Due to the presence of bivalves there can be a net deposition in a tidal flat over a year. Janssen-Stelder (2000) observed also a seasonal trend in the deposition of sediments. According to this study, there is a net deposition on the tidal flats in the summer, because the hydrodynamic conditions are low due to low wind speeds (thus low waves). The current velocities are the dominant processes of sediment transport during these

calm conditions. The combination of waves and tidal currents occurs mostly during winter; these high hydrodynamic conditions result in the erosion of the tidal flats, especially during stormy conditions. During stormy conditions wave action increases and waves become the dominant process in sediment transport.

2.5 Conclusion

There are three categories for the implementation of mussel and oyster beds in the process-based model Delft3D, namely biology, hydrodynamic and sediment dynamic. The main characteristics of mussels and oysters and the most important influences of mussels and oysters on the hydrodynamics and sediment dynamics are presented in this section. The main characteristics of a mussel and oyster bed are:

- Mussels have a shell length of 30 – 100 mm and oysters have a shell length of 80 – 200 mm.
- The length and width scales of mussel and oyster beds varies a lot. Mussel beds have a range from a few meters till several hundreds or thousands of meters, while oyster beds have a range from a few meters till several tens of meters.
- The maximum flow velocity above many mussel beds in the Wadden Sea is $\pm$ 0.5 m s^{-1}. Many oysters settle on existing mussel beds; the maximum flow velocity above oyster beds is therefore similar as the maximum flow velocity above a mussel bed.

The most important influences of mussel and oyster patches on the hydrodynamics are:

- Mussels and oysters increase the roughness of the bed compared to the surrounding area. The flow above a mussel and oyster patch slows down due to this high roughness. The roughness of an oyster patch is higher due to the rougher shell of oysters.
- Mussel and oyster beds are higher than the surrounding area, consequently there is flow routing around these bivalve beds.
- The rough beds of mussels and oysters increase the turbulence above their beds. Oyster beds increase the turbulence more than mussels due to the very rough shells.

The most important influences of mussels and oysters on the sediment dynamics are:

- Mussels and oysters protect the sediment below them by covering the sediments with their shells.
- The high roughness and high bed heights can result in the accumulation of sediment behind the mussel bed due to a calmer zone behind the patch.
- Mussels can accumulate a lot of sediment by climbing on top of the freshly deposited sediment. Mussel beds can accumulate 30 – 40 cm of sediment in one year (mainly young mussel beds). Oyster reefs cannot survive large accumulation of sediment, because they are immobile; the maximum accumulation of sediment is around 40 mm per year.
- The faeces of mussels have a large influence on the settling of sediment in and around mussel beds, because these faeces are heavy compared to the normal sediment in the water column. The settling velocity of mussels faeces is between 0.27 and 1.81 cm s^{-1}. The (pseudo)faeces of oysters will hardly result in an extra settling of sediment, because these faeces are very fluffy and are easily transported.
- The current velocities are the dominant processes of sediment transport during the summer and net sedimentation takes place on the tidal flat. Waves and currents initiate erosion and this process is dominant during the winter.

3 Model set-up

To determine the influence of mussels and oysters on the local hydrodynamics and sediment transport, the process-based model, Delft3D-FLOW, is used. This chapter discusses the set-up of the model. Firstly, Section 3.1 presents the implementation of a mussel or oyster bed in the model. Section 3.2 describes the applied model to simulate flow characteristics above a mussel or oyster patch for laboratory flume conditions. Finally, this model is extended to represent a mud flat inhabited by mussels or oysters (Section 3.3).

3.1 Mussel and oyster bed implementation

A mussel and oyster bed needs to be implemented in a model in order to investigate the influence of these bivalves on hydrodynamics and sediment transport. Section 3.1.1 introduces the hydrodynamic implementation of a mussel and oyster bed, while Section 3.3 presents the sediment dynamic implementation of a mussel and oysters bed.

3.1.1 Hydrodynamic implementation

As be explained in Section 2.2, these bivalves have influence on several hydrodynamic processes, such as roughness, bed height and turbulence. The implementation of these processes is presented in this section.

3.1.1.1 Bed height

Mussels and oysters increase the bed height of the areas they covered compared to the surrounding area and these bivalves increase the roughness of the bed, consequently mussels and oysters increase the resistance of the bed. The height of a mussel bed or oyster bed can be implemented in the flow model by changing the bathymetry at the location of the bivalve bed. The height of a mussel bed or oyster bed is based on the studies of Dankers et al. (2004a) and Walles et al. (2014).

3.1.1.2 Roughness

The roughness of mussels and oysters are implemented in Delft3D with the '(Rigid) 3D vegetation model', because this model takes into account the effect of bivalves on the hydrodynamics, both flow velocities as well as turbulence. The vegetation or bivalves are presented as rigid vertical cylinders and the main input parameters for this model are the density, diameter, height and drag coefficient. A technical description, including the equations of the (rigid) 3D vegetation model, is presented in Appendix B.2. In order to represent mussels and oyster with the (rigid) 3D vegetation model, several assumptions have been made, namely:

- Mussels and oyster can be represented with upright cylinders.
- This cylinders are evenly distributed over a patch.
- Only the upper part of a mussel or oyster bed has influence on the hydrodynamics, therefore only the upper part of mussels or oysters will be represented with cylinders.

The height, width and density of these cylinders correspond with the height, width and density of mussels and oysters found in the field. Figure 3.1B represents a schematisation of a mussel bed in the rigid 3D vegetation model. An oyster patch is similar schematized as a mussel bed, because many oyster reefs are higher than the surrounding area (Walles et al., 2014). However, in contrast with mussel mud, oyster mud does not exist below an oyster reef. The core of an oyster reef consists mainly of oyster shells and sediments (Walles, 2015). The length and width of the cylinders is larger in the model representing an oyster patch in comparison the cylinders representing mussels, because oyster shells are larger and wider.

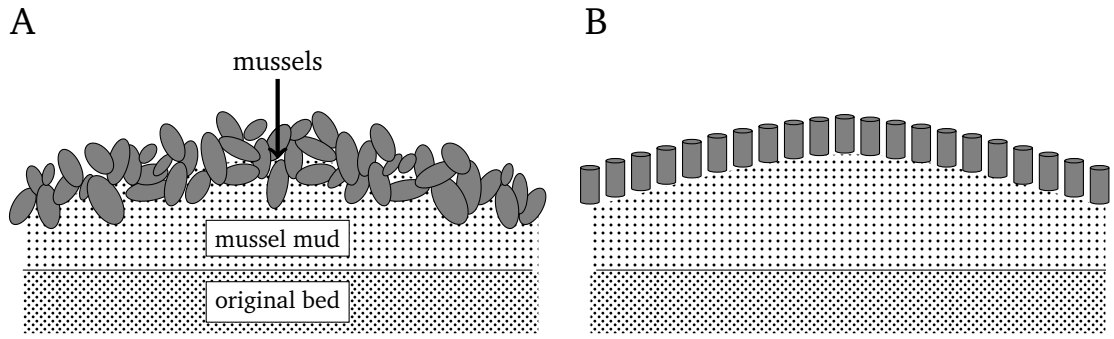

Fig. 3.1. (A) Schematic overview of a mussel bed. (B) Schematic overview of the implementation of a mussel bed with the (rigid) 3D vegetation model.

3.1.1.3 Near-bed velocity and turbulence

Mussels and oysters have an influence on the hydrodynamics, consequently these bivalves have also an effect on the sediment transport. An important parameter that determines the sediment transport is the bed shear stress (τ_b). Shear stress is caused by a moving fluid on a boundary. The bed shear stress can be determined with a combination of the roughness of a bed and the near-bed velocity. The roughness of the mussel and oyster bed is higher compared to the roughness of the surrounding bed. The larger roughness of these bivalves does not result in a larger shear stress on the sediment, because a part of the shear stress is absorbed by the shells of these bivalves, while the other part is absorbed by the sediments on the bottom. The 3D rigid vegetation model accounts for the reduced bed shear stress on the sediment (see Appendix B.2).

3.1.2 Bivalve activity and sediment dynamic

Mussels and oysters have also an influence on the sediment transport by their activity. Mussels and oysters produce (pseudo)faeces due to the filtration of water. In this section the implementation of sediment transport (due to bivalve activity) around and above a mussel and oyster bed is presented.

3.1.2.1 Filtration

Mussels and oyster filter the water column for food and these bivalves produce (pseudo)faeces during the filtration. The (pseudo)faeces of mussels are firm, heavy and resistant to erosion, while the (pseudo)faeces of oysters are fluffy, light and have little stability (see Section 2.3.1.2). Moreover, mussels and oysters produce inhalent and exhalent siphons (or jets). These inhalent and exhalent siphons have influence on the turbulence in the water column (see Figure 2.1). The model in this study does not include the increased turbulence levels as a result of inhalent and exhalent siphons.

The (pseudo)faeces of mussels have a larger settling velocity than the (original) sediment in the water column. Consequently, these faeces of mussels can result in larger deposition of sediment in and around the mussel bed (Widdows et al., 1998; Dankers et al., 2004b). The biodeposition is modelled as a local increase of the settling velocity to account for the larger settling velocity of the (pseudo)faeces. This method is similar to the method of Van Leeuwen et al. (2010). The characteristics of the (pseudo)faeces of mussels and oysters are very different (see Section 2.3.1.2). The (pseudo)faeces of oysters do not settle (or hardly settle) and these faeces are transported in the flow (Dankers et al., 2004b). Consequently, the additional settling above the bivalve bed (velocity due to the filtration rate) does not apply for oysters.

The additional term 'biodeposition' must be included in the suspended sediment transport equations. Suspended sediment transport is calculated with the advection diffusion equation in Delft3D. The advection diffusion equation including the additional term 'biodeposition' is presented in Equation 3.1 (The depth averaged advection diffusion equation including biodeposition is presented by Van Leeuwen et al. (2010)).

$$\frac{\partial c}{\partial t}+\frac{\partial uc}{\partial x}+\frac{\partial vc}{\partial y}+\frac{\partial (w-w_s)c}{\partial z}-\frac{\partial}{\partial x}\left(\epsilon_{s,x}\frac{\partial c}{\partial x}\right)-\frac{\partial}{\partial y}\left(\epsilon_{s,y}\frac{\partial c}{\partial y}\right)-\frac{\partial}{\partial z}\left(\epsilon_{s,z}\frac{\partial c}{\partial z}\right)=E-(D+D_{bio}) \tag{3.1}$$

Where:

c	$[kg\ m^{-3}]$	suspended sediment concentration
u, v, w	$[m\ s^{-1}]$	flow velocity components
w_s	$[m\ s^{-1}]$	settling velocity
$\epsilon_{s,x}\ \epsilon_{s,y}\ \epsilon_{s,z}$	$[m^2\ s^{-1}]$	eddy diffusivities of sediment fraction
E	$[kg\ m^{-3}\ s^{-1}]$	erosion
D	$[kg\ m^{-3}\ s^{-1}]$	deposition
D_{bio}	$[kg\ m^{-3}\ s^{-1}]$	biodeposition

The deposition is described in Delft3 is presented in Equation 3.2.

$$D = w_s\ c \tag{3.2}$$

The biodeposition is described similar to the deposition (Equation 3.3).

$$D_{bio} = fr\ c \tag{3.3}$$

Where:

fr	$[m\ s^{-1}]$	filtration rate

To solve the energy exchange over the vertical, Delft3D devides the water column into different vertical layers. The suspended sediment concentration is calculated for each different layer. Equation 3.2 and 3.3 uses the same suspended sediment concentration in each layer, consequently the terms settling velocity and filtration rate can be combined (see Equation 3.4) (Van Leeuwen et al., 2010).

$$D_{tot} = D + D_{bio} = (w_s + fr)\ c \tag{3.4}$$

The adapted advection-diffusion equation is:

$$\frac{\partial c}{\partial t}+\frac{\partial uc}{\partial x}+\frac{\partial vc}{\partial y}+\frac{\partial (w-(w_s+fr)c}{\partial z}-\frac{\partial}{\partial x}\left(\epsilon_{s,x}\frac{\partial c}{\partial x}\right)-\frac{\partial}{\partial y}\left(\epsilon_{s,y}\frac{\partial c}{\partial y}\right)-\frac{\partial}{\partial z}\left(\epsilon_{s,z}\frac{\partial c}{\partial z}\right)=E-D_{tot} \tag{3.5}$$

The filtration rate is assumed to be constant in this study. A constant filtration rate can be justified with:

- The model represents summer conditions; therefore there is no (hardly) seasonal variability.
- The range of suspended particles in the water column is between 0-100 mg l^{-1} and the filtration rate has a small range for these particle concentrations (see Figure 2.7).
- According to Widdows et al. (2002), the filtration rate is independent of current velocities between 0.05 and 0.8 m s^{-1}. Current velocities are larger than 0.05 m s^{-1} most of the tidal cycle (at locations of bivalve beds). The filtration rate of the Blue mussels is between 1.5 and 6 l h^{-1} ind^{-1} (Troost, 2010).

The simulated mussel bed is based on the study of Van Duren et al. (2006) and the characteristics of this mussel bed are used to estimate the filtration rate. The filtration rate of the blue mussel is 1.5 l h^{-1} (Widdows et al., 1979), based on the average length of the mussel shell of 3.85 cm Van Duren et al. (2006) and the suspended sediment concentration in the Wadden Sea of 50 mg l^{-1} (Postma, 1981). The mussel bed density in the experiment of Van Duren et al. (2006) is 1800 mussels per square meter. The filtration rate per square meter is $1800 \times 1.5 = 2700$ l h^{-1} m^{-2} or 0.75×10^{-3} m^1 s^{-1} m^{-3} or 0.75×10^{-3} m s^{-1}.

According to Jorgensen (1996), there is a large difference between filtration rates measured in a laboratory and the filtration rates that actually happen in the field. The filtration rate in the field corresponds with the laboratory measurements if all the mussels along the bed had the exhalent apertures facing the open water. A mussel bed in the field has a very random variation; as a consequence, some mussels will inhale water that has already been depleted of suspended mater, because neighbouring mussels have already filtered this water. The mean rates measured in the field can be 33% of the filtration rates measured in a laboratory (Jorgensen, 1996). Therefore, the re-filtration of water will be accounted for by decreasing the filtration rate per square meter with 33%. The filtration rate for a mussel bed is 0.25 mm s^{-1}.

Mussels filter only the lowest part of the water column and this has been included in the model by increasing the settling velocity (due to the filtration rate) only in the lowest layers of the water column. This increased settling velocity is implemented in Delft3D by changing the code. It is assumed that mussels can only filter the lowest 10 - 15 cm of the water column, because at these distances higher turbulence levels can be noted due to the filtration of suspended particles (Van Duren et al., 2006).

3.1.2.2 Sediment

There are three types of sediments in and around a bivalve bed, namely the normal sediment, the faecal pellets and the pseudofaecal pellets. The faecal and pseudofaecal pellets of mussels are very heavy compared to the normal sediment; and the faecal pellets are more resistant to erosion (Callier et al., 2006; Chamberlain et al., 2001). Thus, the critical bed shear stress of these faecal pellets is higher than the critical bed shear stress of the normal sediment. In contrast, the pseudofaecal pellets are lighter and easier to erode; besides, pseudofaeces fall easily apart and will (eventually) be similar as the normal sediment. Consequently, the faeces and pseudofaeces have a high critical bed shear stress and a low critical bed shear stress, respectively. The production of pseudofaeces is larger than the production of faeces in the Wadden Sea (see Section 2.3). The

critical bed shear stress in the model is therefore the same as the critical bed shear stress of the normal sediment. In contrast to mussels, the faeces and pseudofaeces of oysters are very light and these (pseudo)faeces hardly settle to the sea bottom (Dankers et al., 2004b). Therefore, it is assumed that the sediment properties in and around an oyster patch is similar to the sediment properties for a situation without an oyster patch.

3.2 Flume model

Van Duren et al. (2006) and De Vries et al. (2012) investigated the influence of respectively mussels and oysters on the hydrodynamics in a flume. They measured for instance, the flow velocity and the turbulent kinetic energy above a mussel and oyster bed, for low, intermediate and high flow velocities. The results of these studies are simulated with two models, each model represents a study, whereby the results are used to calibrate and validate the hydrodynamics of both model. The aim of these models is to mimic the roughness of mussels and oysters as good as possible.

3.2.1 Grid and bathymetry

The influences of mussels and oysters on the hydrodynamics for laboratory flume conditions are determined with the Delft3D-FLOW model. The bathymetries of the models are based on the bathymetries of the flumes. The simulated hydrodynamics are compared with the hydrodynamics of both flumes. The location of the measurements is the same as the location where the hydrodynamics of both models is derived, as a consequence, a good comparison can be made between the flumes and models. The numerical equations of Delft3D are based on finite differences. These numerical equations are solved for a certain volume specified by the grid and layers. The computational grid in the flume model has a dimension of 0.1×0.1 m. To account for the influence of mussels and oysters in the z-direction the volume is also divided into 40 equal vertical layers. The computational grid is small and the amount of layers is large to account for the effects of mussels and oysters on a small scale.

Mussels

One of the models simulates the influence of mussels on the hydrodynamics for the laboratory flume conditions of Van Duren et al. (2006). The dimensions of this model are 16×0.6 m and the water depth is 0.4 m. The bottom roughness height of the flume without mussels was calibrated at 5×10^{-5} m. The horizontal eddy viscosity was determined at 0.001 m^2 /s, and other values for this parameter does not lead to significant changes in the hydrodynamics . The mussel bed was defined at 9.6 m along the flume and the length of this bed was 3 m. The mussel bed consists of young mussels and the size of these young mussels are used as input parameters of a mussel bed in Delft3D. The average height of the mussel bed and the average shell length are 6.1 cm and 3.85 cm, respectively. The range of this mussel bed varies between 4.9 and 8.6 cm. The density of the mussel bed is 1136 mussels m^{-2} and the diameter of the mussels is 2 cm. According to De Vries et al. (2012), the drag coefficient of mussels is 0.42. After calibration of the model, the drag coefficient has been adapted to 0.6, because the simulated velocity profiles above mussel beds with this drag coefficient correspond better with the measurements of Van Duren et al. (2006). An overview of the characteristics of the implemented mussel bed is given in Table 3.1.

Oysters

The other model simulates the influence of oysters on the hydrodynamics for the laboratory flume

Tab. 3.1. Characteristics mussel and oyster patch as used for the numerical modeling (based on the measurements of Van Duren et al. (2006); De Vries et al. (2012).

		Mussels	Oysters
Density	[ind m^{-2}]	1136	148
Average height	[cm]	3.9	8.8
Range height	[cm]	2.7 - 6.4	5 - 12.5
Diameter	[cm]	2	5
Drag coefficient	[-]	0.6	1.84

conditions of De Vries et al. (2012). The grid of this model has a total length, width and water depth of 16, 0.5 m and 0.4 m, respectively. The bottom roughness height of the flume without oysters and the eddy viscosity is calibrated 5×10^{-5} m, the horizontal eddy viscosity was set to 0.001 m^2/s.. The length of the oyster bed was 3.3 m and this bed was defined at 7.6 m along the flume. The average oyster shell length is 8.8 cm, with a standard deviation of 2.5 cm. The density of the oyster bed is 148 oyster m^{-2} and the diameter of the oysters is 5 cm. The drag coefficient is based on the measurements of De Vries et al. (2012) (see Appendix A.2.2). The sum of $[c_D\ d(z)\ n(z)]$ (part of Equation B.6) of mussels and oysters is similar in size, however the height of oysters is significantly larger than the height of mussels. As a consequence, the total resistance force (F) (over the total bivalve height) imposed by oysters on the mean flow is higher than the total resistance force imposed by mussels. Table 3.1 presents an overview of the characteristics of the oyster patch. The set-up of both models are presented in Figure 3.2. The flume studies are described in Appendix A.

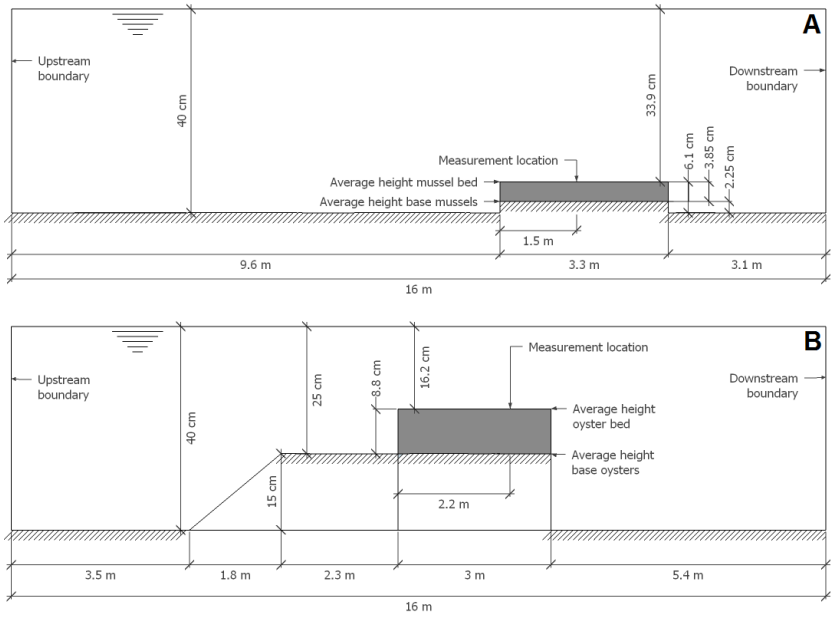

Fig. 3.2. The model set-up of the flume experiments conducted by Van Duren et al. (2006) (A) and De Vries et al. (2012) (B). The gray area indicates the bivalve height.

3.2.2 Hydrodynamics

The flow in the studies of Van Duren et al. (2006) and De Vries et al. (2012) is a steady flow, so the water depth and flow velocity do not vary in time. The model has two open and two closed boundaries to simulate the flow in a laboratory flume. The two closed boundaries represent the

walls of the flume, while the open boundaries describe the flow. To simulate a steady flow in Delft3D, the upstream boundary has a constant discharge and the downstream boundary is a constant water level. The downstream boundary is 0.4 m for both studies. For the upstream boundary several constant discharges are used to simulate the model, these discharges are presented in table 3.2. The discharges are determined with the 'law of the wall' (see Appendix A.3.1).The intermediate discharge is used to calibrate the models, while the low and high discharges are used to validate the models.

Tab. 3.2. The upstream boundary for the model with mussels or oysters. $\bar{U}$ = depth average flow velocity, Q = discharge

Velocity	Mussels		Oysters	
	$\bar{U}$ [m/s]	Q [m^3/s]	$\bar{U}$ [m/s]	Q [m^{-3}/s]
Calibration				
Intermediate	0.106	0.024	0.226	0.018
Validation				
Low	0.051	0.011	0.107	0.009
High	0.340	0.064	0.321	0.026

3.3 Field model

Another model has been set up, based on the flume model, in order to investigate the influence of mussels and oysters on the sediment dynamics. The model represents a tidal flat which is populated with mussels or oysters. Hereby, it is important to distinguish the effects caused by the chosen model domain and boundaries and the effects caused the mussel or oyster bed themselves. Moreover, it must be easy to vary several characteristics of the mussel or oyster bed, such as shell height and bivalve density, in the model in order to investigate the influence of these characteristics on the hydrodynamics and sediment transport. Taken these conditions into account, an idealized model has been chosen to represent a mussel or oyster patch on a tidal flat.

Mussel beds occur in the mid intertidal to subtidal, while oyster beds occur low in the intertidal to subtidal. So, both bivalves occur mostly in the same area. According to Dankers and Fey-Hofstede (2015); Brinkman et al. (2002); Troost (2010) there are also many mussel and oyster beds in the subtidal area. Besides, the flume studies investigated the influence of mussels and oysters on the hydrodynamics when they are constantly submerged. The influence of mussels and oysters on the sediment dynamics will therefore be investigated for subtidal conditions. The erosion of mussels and oysters is not included in this study. The model will represent summer conditions for a subtidal flat, because there is hardly any erosion of mussels and oysters in the summer. Moreover, currents are more dominant in the summer than the hydrodynamic forces caused by waves (Janssen-Stelder, 2000). Waves are therefore not included in the model.

The hydrodynamic flow conditions in the idealized model must be realistic for a mussel and oyster bed. Brinkman et al. (2002) investigated suitable areas for natural establishment of mussel beds (see Section 2.1.1) and this study is used to realize a model with realistic flow conditions for a mussel bed. Moreover, the PACE model of Duran-Matute et al. (2014) and Van Kessel (2015) is also used to estimate the flow velocities at several locations of existing mussel beds. The flow velocity above a mussel bed varied (most of the time) between 0.2 and 0.4 m s^{-1}. The results of

Brinkman et al. (2002) and Duran-Matute et al. (2014) are used to determine the hydrodynamic flow conditions. The oyster patch is simulated for similar hydrodynamic conditions as the mussel bed, because Pacific oysters prefer to settle on mussel beds(Reise, 1998). Consequently, the physical conditions of the Pacific oyster beds are similar to the physical conditions of mussel beds. Simulating a mussel and oyster bed in the same idealized model has an additional benefit, namely it is easier to compare the model results of a mussel patch and an oyster patch.

3.3.1 Grid and bathymetry

The influence of mussels and oysters on the sediment dynamics is determined with the Delft3D-FLOW model, hereby using hydrodynamic and morphological computations. The morphological computations are sensitive to the boundaries of the model, these boundaries must therefore be far enough away from the area of interest to avoid boundary effects. First of all, the hydrodynamic and sediment boundary conditions need time to develop a profile which corresponds with the model conditions. The hydrodynamics adapt quicker to the model conditions in comparison with the sediment dynamics. The morphodynamic computations determines therefore the length and width scale of the model. In Appendix B.3.4, the model dimensions have been determined for fine sediment dynamics. The length of the model is 2200 m and the width of the model is 300 m.

The computational grid cell has a dimension of 2×2 m in the center of the model. The grid size increases towards the lateral boundaries and the grid size near the boundaries is $\pm 60 \times 10$ m. An overview of the model grid and model dimensions (including the location of the mussel or oyster patch) is presented in Figure 3.3. The minimum size of a mussel or oyster patch is 10×10 m, because important geometrical and hydrodynamic phenomenon must at least be covered with 5 grid cells to solve the numerical equations adequately (Deltares, 2014). Given the size of the model it is not feasible to choose a smaller grid size (due to computational limitations), however this is unnecessary since this study aims to determine a larger scale influence of mussels and oysters. The depth of the idealized subtidal flat is 1.5 m and it is assumed that the depth does not vary in the direction of the flow and the transverse direction of the flow. The computational grid is divided in 20 vertical sigma layers to account for the influence of mussels and oysters in the z-direction. The vertical steps of these layers are small near the bed (and the top of the bivalves) and increases towards the water surface.

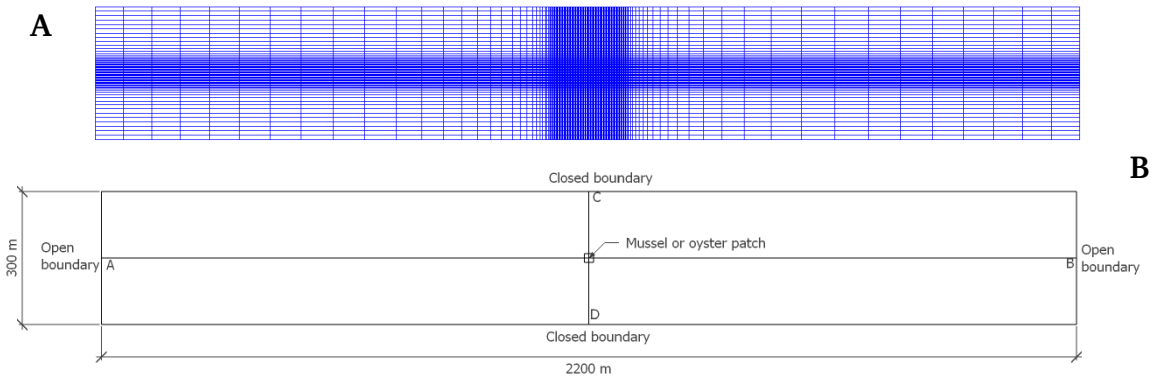

Fig. 3.3. A schematic overview of the model grid (A) and dimensions (B).

3.3.2 Bivalve implementation

The characteristics of the mussel and oyster patch are based on the flume model (Section 3.2). The size of the bivalve bed and the height of the bivalve bed are also important parameters which influence the sediment transport. The length and width of the mussel and oyster bed is 20 by 20 m and these distances correspond with a small/medium sized mussel or oyster bed. The height of a mussel and oyster bed has a large variation. The height varies of a mussel and oyster between $\pm$ 10 cm and $\pm$ 1 m (Dankers et al., 2004b; Walles et al., 2014). The height of the bivalve bed (without the shells) is 20 cm, based on the height of many mussel beds in the Wadden Sea (Figure 2.3).

3.3.3 Hydrodynamics

The outer dimensions of the model are rectangular and have four boundaries. Similar to the models representing the flume studies, this model has two open and two closed boundaries to simulate a tidal flow. The two closed boundaries are in the transverse direction of the tidal flow, while the two open boundaries describe the tidal flow. The bidirectional flow is similar during flood and during ebb, because this similarity will result in symmetric sedimentation patterns. The processes responsible for these patterns can be better understood and visualized with a symmetric tide. The bidirectional tidal flow changes every 6 hours in direction. A disadvantage of this similar tide during flood and ebb is that it was not feasible to force a water elevation over the tidal period. There is little variation in the water elevation and the water level can be assumed to be constant and this does not correspond with the field conditions (in the Wadden Sea).

The maximum flow velocity during the tide is 0.5 m s^{-1} and this velocity corresponds with the preferred habitat of mussels according to Brinkman et al. (2002). The bed shear stress, produced by this tidal flow, is above the critical bed shear stress for erosion during most of the tidal period. The bottom roughness height is set to a Nikuradse roughness height (k_s) of 5 $\times$ 10^{-3} m in the model (simulating the sediment dynamics), corresponding with a tidal flat (Paarlberg et al., 2005). An overview of the hydrodynamic parameters is presented in Table 3.3.

3.3.4 Sediment transport

Morphodynamic computations are included in the model in order to determine the influence of mussels and oysters on the sediment dynamics. There are many types of sediments, for example coarse sediments, such as coarse sands, and very fine sediments, such as clay. These sediments are specified in groups and have certain properties, for example sediments can be specified in a cohesive and non-cohesive group. Fine sediments have a cohesive behavior, because they consists of very fine particle sizes and the electro-magnetic properties of these sediments are relatively large and this binds the sediments together. The sediments around mussel beds are often very fine, such as silt, due to the settling of faeces (Hertweck and Liebezeit, 1996). Mussels live therefore often in a cohesive environment. Many oysters live in a sandy (non-cohesive) environment, for example in the Eastern Scheldt (Walles, 2015). However, mussels and oysters occur also in a non-cohesive and cohesive environment, respectively. The influence of mussels and oysters will therefore be determined in a cohesive and non-cohesive environment.

The properties of the cohesive sediments are based on the study of Van Ledden (2003). The settling velocity of the cohesive sediment is 0.5 mm s^{-1}. The critical shear stress and the erosion coefficient are 0.5 N m^{-2} and 1 $\times$ 10^{-4} kg m^{-2} s^{-1}, respectively. The density of the sediment is

Tab. 3.3. Parameters settings for the model simulations. Bold numbers indicate variables in the model simulations. l_{shell} indicates the range of shell length of the bivalve bed.

	Symbols [unit]	Reference run	Physical factors	Biology factors			
			u	h_{bed}	l_{shell}	n	fr
Flow velocity amplitude	u [m s^{-1}]	0.5	**0.4-0.6**	0.5	0.5	0.5	0.5
Water depth	h [m]	1.5	1.5	1.5	1.5	1.5	1.5
Roughness	k_s [m]	5×10^{-3}	5×10^{-3}	5×10^{-3}	5×10^{-3}	5×10^{-3}	5×10^{-3}
Mussels							
Bed height	h_{bed} [cm]	20	20	**0-40**	20	20	20
Length shell	l_{shell} [cm]	2.7-6.4	2.7-6.4	2.7-6.4	**0-3.5**	2.7-6.4	2.7-6.4
Density	n [ind m^{-2}]	1136	1136	1136	1136	**284-1136**	1136
Filt. rate	fr [mm s^{-1}]	0.25	0.25	0.25	0.25	0.25	**0-0.5**
Oysters							
Bed height	h_{bed} [cm]	20	20	**0-40**	20	20	20
Length shell	l_{shell} [cm]	5-12.5	5-12.5	5-12.5	**0-7.5**	5-12.5	5-12.5
Density	n [ind m^{-2}]	148	148	148	148	**37-148**	148
Filt. rate	fr [mm s^{-1}]	-	-	-	-	-	-

2650 kg m^{-3}, while the density of deposited sediment is 500 kg m^{-3} (corresponding with a very loose bed). It takes time for cohesive sediment to consolidate and the time scales in this model are too short for consolidation, consolidation plays therefore a minor role and is assumed to be zero in this model. The suspended sediment concentration in the model corresponds with the average suspended sediment concentration in the Wadden Sea (50 mg l^{-1}) (Postma, 1981; Van Ledden, 2003). The simulated mudflat represents summer conditions and there is a net deposition of sediment corresponding with the study of (Janssen-Stelder, 2000). The cohesive sediment transport is calculated with the Partheniades (1965) formulations (see Appendix B.3.1)

The properties of the non-cohesive fine sediments are based on the study of Brinkman et al. (2002) and Huisman and Luiendijk (2009). A median grain size of 0.2 mm occurs at mussel bed locations in the Wadden Sea (Brinkman et al., 2002). Many oyster beds occur in the Eastern Scheldt, and the grain size in the Eastern Scheldt is 0.15-0.2 mm (Huisman and Luiendijk, 2009). The median grain size in the fine (non-cohesive) sediment model is therefore 0.2 mm. The density of the sediment is 2650 kg m^{-3} and the dry bed density is 1600 kg m^{-3}. The boundaries do not transport sediment inside the model (only outwards the model) and the transport is initiated by picking up sediment from the bottom. After a certain length, the sediment transport is adjusted to the flow and this adjustment length is taken into account by the larger model dimensions. The non-cohesive sediment transport is calculated with Van Rijn (1993) (see Appendix B.3.2). The hydrodynamic and sediment dynamic settings, with an exception for the water elevation, correspond with typical field conditions (Brinkman et al., 2002; Van Ledden, 2003; Paarlberg et al., 2005; Huisman and Luiendijk, 2009). The influence of mussels and oysters on the hydro- and sediment-dynamics are determined for a reference run with the parameter settings listed in Table 3.3. The sensitivity of the hydro- and sediment-dynamics is investigated for a variation in flow velocity, bed height, shell length, density and filtration rate.

4 Hydrodynamic results

Two models are presented in this section; one model simulates the flow over a mussel bed, while the other model represents the water flow over an oyster bed. The model set-ups of these two models are presented in Section 3.2. The results of both models will be compared with the results of the flume studies of Van Duren et al. (2006) and De Vries et al. (2012).

4.1 Calibration

This section presents the calibration of both models. The calibration of the mussel bed model and oyster bed model is presented in Section 4.1.1 and Section 4.1.2, respectively.

4.1.1 Mussel patch

Van Duren et al. (2006) measured the flow velocity and turbulent kinetic energy (TKE) above a mussel bed; moreover, this study also measured the flow velocity and TKE above the flat bottom of the flume. First of all, the performance of the model will be determined for the flow conditions above a flat bottom. Hereafter, the model simulates the flow above a mussel bed and the settings of this model will be calibrated. A detailed description of the measurements conducted by Van Duren et al. (2006) is presented in Appendix A.

The simulated flow velocity and TKE above a flat bottom is represented in Figure 4.1. It can be noted that the measured flow velocity does not completely follow a logarithmic profile; the measured profile is (more) linear. This is also visible in Figure A.5, especially for the intermediate and high flow velocity, in these cases the flow profile follows a (small) concave shape (Van Leeuwen, 2008). Furthermore, the roughness length (z_0) over a flat bottom is not constant for the three different flow velocities. This is remarkable, because the roughness length will normally be constant for a variable flow velocity. The profile cannot be logarithmic due to several reasons, for example due to the flow generation by the conveyor belt system (acting like a paddle wheel).

The results of Van Duren et al. (2006) cannot be disqualified a priori for the fact that the velocity profiles do not show a logarithmic profile. However, the assumptions of 'law of the wall' are not valid for these measurements (Van Leeuwen, 2008). Consequently, the calculated discharge of the flow must be taken with caution (see Appendix A.3). This could also be one of the reasons for the bad similarity between the measured and simulated velocity profile. However, the simulated velocity profile above a mussel bed corresponds reasonably well with the measurements and this is an indication that the calculated discharge is quite correct. The approximated error of the calculated discharge is 5-10%. Moreover, Delft3D assumes a logarithmic velocity profile, consequently this could be a reason that the simulated flow profile does not correspond well with the measured profile. The simulated TKE shows reasonable agreement with the measured turbulence levels.

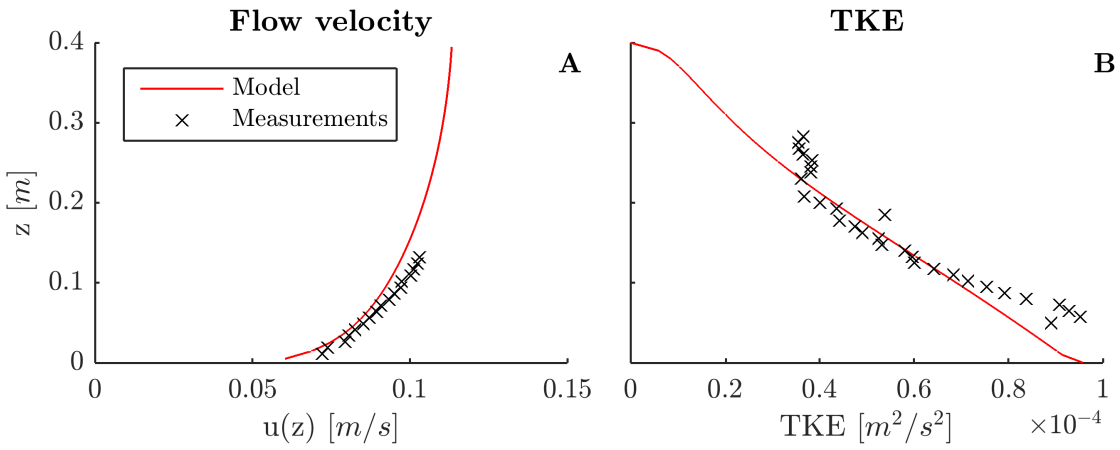

Fig. 4.1. Flow velocity (A) and TKE (B) above a flat bottom (glass) in a flume. Measurements are conducted by Van Duren et al. (2006).

First of all, before modeling the velocity and TKE profile above a mussel patch, it can be noted that the flow is not completely developed at the measurement location. The Reynolds stresses do not have a linear distribution over the water depth (see Appendix A.2.1) as it would be expected from a completely development flow according the measurements of Nezu and Rodi (1986). So, it can be concluded that the boundary layer is not completely developed.

The characteristics of the mussel bed are shown in Table 3.1 and the corresponding velocity profile and TKE above a mussel bed for an intermediate velocity is presented in Figure 4.2. The mussel bed is simulated for two cases, namely a mussel bed with a constant height ($h_{mus\ con}$) and a mussel bed with a variable height ($h_{mus\ var}$). The constant total mussel bed height is 6.1 cm and the average shell (cylinder) height is 3.9 cm. The flow velocity above a mussel bed with a constant height shows good agreement with the measured flow velocity; however the turbulence levels are strongly overrated by the model. The overestimated turbulence levels are almost a factor 4 to large.

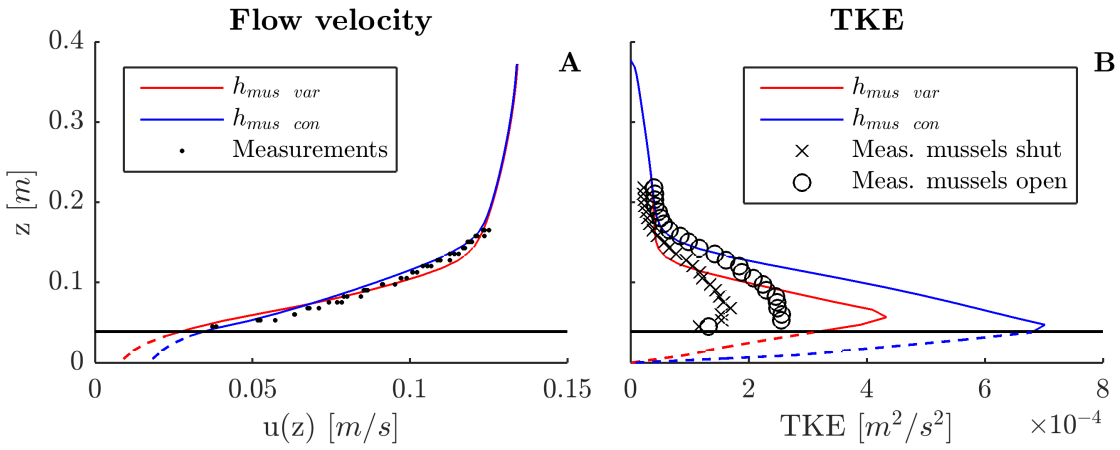

Fig. 4.2. Velocity (A) and TKE (B) profile above a mussel patch at intermediate flow velocity. The black marks indicate the measurements of Van Duren et al. (2006). The turbulence levels above active and inactive mussels are indicated with the black circles and black crosses, respectively. The black horizontal line indicates the average mussel height.

In order to reduce this large overestimation of the turbulence, a random variation for the mussel height is implemented in the model. This variation is implemented in Delft3D by varying the

mussel bed height per grid cell and is implemented by changing the height of the cylinders in the 3D (rigid) vegetation model. A random function determines the mussel bed height at each grid cell. The mussel bed height has 5 possible values and these values are within the range of the measured mussel bed height. Figure 4.3 represents a mussel bed with a variable height. The flow velocity and turbulence are average over the total width of the flume in order to prevent extreme and unrealistic values. Otherwise, the results could be unrealistic as a result of unfavorable consecutive heights, for example 5 consecutive high mussel bed heights and these consecutive heights will result in a large TKE peak high in the water column. In this case the results are averaged over the 6 grid cells. The influence of several different random bed heights is presented in Appendix C.1.1.

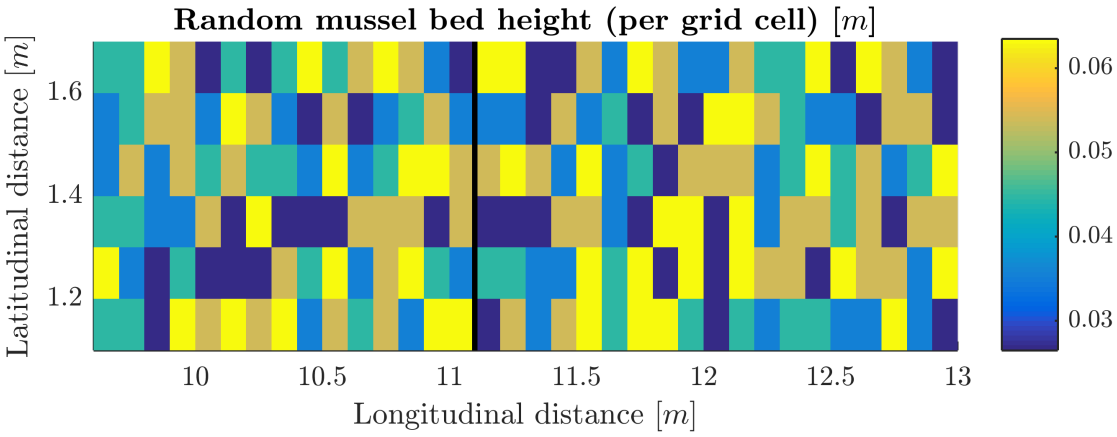

Fig. 4.3. A variable mussel bed height. The variation is determined with a random function. The vertical black line indicates the measurement location.

4.1.2 Oyster patch

De Vries et al. (2012) did not measure the flow velocity and turbulence above the flat bottom of the flume; therefore it is not possible to determine the performance of the model above the flat bottom. The measurements of De Vries et al. (2012) must be taken with caution, because the flow was not completely stable and the wave dampener did not worked perfectly. Moreover, there is a lack of data points over the water depth and there is not a clear pattern visible in the TKE for most of the turbulence profiles. Consequently, these measurements should be taken with caution. Appendix A presents a detailed description of the flow velocity profiles and the TKE measured by De Vries et al. (2012).

The characteristics of the oyster bed are given in Table 3.1. Figure 4.4 represents the flow velocity and TKE above an oyster bed for an intermediate flow velocity. Comparison between the measurements and the simulated flow velocity and TKE revealed that the model simulations above an oyster bed with a constant height ($h_{oys\ con}$) are completely inaccurate. The turbulence peak over a constant height is not included in Figure 4.4 B, because this peak is extremely large (0.08 $m^2\ s^{-2}$). Hence, an oyster bed cannot be presented with a constant bed height. In contrast, the model, including a variable oyster bed height ($h_{oys\ var}$), shows good agreement with the measurements, both the flow velocity as well as the TKE. The implementation of this variable oyster bed height is similar to the implementation of a variable mussel bed height (Section 4.1.1). The variation of this oyster bed corresponds with the measured variation. The flow velocity and turbulence are also averaged over the total width of the flume; in this case the results are averaged over the 5 grid cells.

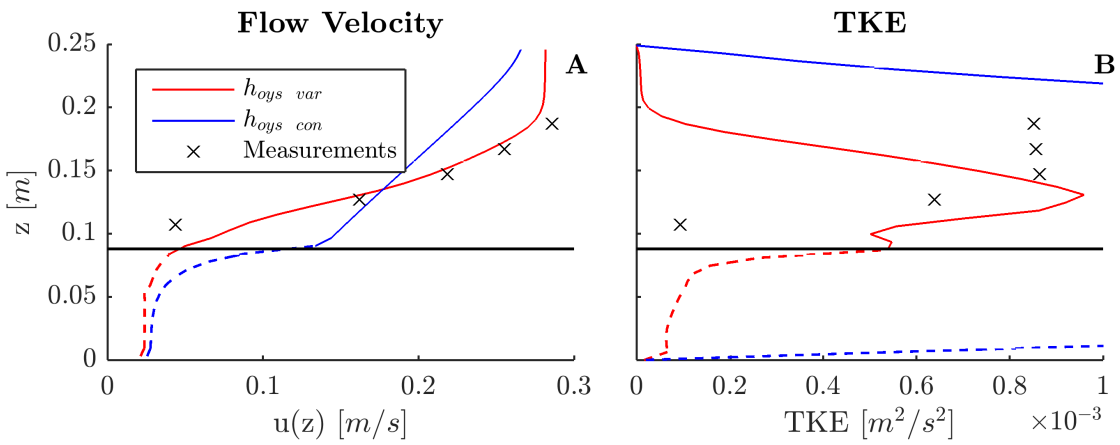

Fig. 4.4. Velocity (A) and TKE (B) profile above an oyster patch at intermediate flow velocity. The black crosses indicate the measurements of De Vries et al. (2012). The black horizontal line indicates the average oyster height.

The simulated velocity pattern (over a variable oyster bed height) corresponds with the measurements; there is only a small overestimation of the velocity near the canopy. The TKE is estimated reasonably by the model, the magnitude of the turbulence corresponds well with the measurements; in contrast, the location of the turbulence peak is lower compared to the measured location. The turbulence within the oyster bed is very small due to the low vertical velocity gradient within the canopy (See Section B.2). The small TKE peak at a distance of 0.09 m from the bed originates from a large turbulence production at one of the grid cells at this height. This large turbulence production is generated at this height due to a several consecutive low oyster bed heights and is reduced by averaging over the total width of the flume.

Both models proved capable of reproducing the general features of the measured flow if a variation in the bivalve bed height is included. According to Figures 4.3 and 4.4, a variable shell height will strongly reduce the turbulence levels. Mussels and oysters are very close to each other and the influence of each bivalve on the flow will affect the hydrodynamics several decimeters behind this bivalve. This is probably one of the reasons for the extreme turbulence production over a bivalve bed with a constant height. The turbulence peak created by every single bivalve is produced at the top of the canopy (at the same height) and this is consistent with the studies of (Okamoto and Nezu, 2013; Bouma et al., 2007; Stoesser and Nikora, 2008).

A schematic overview of the turbulence enhanced by bivalves with exactly the same height and with a variable height is presented in Figure 4.5. The distance between the bivalves is small and the turbulence generated by one bivalve has not been developed between these small distances. Moreover, every bivalve increases the turbulence strongly at the same height (if every bivalve has exactly the same height). This turbulence peak is enhanced by each bivalve and the total turbulence peak will strongly increase. The turbulence peak above a mussel bed with a variable height is smaller and this reduction is probably the direct effect of a variable bed, because the flow is partly obstructed by the bivalves and the turbulence peak is generated at different depth.

4.2 Validation

The calibrated model of a mussel and oyster bed is validated with other measurements in this section. The simulated flow above a mussel and oyster bed with a constant height ($h_{mus\ con}$ and

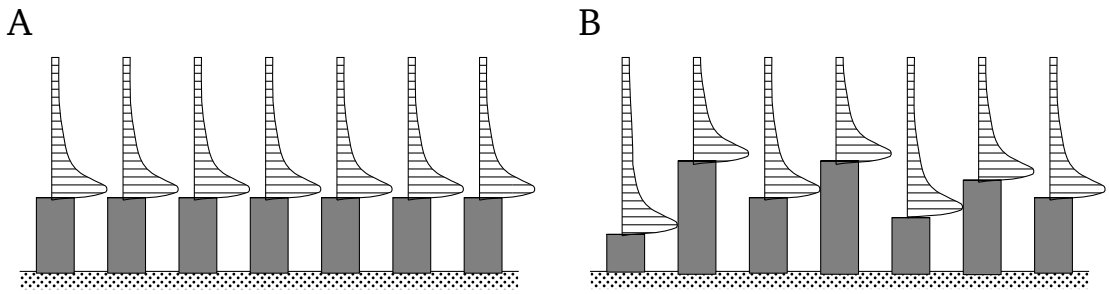

Fig. 4.5. (A) Schematic overview of a bivalve bed with a constant shell height. (B) Schematic overview of the implementation of a bivalve bed with a variable shell height in the (rigid) 3D vegetation model.

$h_{oys\ con}$) showed similar results as in Section 4.1. A constant bed height results in overestimation of the turbulence levels above a bivalve bed. The model simulations above a mussel and oyster patch with a variable bed height ($h_{mus\ var}$ and $h_{oys\ var}$) showed good agreement with the measured velocity profile (Van Duren et al., 2006; De Vries et al., 2012) (Figures 4.6 and 4.7), except the velocity is overestimated close to the canopy of oysters. The flow is reduced within the bivalve bed due to the friction of the shells, while the flow is forced to flow above the bed and this results in an increased flow velocity above the bed. The simulated TKE above the mussel bed ($h_{mus\ var}$) corresponds reasonably well with the measurements, the simulated TKE peak is slightly overestimated while the location of the peak is correct. The simulated turbulence above an oyster bed ($h_{oys\ var}$) showed good agreement with the measurements, only in case of low velocities is the TKE peak overestimated. The turbulence peak at a distance of 0.09 m from the bed is also visible for the low and high velocities and this peak originates also from a large turbulence production at one of the grid cells at this height.

Comparison of the simulated velocity profiles and TKE of mussels and oysters revealed that the free stream flow velocity is roughly equal for the intermediate velocity above mussels (Figure 4.2A) and the low velocity above oysters (Figure 4.7A). The simulated turbulence peak above a mussel and oyster bed are roughly $\pm\ 4 \times 10^{-4}$ m^2 s^{-2} and $\pm\ 3.5 \times 10^{-4}$ m^2 s^{-2}, respectively. Consequently, the TKE above a mussel bed of 1136 individuals is comparable with the TKE above an oyster bed of 148 individuals. To conclude, an individual oyster produces a significantly larger amount of turbulence than an individual mussel. These results can be explained by the rougher and larger shell of oysters compared to mussels. A larger and rougher shell will decrease the flow velocity to a larger extend. These findings correspond with the study of De Vries et al. (2012).

The influence of the bivalve bed characteristics, such as the density, the diameter, the shell height and the drag coefficient, on the velocity and turbulence profiles is presented in Appendix C.1. The density, diameter and drag coefficient have similar influence on the hydrodynamics above the patch. The variation of the shell height has a large influence on the flow velocity and especially on the turbulence levels. A larger variation results in lower turbulence levels and otherwise.

4.3 Results in the longitudinal direction

As explained in Section 4.1.1 the flow is not completely developed in both flumes; therefore, this section presents the velocity profiles for the longitudinal direction (the direction of the flow). According to Figure 4.8, the flow is not developed at the measurement location (longitudinal distance of 11.1 m), because the velocity is not constant over the length of the mussel bed. The

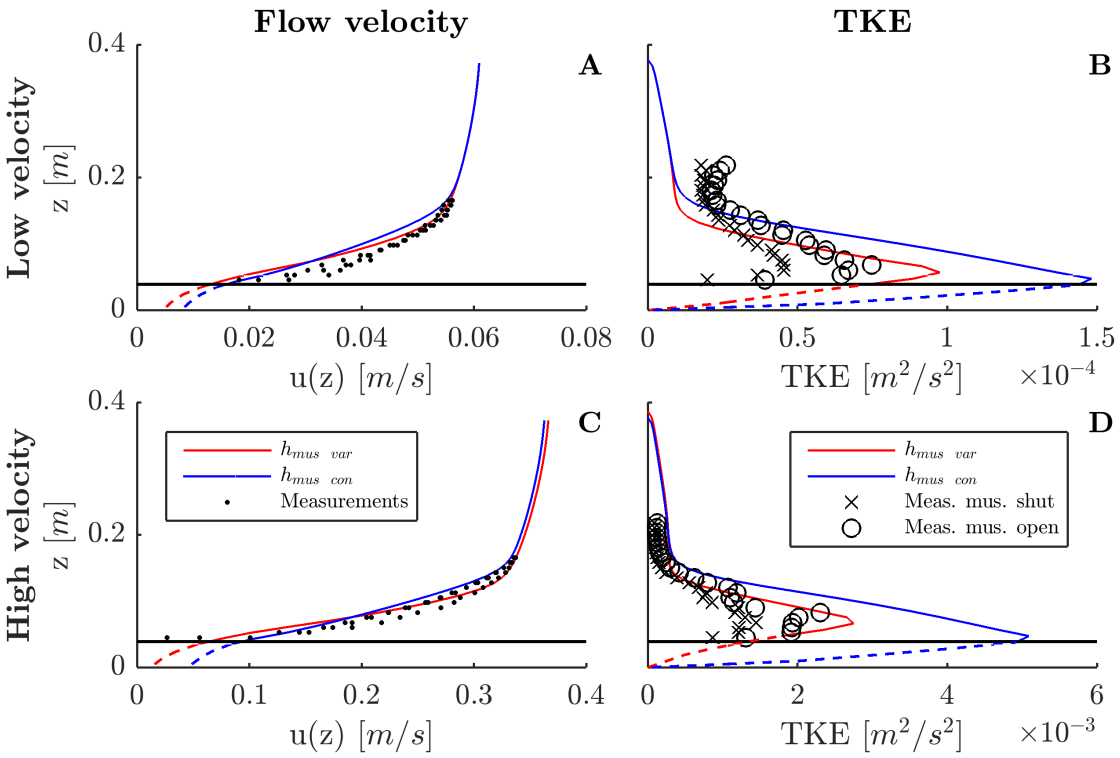

Fig. 4.6. Velocity (A) and TKE (B) profiles above a mussel patch at low and high flow velocities.The black marks indicate the measurements of Van Duren et al. (2006). The turbulence levels above active and inactive mussels are indicated with the black circles and black crosses, respectively. The black horizontal line indicates the average mussel height.

boundary layer is not completely developed and this corresponds with the measurements of Van Duren et al. (2006); Nezu and Rodi (1986) (see Appendix A.2.1). The velocities profiles above a constant mussel bed height and above a variable mussel bed height are comparable. A variable bed height is a lower flow velocity near the canopy while the velocity at $\pm$ 0.15 m is higher in comparison with a constant bed height. Appendix C.1.2 represents the development of the TKE over the longitudinal direction. The flow development above the oyster patch (in the lengthwise direction) is comparable with the development above a mussel patch; hence these results are not presented. As a consequence of only one measurement location during the experiments of Van Duren et al. (2006) and De Vries et al. (2012), both models cannot be compared over the longitudinal distance.

4.4 Grid dimensions

The grid dimensions in the flume are small, namely 0.1 $\times$ 0.1 m. Both models are capable to reproduce the general hydrodynamic features above a mussel or oyster bed for these small grid dimensions. However, these dimensions are too small to implement a mussel or oyster patch on a tidal flat scale, because the computational time will increase several magnitudes. It is therefore not feasible to resolve the numerical equations of Delft3D for these grid dimensions above/around a bivalve patch. The grid size must increase in order to implement a bivalve bed on a tidal flat scale.

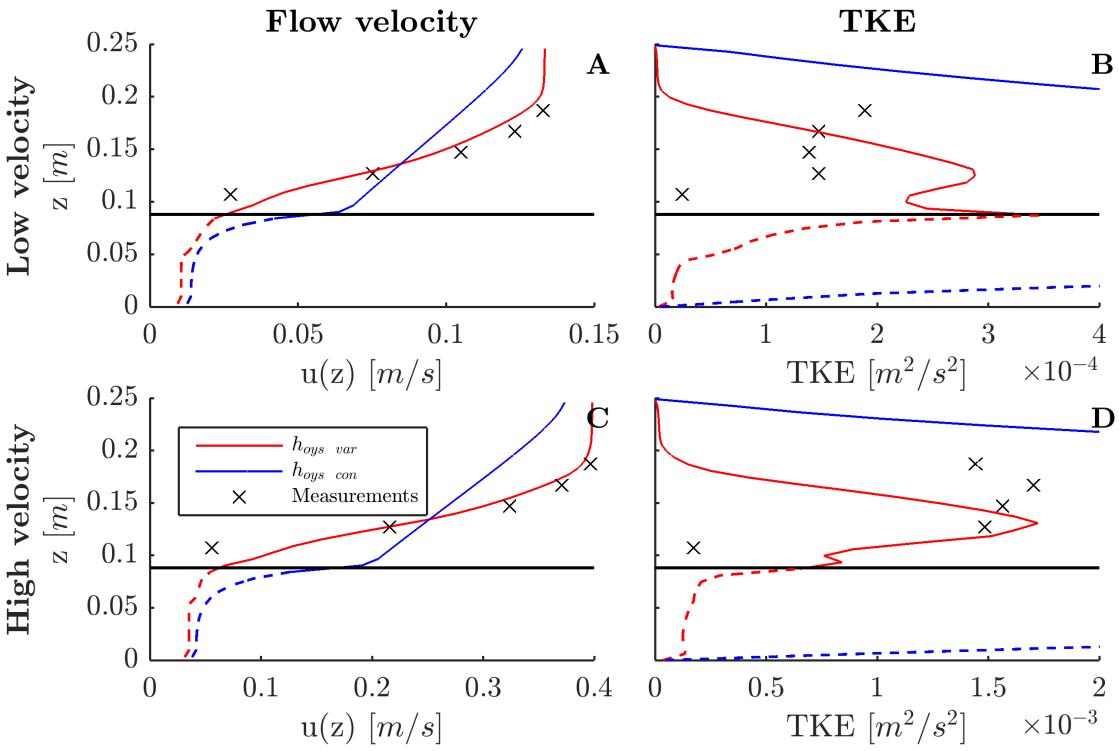

Fig. 4.7. Velocity (A) and TKE (B) profiles above an oyster patch at low and high flow velocities. The black crosses indicate the measurements of De Vries et al. (2012). The black horizontal line indicates the average oyster height.

The grid dimensions and width of the model is increased are increased from 0.1 × 0.1 m to 0.5 × 0.5 m. The width and discharge of the model is also increased with a factor 5; consequently the average flow velocity will be similar as the initial model. The length and water level are unaltered. The height of the mussel and oyster bed is also varied per grid cell and as a consequence of the larger grid is the variation of the bivalve bed height less pronounced. The bivalve bed height has at least a uniform bed height for a length and width scale of 0.5 m; the hydrodynamics will therefore be more comparable with a uniform bed height.

Figure 4.9 presents the velocity and TKE profile above a mussel and oyster bed for a grid dimension of 0.5 × 0.5. The blue line presents a mussel or oyster bed, whereby the height is varied per grid cell ($h_{mus\ var\ grid}$ or $h_{oys\ var\ grid}$). In the case of a variable mussel height ($h_{mus\ var\ grid}$), the simulated velocity profiles are very similar to the measurements. The simulated TKE above a mussel bed corresponds good with the smaller grid size model and these simulations shows fairly good correspondence with the measurements. On the other hand, the simulated velocity profile and TKE above an oyster patch with a grid dimension of 0.5 × 0.5 ($h_{oys\ var\ grid}$) does not correspond well with the measurements. The velocity close to the bed is overestimated, while the velocity in the upper part of the water column is underestimated. The turbulence is extremely overrated due to less variation in the bed height. Each oyster produces a large amount of turbulence and this total turbulence is enhanced by every oyster resulting in a large turbulence production. The three turbulence peaks are the result of a variation in the oyster bed height. This model result is comparable with the model results above an oyster bed with a constant bed height (see Section 4.1.2).

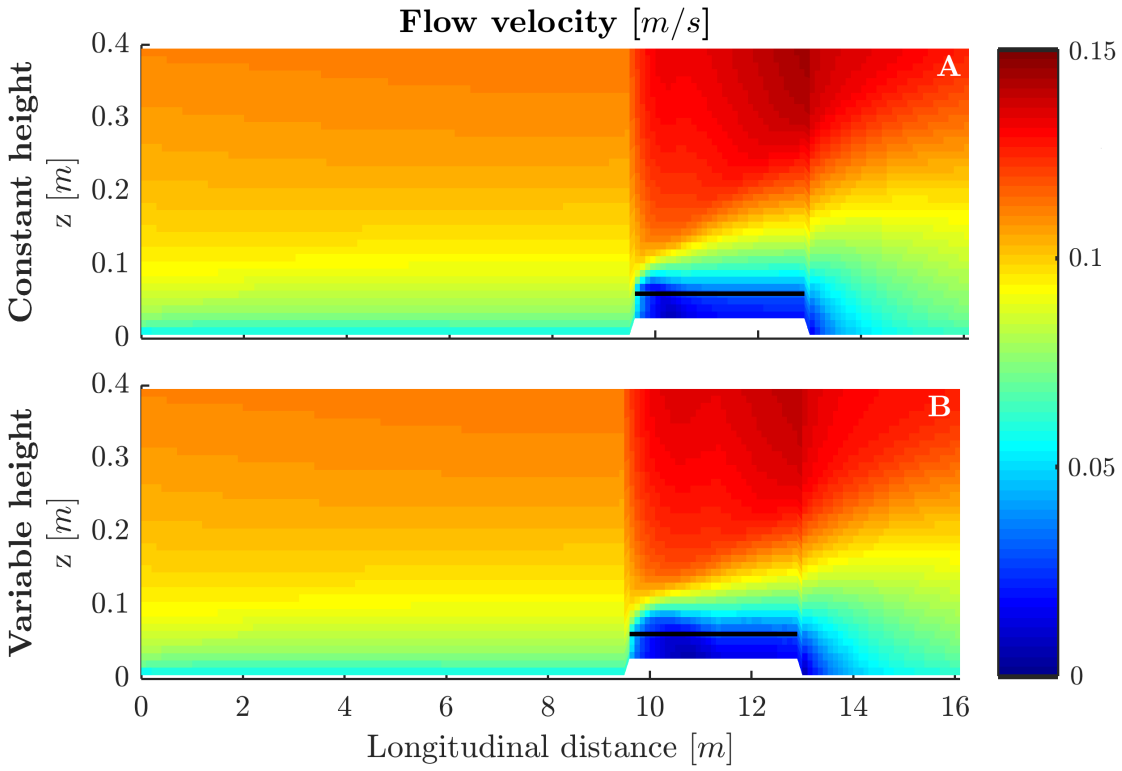

Fig. 4.8. Side view of the intermediate flow velocity above a mussel patch with a constant shell height (A) and a variable shell height (B). The flow velocity is averaged over the width of the flume and the measurement location of Van Duren et al. (2006) is at 11.1 m. The black horizontal line indicates the average mussel height.

In order to decrease the influence of a larger grid size on the hydrodynamics above an oyster bed another method is implemented in Delft3D to account for the variable bivalve bed height. Hereby, the bivalve bed height is varied by changing the numbers of bivalves m^{-2} over the height. The number of bivalves m^{-2} is largest close to the bed and the smallest at the top of the canopy. This variation can be implemented within the grid cell; consequently the model is not dependent on grid size in combination with the variation of the bivalve bed.

Figure 4.9 presents the simulated flow velocity and TKE for a mussel or oyster patch, whereby the height is varied within the grid cell ($h_{mus\ var\ cel}$ and $h_{oys\ var\ cel}$). This simulated flow velocity above a mussel or oyster patch corresponds well with the measurements. The predicted TKE above a mussel patch corresponds reasonable, however, the results above a mussel bed with a variation per grid cell is better. It cannot be explained why there is a significant difference between the model results of $h_{mus\ var\ grid}$ and $h_{mus\ var\ cel}$. A possible explanation is that there is too little variation between the mussel heights and that the model interpolates between these heights, consequently the model simulates the flow above this bivalve bed more like a bivalve bed with a constant bed height.

The model simulates the flow velocity and turbulence levels above an oyster patch with a variation within the cell ($h_{oys\ var\ cel}$) fairly good (Figures 4.9 and C.3). The magnitude of the turbulence peak corresponds reasonable well with the measurements. A big advantage of a model with a variation within the cell is the results above a bivalve patch are independent on the grid dimensions. Consequently, this model can be implemented in a model with larger grid dimensions to investigate the influence of a bivalve patch on the sediment dynamics.

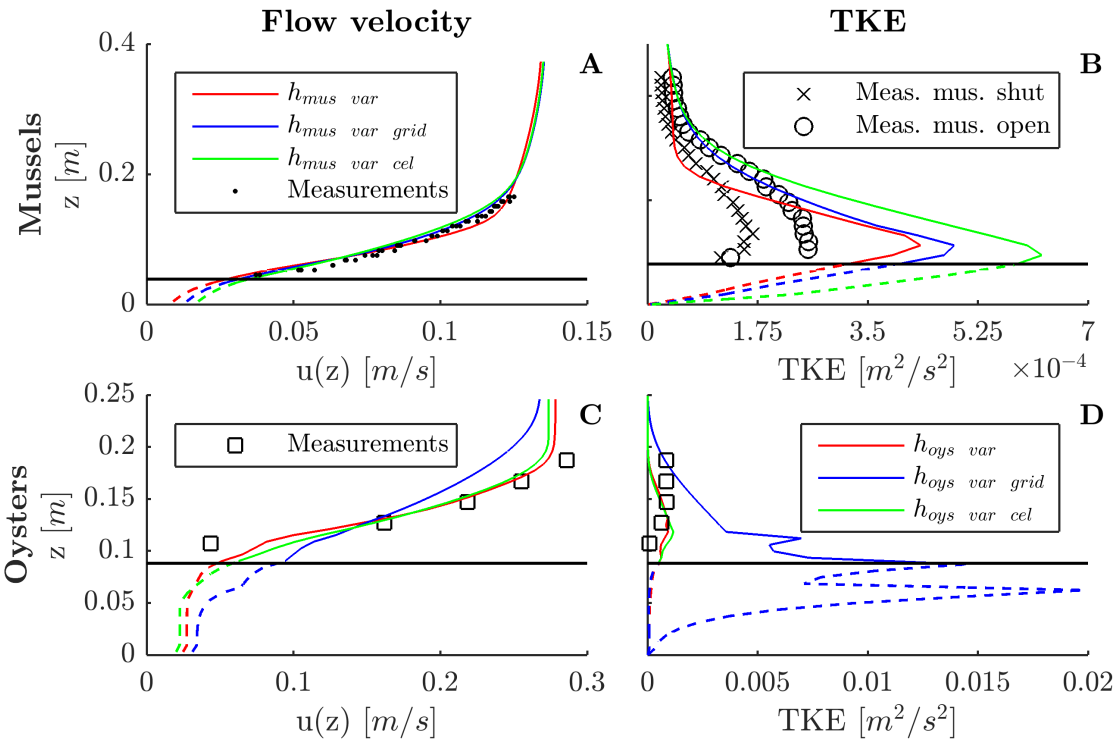

Fig. 4.9. Velocity profile (A,C) and TKE (B,D) above a bivalve patch at intermediate flow velocity. Three model results are presented; firstly, the simulations above a bivalve patch with a grid size of 0.1 × 0.1 m ($h_{mus\ var}$ and $h_{oys\ var}$). Secondly, the simulations above a bivalve patch with a grid size of 0.5 × 0.5 m, the bivalve height is varied per grid cell ($h_{mus\ var\ grid}$ and $h_{oys\ var\ grid}$). Finally, the model results for a bivalve patch with a grid size of 0.5 × 0.5 m, these bivalve heights are varied within the cell ($h_{mus\ var\ cel}$ and $h_{oys\ var\ cel}$). The black marks indicate the measurements of Van Duren et al. (2006) and De Vries et al. (2012). The turbulence levels above active and inactive mussels are indicated with the black circles and black crosses, respectively. The black horizontal line indicates the average bivalve height.

4.5 Sediment transport

The hydrodynamic conditions determine for a large part the transport of sediment. Mussels and oysters have a large influence on the hydrodynamics; they reduce the flow velocity near the bed and they increase the flow velocity in the upper part of the water column. As a consequence, mussels and oysters have a large influence on the sediment transport. An important parameter of sediment transport is the bed shear stress. The current just above the bed (and the roughness height) determines for a large part the bed shear stress (See Appendix B.3). The near bed flow velocity is reduced due to the obstruction of the flow by mussels or oysters; consequently, the bed shear stress on the sediment between the bivalves is also reduced (compared to the surrounding bed). The bed shear stress for a bivalve patch (with the normal height) is very low (see Figure 4.11) and it is implausible that sediment erodes from the bivalve bed. This section determines the possibility of erosion due to a decreased shell height. The shell height can decrease if sediment is deposited in a bivalve patch. The height of the bivalve shells is decreased with 1, 2 and 3 centimeters to determine the increase of bed shear stress (on the sediment). The difference between the highest and lowest bivalve shell height remains the same for these shell height reductions, and every shell has been reduced with the same length.

Firstly, the influence of a decreased mussel shell height on the velocity is determined (Figure 4.10A).The flow velocity pattern above the canopy does not change for the different shell heights,

except the near-bed flow velocity increases slightly, consequently the bed shear stress increases as well. Figure 4.11 presents the influence of the shell height reduction on the bed shear stress. The critical bottom shear stress for resuspension of sediment (in a flume) is around 0.10 N m^{-2} (Wright et al., 1997). It is unlikely that erosion occurs from a mussel or oyster patch for these flow velocities, if the bed shear stress within the mussel patch is compared with the critical bed shear stress.

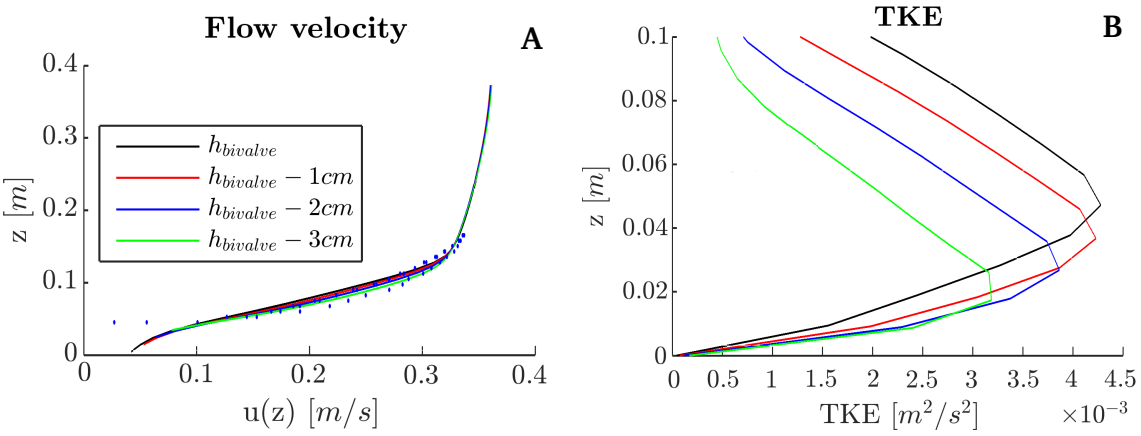

Fig. 4.10. The flow velocity (A) and TKE (B) profile for four different bivalve heights (in this case a mussel bed). The mussel height is reduced by lowering the height of the cylinders in the rigid 3D vegetation model with 1, 2 or 3 cm.

Another phenomenon that can be noted from Figure 4.11 is the bed shear stress peak around the leading edge of the bivalve patch. The flow velocity above the bivalve patch is increased due to a decreased cross sectional area of the flume (compared to the surrounding area). This results in an uplift of water just in front of the patch. The flow is accelerated just in front of the patch due to this uplift of water and this cause an increased bed shear stress (Borsje et al., 2014). The bed shear stress inside the patch is strongly decreased and the bed shear stress at the lee side of the patch is also reduced over several meters. These results are comparable with the results of Bouma et al. (2007) and Borsje et al. (2014), and both studies used the 3D rigid vegetation model of Uittenbogaard (2003). The bed shear stress in front of a tube building worm (*Lanice conchilega*) increases, while the shear stress decreases in the patch and at the lee side of the patch (Borsje et al., 2014). Bouma et al. (2007) found similar results around marsh vegetation patches (*Spartina anglica*).

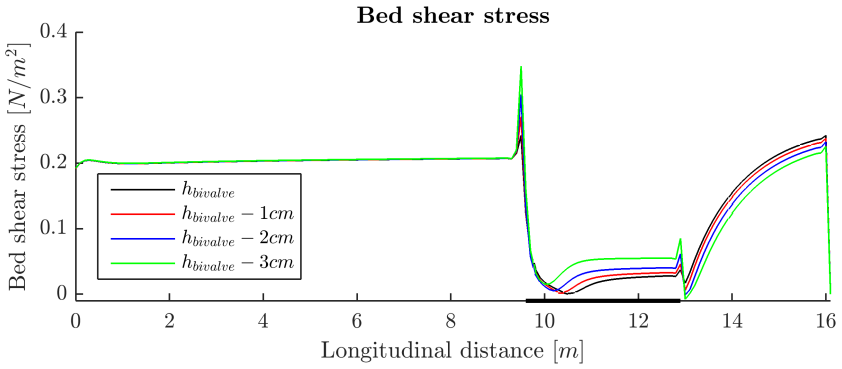

Fig. 4.11. The bed shear stress for four different bivalve heights (in this case a mussel bed) The mussel height is reduced by lowering the height of the cylinders in the rigid 3D vegetation model with 1, 2 or 3 cm. The black horizontal line indicates the location of the bivalve bed.

Turbulence is also an important parameter to determine the sediment dynamics. Turbulence is caused by bottom friction and velocity differences between water layers. In the case of a mussel or oyster patch, the friction is mostly caused by the shells. Turbulence, i.e. velocity fluctuations and vortices, is able to lift sediment grains from the bed and bring it to higher water levels, so the sediment is brought into suspension and is distributed over the water column (Borsje, 2014). Mussels and oysters patches create a lot of turbulence compared to the surrounding area. This high turbulence levels can bring sediment high in the water column. Moreover, high turbulence levels can results in erosion if these (high) turbulence levels are close enough to the sediment. According to the figures in Section 4.1 and 4.2 above, the highest turbulence levels occurs around the top of the canopy and it is therefore unlikely that these high turbulence levels can result in erosion. If the elevation of a bivalve patch is reduced the high turbulence levels are closer to the bed and it is likely that erosion can occur due to large turbulence levels (Figure 4.10).

Concluding, it is implausible that erosion occurs from a bivalve bed (with a normal elevation), because the bed shear stress is too low. Besides, the high turbulence levels are probably too high in the water column in order to lift sediment grains from the bed. The field model can give some clarification to this subject. This conclusion corresponds with the measurements of Widdows et al. (1998) and Widdows et al. (2002). These studies determined that erosion hardly occurs from a mussel bed in a sandy substrate or cohesive mud substrate. The density of the mussel bed used in this model corresponds with these high density percentages. Nonetheless, it is likely that erosion can occur if the elevation increases or if the density decreases.

4.6 Conclusion

Both models, representing a mussel or oyster patch, are able to reproduce the general features of the measured flow. The flow velocities are reduced within the bivalve patch and the water, while above the patch the velocities are increased, corresponding with the measurements. The turbulence levels are also similar to the measured TKE. Overall, the results of both models correspond reasonable well with the flume studies; however, due to a lack of longitudinal measurements over a mussel and oyster patch it is hard to evaluate the model over longitudinal direction, especially the leading edge. The leading edge is the part of the bivalve patch that first contacts the water flow. More qualitative good measurements are needed over the longitude of the flume; consequently, the model can be validated at several locations.

One essential parameter for the implementation of a bivalve bed in Delft3D is the variability in shell (cylinder) height over the bivalve bed. A variable shell height is needed to simulate the flow velocity above the bivalve patch correctly, especially for oysters. Variability in shell height decreases the turbulence levels above the canopy of the bivalve bed, and these turbulence levels correspond with the measurements of two flume studies. The precise influence of a variable bed on the simulated turbulence levels is unknown. The results of this model can be circumstantial results, originating form coincidences which have a positive effect on the simulations. However, it is also very likely that these results are a direct effect of the variable bed and that the model reduces the turbulence, because the flow is partly obstructed by the bivalves and the turbulence is generated at different depths (See Figure 4.5). As a consequence, more research needs to be done to this phenomenon, both experiments as modeling. The best method is to integrate experiments with modeling. Firstly, with experiments the effect of variable cylinders heights on the flow can be determined and with these experiments the results of the model (in this study) can be verified.

The results of the experiments can be simulated with a model and used as validation for the model. With this model the processes around a variable cylinder bed can be better understood.

5 Results hydro- and sediment-dynamics

The influence of mussels and oysters on the hydrodynamics was determined in Section 4 and these bivalves have been implemented in Delft3D with the 3D rigid vegetation model. These models have been calibrated and validated with measurements of two flume studies. Subsequently, these models are implemented in a larger scale 3D model to determine the influence of mussels and oysters on the hydro- and sediment-dynamics on a tidal flat. The results of this field model (including sediment dynamics) are presented in this section.

5.1 Reference model (bare bed)

The mussel and oyster patch are located in the center of the model and the conditions at this location should be similar as conditions found in the field (see Section 2.1.1 and 2.1.2). Figure 3.3 presents the conditions for the two types of sediments, namely cohesive and non-cohesive sediments. The hydrodynamic forcing is identical in both environments. The mussel and oyster bed is imposed to a bidirectional tidal flow, which changes every 6 hours in direction. The maximum flow velocity is 0.5 m s^{-1} and corresponds with the maximum flow velocity of many mussel beds in the Wadden Sea (Brinkman et al., 2002).

The maximum suspended sediment concentration (SSC) of cohesive sediment is $\pm$ 0.05 kg m^{-3} at a distance to bottom (z) of 10, 75 cm and 137 cm (Figure 5.1C), corresponding with the uniform SSC in the Wadden Sea (Postma, 1981; Van Loon, 2005). The SSC profile in the Wadden Sea is uniform due to the high turbulence and low water depths. The SSC for non-cohesive sediments is not uniform due to the large settling velocity of these sediments and the largest concentrations are found near the bed. The settling velocities of cohesive and non-cohesive sediments are 0.50 mm s^{-1} (Paarlberg et al., 2005; Van Ledden, 2003) and $\pm$ 23.5 mm s^{-1} (based on Van Rijn (1993)), respectively. The highest SSC's occur during high flow velocities, because high (near-bed) velocities results in high bed shear stresses and these stresses can initiate sediment transport. Moreover, the sediments have less time to settle to the bottom during high flow velocities.

Figure 5.1E presents the cumulative sedimentation for a bare bed with cohesive sediments. There is a deposition during small flow velocities and erosion during high flow velocities. The high flow velocities do not have enough force to erode all the deposited sediments resulting in a net sedimentation on the tidal flat corresponding with a tidal flat in the summer (Janssen-Stelder, 2000). The cumulative sedimentation during the tidal cycle is harmonic, because the sedimentation pattern during flood is the same as the sedimentation pattern during ebb. This perfect harmonic accumulation is a result of the choices regarding the model. The cumulative sedimentation above a bare bed is 0.25 mm day^{-1} for cohesive sediments and is uniform in the area of interest (the center of the model).

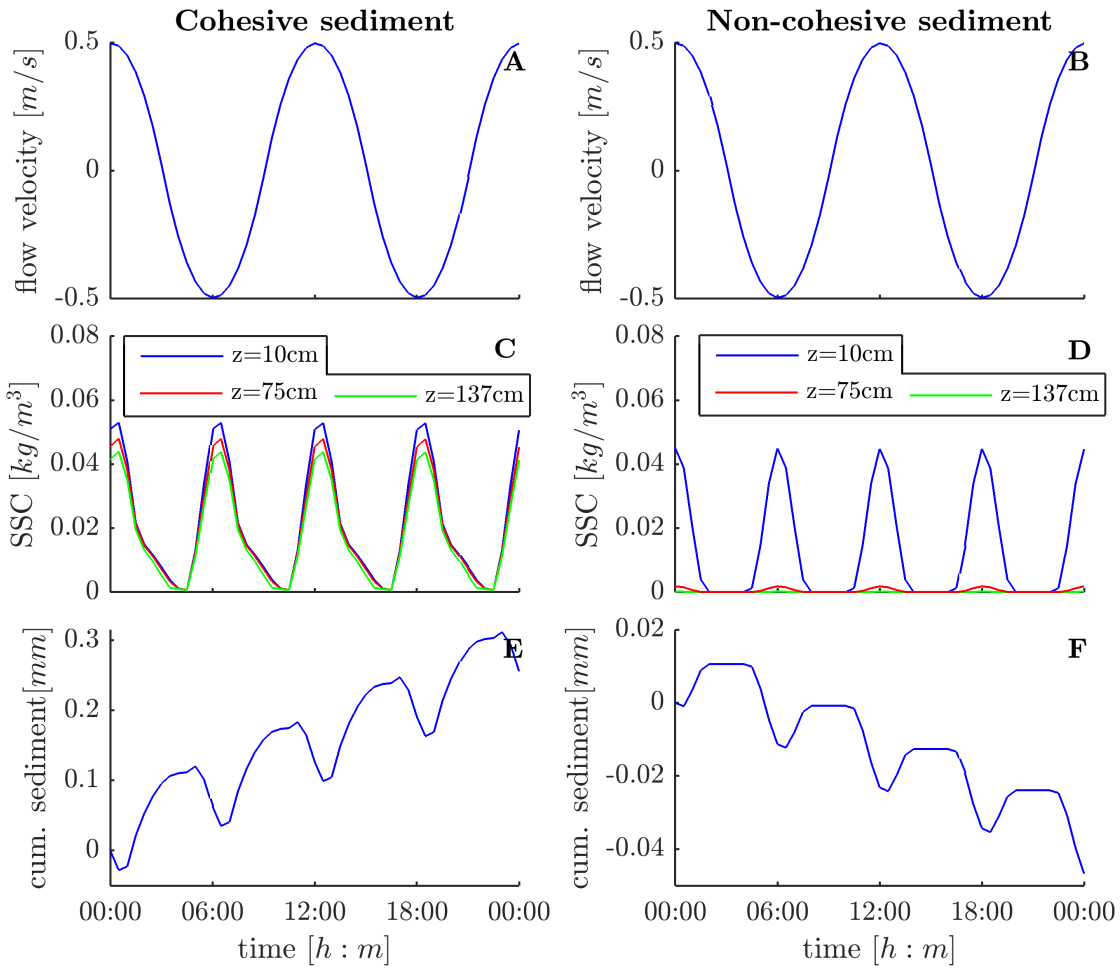

Fig. 5.1. The flow velocity, SSC and cumulative deposition in the center of the model during a tidal cycle of 1 day. (A), (C) and (E) represent a cohesive environment, while (B), (D) and (F) represent a non-cohesive environment.

The net erosion on a tidal flat with non-cohesive sediments is 0.05 mm day^{-1} (see Figure 5.1F). There is net erosion on the tidal flat due to model choices. Non-cohesive sediments are not transported into the model, because it is very hard to determine the boundary conditions for this type of sediment. Hence, the model domain is large and the sediments can be picked up from the bottom and transported through the model domain. The SSC can adjust to the flow conditions due to the large model length. This approach is more convenient to model non-cohesive sediments (and is similar as the approach of Borsje et al. (2014). The cumulative erosion is uniform in the area of interest (the center of the model).

5.2 Reference model (bivalve bed)

The influence of a mussel and oyster bed on the hydrodynamics on a tidal flat is presented in this section. The parameter settings of the mussel and oyster bed are presented in Table 3.1. The mussel and oyster bed have a dimension of 20 by 20 m and these bivalve beds are placed in the center of the model (see Figure 3.3). Hereafter, the influence of a mussel and oyster bed on the sediment dynamics is determined.

5.2.1 Hydrodynamics

A mussel and oyster bed have an effect at the front, the lee and the left and right side of a bivalve patch. The influence of a bivalve patch on the hydrodynamics is clearly visible; the patch has a stabilizing and destabilizing effect on the environment (Figure 5.2). The horizontal flow velocity above a bare bed is 0.35 m s^{-1} at a height of 5 cm from the bottom. The flow inside the bivalve patch is strongly reduced and this reduction is more pronounced inside an oyster bed compared to a mussel bed due to the higher total resistance force of oysters (Figure 5.3).The flow velocity above the oyster bed is also more reduced in comparison with a mussel bed (Figure 5.4). The velocity in the upper part of the water column is similar for a mussel and oyster patch.

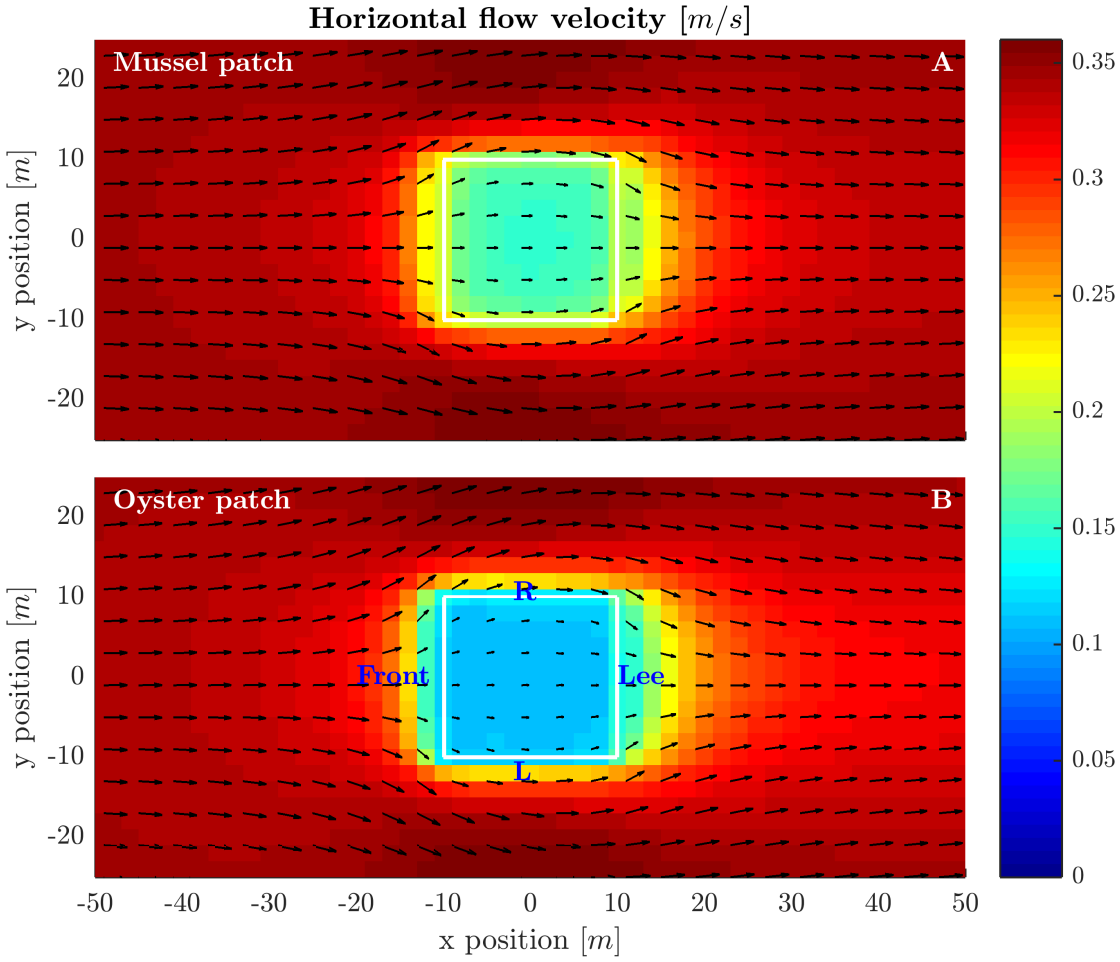

Fig. 5.2. The interaction between a mussel and oyster patch of 20 by 20 m and the environment. Top view of the horizontal flow velocity (m s^{-1}) at the height of z = 4.5 cm from the bivalve bed. (A) represents the mussel bed and (B) represents the oyster bed. The white framed box indicates the location of the bivalve bed. The arrows indicate the velocity vectors (u and v) strength and angle. The cross-patch velocity component (v) is multiplied by a factor of 5 for visualization purpose.

According to Figures 5.2 and 5.3, there is a clear interaction between the bivalve patches and the environment. The flow velocity inside the bivalve patches is low due to the obstruction of the bivalves; consequently more water flows in the upper part of the water column and around the bivalve patch. The flow velocity reduces in front of the patch due to flow routing. Hence, more water flows around the patch; the hydrodynamic forces at left and right (LR) sides of the bivalve patch increases. From now on, the left and right (LR) side of a bivalve patch referred to the position relative to y = 0 m. The front and lee side referred to the direction of the flow

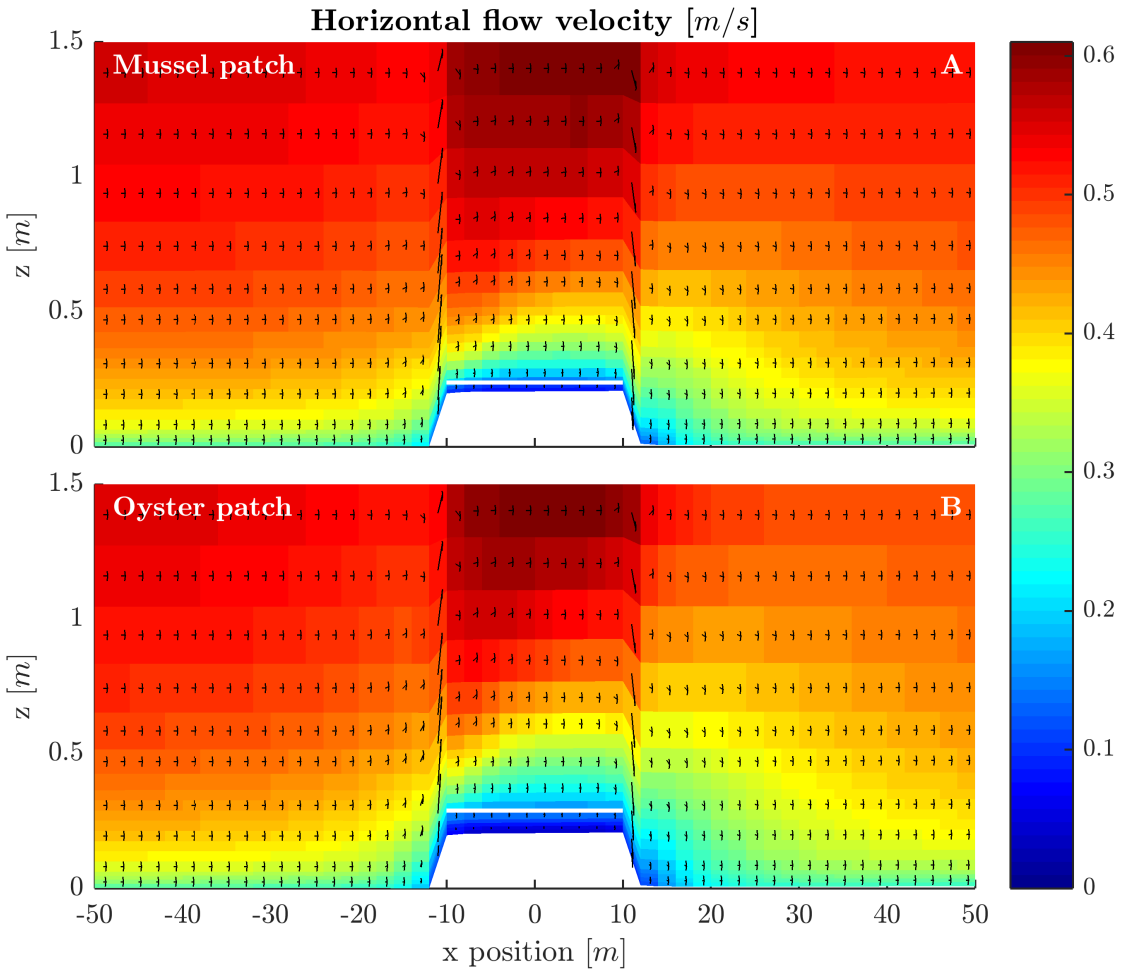

Fig. 5.3. The interaction between a mussel and oyster patch of 20 by 20 m and the environment. Side view of the horizontal flow velocity (m s^{-1}) in the center of the patch (y = 0 m). (A) represents the mussel bed and (B) represents the oyster bed. The white framed box indicates the location of the bivalve bed. The arrows indicate the velocity vectors (u and v) strength and angle. The vertical flow velocity component (w) is multiplied by a factor of 5 for visualization purpose.

(position relative to x = 0 m) (see also Figure 5.2B). Close to the bivalve bed (at the LR side edges) the flow experiences the large roughness of the patch and is reduced. The hydrodynamic conditions are calmer at the lee side of the patch, because less water flows over the patch leading to lower flow velocities behind the patch. The effect of a bivalve patch on the horizontal flow velocity (at the lee side) can be several hundreds of meters.

An oyster patch has a larger total resistance force compared to a mussel bed; consequently, less water flows over the oyster patch and more water is forced around the oyster patch (Figure 5.4). Flow routing is even at 90 meters from the oyster patch visible (in latitudinal direction). The flow velocities directly around the oyster bed are lower and the zone behind the oyster patch is calmer and larger in comparison with the mussel bed. The effect of oysters on the horizontal flow velocity can be seen at least 300 m behind the patch. However, the largest differences between flow velocities occur directly behind the patch (several tens of meters).

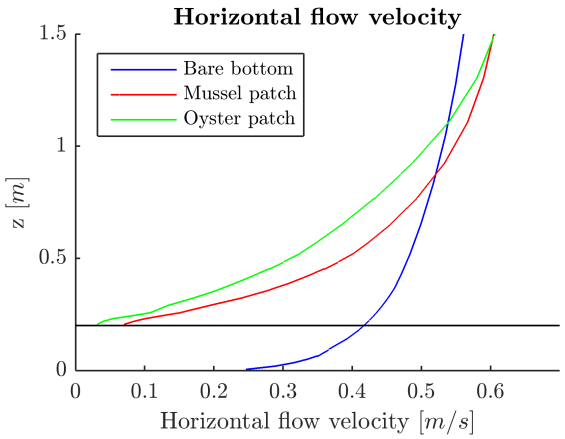

Fig. 5.4. The horizontal flow velocity (m s^{-1}) in the center of the patch (x = 0 m and y = 0 m). The black line indicates the base height of the bivalve bed.

5.2.2 Sediment dynamics

Mussels and oysters have a significant influence on the hydrodynamics above and around their patches; as a consequence they have also an influence on the sediment dynamics. The transport of sediment is determined with the bed shear stress (both for cohesive and non-cohesive sediment) (see Section B.3). If the bed shear stress is higher than the critical bed shear stress, sediment is transporter in the direction of the flow. As explained in Section C.2.5, bivalves absorb a large part of the bed shear stress with their physical structure. The shells reduce the flow near the bed and the bed shear stress on the sediment (inside the patch) is reduced. The bed shear stress on the bare bed is 0.69 N m^{-2} in the center of the model during the maximum velocities of the tidal cycle. This bed shear stress is higher than the critical bed shear stress of the sediment; consequently the sediment is eroded during the higher velocities.

Mussels and oysters can significantly reduce the bed shear stress on the sediment between their shells (see τ_{bed} Figure B.2). The maximum shear stress on the sediment inside a mussel and oyster patch (in Figure 5.5) is 0.06 and 0.012 N m^{-2}, respectively (in the center of the patch). The shear stress inside an oyster bed is lower than the stress inside a mussel bed, because the oysters reduce the near-bed velocity more due to the higher shell height. The shear stress in a bivalve bed are significantly lower than the critical bed shear stress of cohesive (0.5 N m^{-1}) or non-cohesive sediment ($\pm$ 0.17 N m^{-2}) (Berenbrock and Tranmer, 2008). Consequently, the bed shear stress is too low to erode the sediment between the shells. Hence, there is no erosion inside a bivalve patch for a maximum current velocity of 0.5 m s^{-1}.

Besides, a bivalve patch can have a large influence on the sediment dynamics around their patch due to their influence on the hydrodynamics (Oost, 1995). The edges around a bivalve patch have lower bed shear stress due to the obstruction of the flow (and the large roughness of these patches). The shear stresses around an oyster patch are higher than the shear stresses around a mussel patch and this is conforming to the presented horizontal velocity. Moreover, the shear stresses in front and at the wake of the oyster bed are lower in comparison with the mussel bed. The bed shear stress behind the oyster patch is reduced for a longer length (Figure 5.5); the effect of oysters on the bed shear stress can be noted at 300 m behind the patch. The bed shear stress is 0.65 N m^{-2} after 120 and 200 m for mussels and oysters, respectively. The biggest reduction of the bed shear stress occurs within these length scales. The large influence of mussels

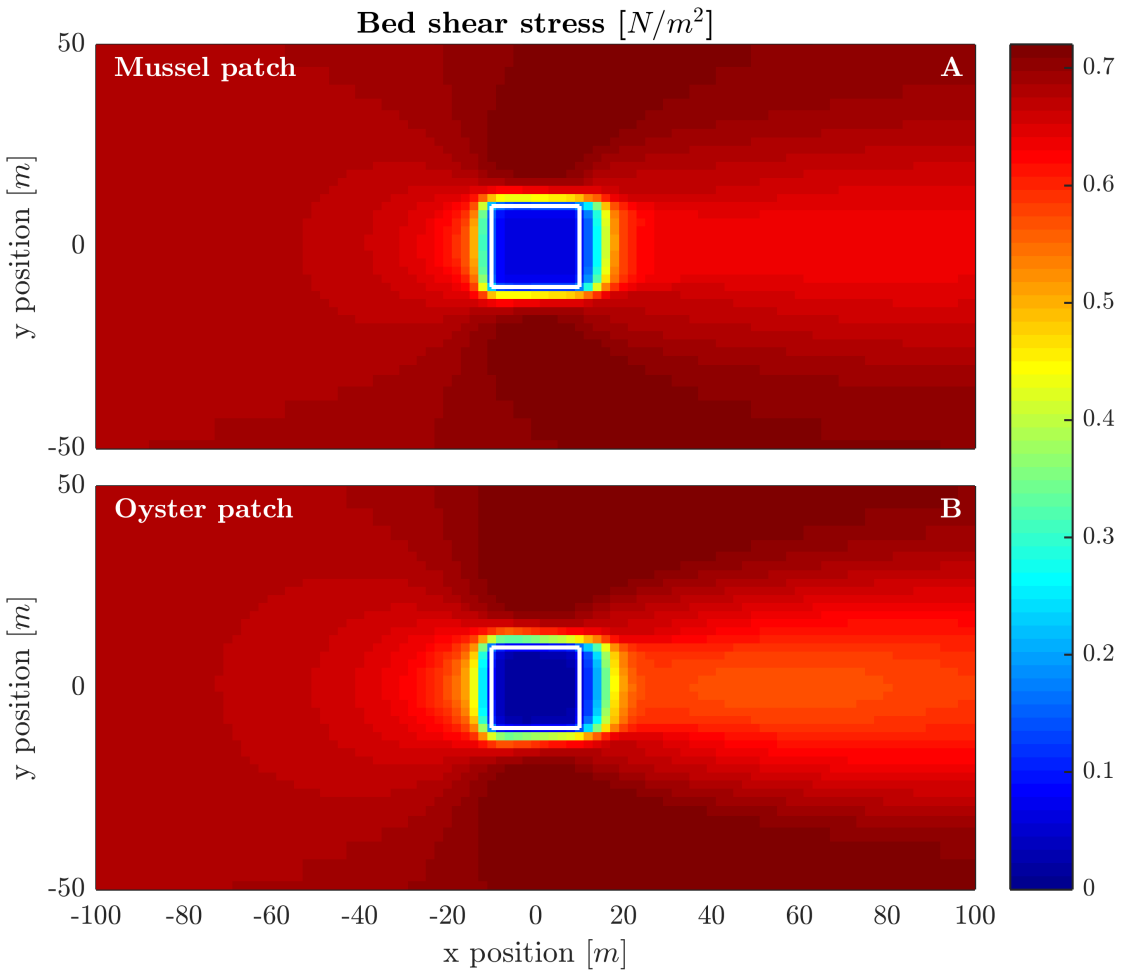

Fig. 5.5. The bed shear stress inside and around a bivalve bed. (A) represents the mussel bed and (B) represents the oyster bed. The white framed box indicates the location of the bivalve bed.

and oysters on the flow velocity and bed shear stress results will have an effect on the sediment dynamics in and around the patches. The influence of a mussel and oyster patch on the sediment dynamics have been tested for two cases, namely a cohesive environment and a non-cohesive environment.

Cohesive sediment

Sediment is accumulated inside the bivalve patch in a cohesive environment due to the velocity reduction inside the patch. Figure 5.6 presents the cumulative erosion/sedimentation after two days in a cohesive environment. The net accumulation of sediment in the center of the mussel and oyster patch is 2.5 mm day^{-1} and 1.6 mm day^{-1}, respectively. In contrast, the average sedimentation for cohesive sediment is 0.25 mm day^{-1} in the center of the model with a bare bed and is uniform in the area of interest. The estimated sedimentation rates per month are 75 and 48 mm month^{-1} for a mussel and oyster bed, respectively. The accumulation rates of mussels corresponds reasonably well with the literature, while the accumulation rates of oysters are not realistic if these rates occur consecutive (Dankers et al., 2004a; Reise, 1998) (see Section 5.2.3).

These rates correspond with the expectations, because the maximum bed shear stress was low compared to the critical bed shear stress. Sediments that settle inside the bivalve patch are trapped

and cannot erode during a maximum tidal flow velocity of 0.5 m s^{-1}.The higher accumulation rates inside the mussel patch can partly be related to the filtration rate of mussels and partly be related to the availability of sediment above a mussel patch. The filtration rate increases the flux of sediment towards the mussel bed (simulating the deposition of the (pseudo)faeces of mussels) and more sediment will settle inside the mussel bed. The flow velocity above the mussel patch is higher in comparison with the velocity above an oyster patch (due to the smaller total resistance force of a mussel bed); more sediment is transported leading to a larger availability of sediment above the mussel patch.

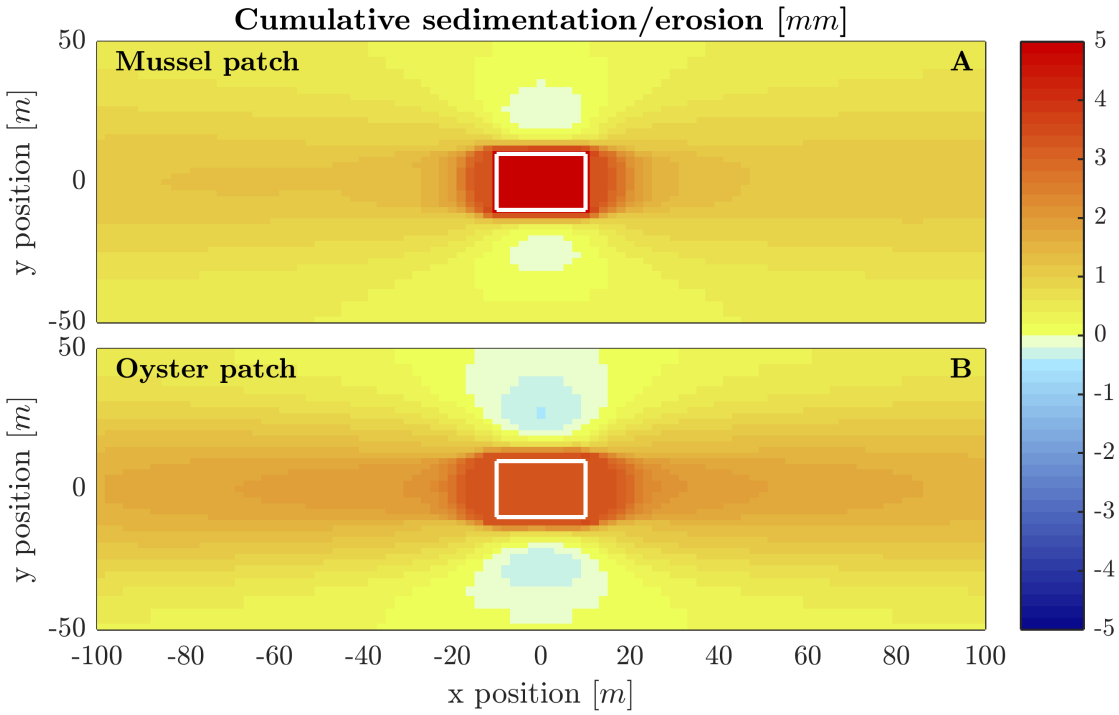

Fig. 5.6. The cumulative sedimentation/erosion inside and above a mussel bed (A) and oyster bed (B) after two days in a cohesive environment. The white framed box indicates the location of the bivalve bed.

There is also a clear pattern visible around the bivalve patches. The sedimentation patterns show a symmetric effect and this effect is a consequence of model choices. The model has a symmetric tide, so the flow velocities during flood are equal to the flow velocities during ebb. The reduced bed shear stress behind the oyster patch leads to a net accumulation of sediment in this area, while the increased bed shear stress at the LR side of the bivalve patch results in erosion. The flow velocities in front and at the lee side of an oyster bed are more reduced compared to a mussel patch. At the same time, the flow velocities at the LR side of an oyster patch are higher compared to a mussel patch. These effects can also been seen in the net sedimentation/erosion around a mussel and oyster patch. The net sedimentation is larger at the lee side of the oyster bed and the net erosion is larger at the LR side of the oyster bed (in contrast to the mussel bed).

Non-cohesive sediment

Sediment is also accumulated inside the bivalve patch in a non-cohesive environment due to the velocity reduction inside the patch. The net sedimentation and erosion patterns of non-cohesive sediment around a mussel and oyster bed are presented in Figure 5.7. The settled non-cohesive sediments are also trapped inside the bivalve bed, because the bed shear stresses are too small to erode the sediment. The net sedimentation in the center of the mussel and oyster bed is 1.8

and 1.3 mm day^{-1}. On the other hand, the average erosion for non-cohesive sediment is 0.05 mm day^{-1} in the center of the model with a bare bed and is uniform in the area of interest. The sedimentation rates per month are estimated at 54 and 39 mm month^{-1} for a mussel and oyster bed, respectively. The accumulation rates of mussels corresponds reasonably well with the literature, while the accumulation rates of oysters are not realistic if these rates occur consecutive (Dankers et al., 2004a; Reise, 1998) (see Section 5.2.3).

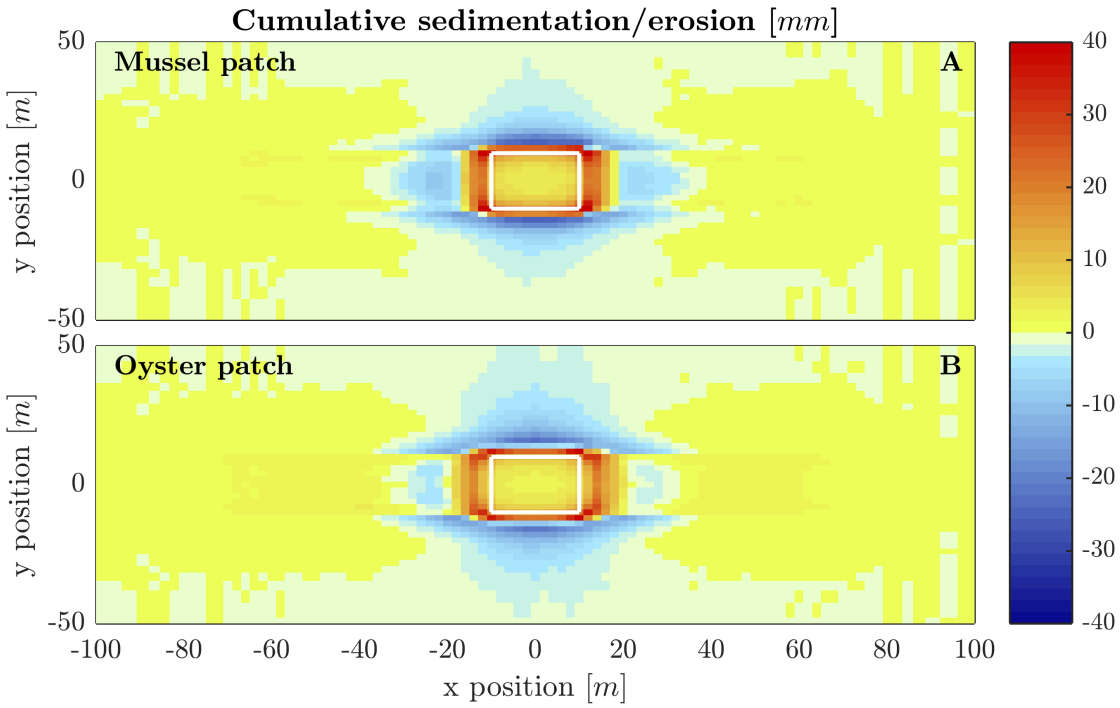

Fig. 5.7. The cumulative sedimentation/erosion inside and above a mussel bed (A) and oyster bed (B) after two days in a non-cohesive environment. The white framed box indicates the location of the bivalve bed.

The water is forced to flow around the patch due to the obstruction of the flow. A part of the flow is forced over the bivalves while the other part is forced to flow around the patch. The influence of flow routing is clearly visible on the erosion rates at the LR side of the patch. There is a net erosion of sediment at the LR side due to these higher flow velocities. An oyster bed obstructs the flow more than a mussel bed and more water flows around the oyster bed causing higher flow velocities and bed shear stresses (Figure 5.2 and 5.5). Consequently, there is a larger erosion area at the LR side of the oyster patch. In contrast, more water flows over the mussel patch due to the smaller total resistance force of mussels causing higher velocities above the mussel bed (see Figure 5.4). More sediment is transported with these higher velocities and a larger part of these sediments settle in the mussel patch leading to a slightly higher sedimentation inside the mussel patch (in comparison with the oyster patch). The influence of the filtration rate of mussels on the sediment transport of non-cohesive sediments is low, because the filtration rate is 0.25 mm s^{-1}, while the settling velocity of non-cohesive sediment is 23.5 mm s^{-1}. A large settling of sediments occurs also just in front of the patch (the flow velocity just in front of the patch is very low due to the obstruction of the flow by the higher bivalve bed).

Net erosion takes place close to the lee side of the patch (at x = $\pm$ -20 and 20 m) as a results of the sudden increase in bed shear stress behind the bivalve patch. The flow must adapt to the sudden change in the water depth and gains speed as it propagates away from the patch (see

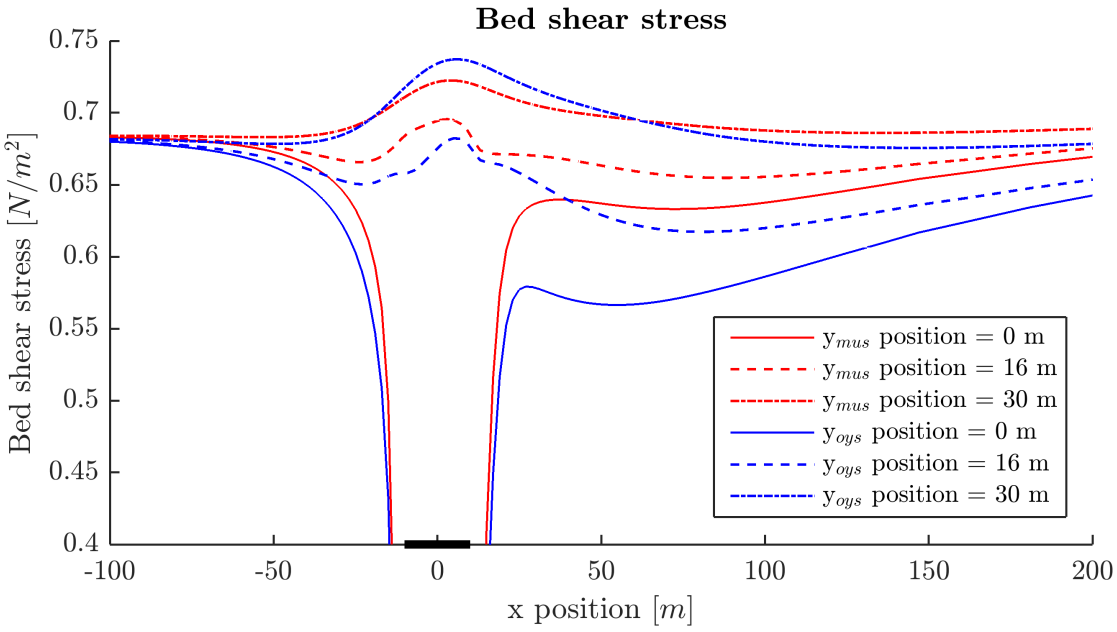

Fig. 5.8. A side view of the bed shear stress around a mussel and oyster bed in the center of the patch (y = 0 m), at the gully (y = 16 m) and at the right side of the patch (y = 30 m). The black line indicates the location of the bivalve bed.

Figure 5.2). The bed shear stress increases strongly due to the larger flow velocity and on the point that the bed shear stress exceeds the critical bed shear stress sediment transport occur leading to a net erosion of sediment. Figure 5.8 reveals the strongly increased bed shear stress behind the bivalve patch (at x = $\pm$ 20 m). Moreover, the water column directly behind the patch is depleted from sediment, because a large part of sediment particles have settled inside the patch. So, hardly any sediment settles behind the patch to counteract the effect of this erosion. Mussels have a larger effect on the erosion at the lee side of the patch, because the velocities above and behind the patch are larger resulting in higher bed shear stresses (see Figure 5.3 and 5.8). The erosion at the lee side of the mussel patch is from 10 till 30 m, while the erosion at the lee side of the oyster patch is from 10 till 20 m.

The erosion at the LR side edges of a mussel patch is larger in comparison with an oyster patch due to the larger flow velocities above and close around the patch. The velocities around a mussel patch are higher thanks to the smaller total resistance force of the mussel bed (Figure 5.2); consequently the bed shear stress is higher and more erosion occurs at the LR side edges of the mussel bed (Figure 5.8). In contrast, the water flows further around the oyster patch in comparison with the mussel patch leading to a larger erosion zone at the LR side. Lastly, there is a small sedimentation of a few mm at the lee side of both patches (yellow areas in Figure 5.7) due to the slightly calmer hydrodynamic conditions at the lee side of the patch.

5.2.3 Relating results to other studies

The sedimentation rates of the mussel bed correspond reasonably well with the sedimentation rates of a (young) mussel bed during the summer. According to Dankers et al. (2004b), a mussel bed can rise 30-40 cm in four months. The simulated accumulation rates in an oyster bed are higher in comparison with the sedimentation rates found in the field. The sedimentation rates of

the oyster bed are too high and the oysters will suffocate if these rates occur for a month or more (Reise, 1998).

Van Leeuwen et al. (2010) found similar sedimentation rates in and around a mussel bed in a cohesive environment as this study. The net sedimentation inside a mussel bed is 10 cm in 60 days, while the net sedimentation in this study is 4.91 mm in two days for cohesive sediment ($\pm$ 15 cm in 60 days). The net sedimentation rates, according to Van Leeuwen et al. (2010), are lower due to lower SSC of the ebb flow. The simulated sedimentation patterns around the mussel bed are similar to the sedimentation patterns of Van Leeuwen et al. (2010). There is a net sedimentation in the wake of the mussel patch, while there is less deposition at the left and right side (relative to the flow direction) of the patch.

The bed shear stress patterns found in this study are comparable with the bed shear stress patterns around a high density bamboo patch (in the field) (Bouma et al., 2007). They found a reduction of the bed shear stress in front of the patch, while the bed shear stress slightly increased at the sides of the bamboo patch. Behind the patch there is a large reduction of the bed shear stress and this effect is similar behind bivalve patches. These stress patterns lead to similar erosion and sedimentation patterns around these bamboo patches. Erosion occurs at the left and right side of the bamboo patch in a sandy environment due to this increased bed shear stress (Bouma et al., 2007).

Walles et al. (2014) investigated the relationship of natural Pacific oysters and the morphological changes in the intertidal soft sediment environments. The oyster reefs showed an elevated area connected to each reef at the lee side of the patch as a result of the reduction of tidal currents and wave energy. According to the results in this study, there is also sedimentation at the lee side of the patch (especially in a cohesive environment). Sedimentation occurs in this model at both (lee) sides due to the bidirectional tidal flow and the absence of waves. Waves increase the hydrodynamic forces above and around a bivalve patch and these increased forces can result in different sedimentation patterns. Waves have often a dominant direction and there is often a net accretion of sediment at the lee side of of this dominant wave direction. According to the results in this study, currents can contribute to the net accretion of sediment behind a patch if the wave and current have the same (dominant) direction. If the current and waves are normal to each other, the sedimentation (erosion) caused by currents and waves can counteract each other, leading to less sedimentation.

5.3 Conclusions of the field model

The model presents the fine sediment dynamics (cohesive and non-cohesive) on a subtidal flat for (calm) summer conditions. There is a small net sedimentation in a cohesive environment, corresponding with the summer conditions on a tidal flat and a small erosion in a non-cohesive environment due to model choices. The hydrodynamic forces are idealized and these forces correspond with the forces found around mussel and oyster beds in the field. The erosion and sedimentation are uniform in the area of interest.

There are high sedimentation rates inside a mussel and oyster bed, moreover, sedimentation occurs at the lee side of the bivalve patch due to calmer flow conditions. The resistance of a mussel and oyster bed slows down the near-bed velocity and increases the deposition of sediment. Sediment that settles inside a bivalve patch is trapped and cannot erode with current velocities

of 0.5 m s^{-1}. The production of heavy faeces by mussels increases the deposition of sediment inside the mussel bed as well. The flow velocities at the LR side of the mussel and oyster patch increases as a result of flow routing, leading to erosion (or less deposition) at these sides.

The flow velocity, bed shear stress and sediment transport patterns of a mussel bed and oyster bed are similar. Mussels have a smaller total resistance force and a higher filtration rate in comparison with oysters. These differences result in higher sedimentation rates inside the mussel patch and less flow routing around the mussel patch. The flow velocities close to the LR side edges are higher due to the smaller total resistance force mussels, while the flow velocities further away from the LR side are lower in comparison with an oyster patch. The bed shear stress inside an oyster bed is significantly lower than the bed shear stress inside the mussel bed as a result of the higher total resistance force of the oysters.

5.4 Sensitivity analysis

The effects of mussels and oysters on the hydro- and sediment-dynamics on a tidal flat is determined for a pre-defined set of parameters and these parameters are based on several studies, such as Brinkman et al. (2002) and Van Ledden (2003). The sensitivity of the model to these parameters has been determined. The parameters are the flow velocity, the height of the bed, the density, the height of the shells and the filtration rate. The influence of these parameters on the bed shear stress and cumulative erosion/sedimentation in the center of the bivalve patch is also presented in Table C.1 and C.2. The results of the sensitivity analysis with an extended discussion are presented in Appendix C.2.

According to the implementation of mussels and oysters in this model, currents have no negative feedback at the sedimentation inside the model, because the bed shear stress never exceeds the critical bed shear stress Therefore, there must be other factors that can lead to erosion of the sediments between the bivalve shells and these factors are discussed in Section 6. Decreasing the height of the mussel or oyster shells is promising for modeling studies where the influence of currents and waves on the sediment dynamics around a bivalve patch is determined. The velocity and turbulence patterns above a bivalve patch with a decreased height are similar to the reference model, while the bed shear stress on the sediment between the shells significantly increases. Moreover, only two parameters have a significant influence on the cumulative sedimentation/erosion in and around the bivalve patches, namely the flow velocity and the filtration rate (taking into account that erosion cannot occur).

6 Discussion

The influences of mussels and oysters on the hydro- and sediment dynamics have been determined for the first time with a 3D model. The characteristics of these mussel and oyster beds are based on previous studies; moreover, previous studies have been used to calibrate and validate the hydrodynamics above a mussel and oyster bed. The calibrated and validated parameters representing a mussel or oyster bed are used for the implementation of these bivalves in a sediment dynamic model. This model represents these bivalve beds on a subtidal flat for a summer condition. The simulations show that sediment inside a bivalve patch cannot erode for a variety in flow velocities, bed heights, shell heights, densities and filtration rates.

6.1 Methodology

A mussel and oyster bed has been implemented in Delft3D, hereby several assumptions and model choices have been made. These assumptions and model choices can have an effect on the results of this model. These assumptions and model choices have been presented and defended in previous sections in this report; however some important assumptions will be discussed in this section.

6.1.1 Waves

A mussel and oyster bed has been implemented in Delft3D for (calm) summer conditions. The current velocities are the dominant processes of sediment transport during these summer conditions in comparison with waves (Janssen-Stelder, 2000); waves are therefore neglected in this study. However, small waves occur also in the summer and can increase the bed shear stress inside (and outside) the bivalve patch. On the other hand, the bed shear stress has been varied from 0.32 up to 1 N m^{-2} (on a bare bed) by varying the flow velocity between 0.3 and 0.6 m s^{-1} (see Appendix C.2). Despite the large variation of shear stresses on a bare bed, the bed shear stress inside a bivalve patch never exceeds the critical bed shear stress. The bed shear stress inside a bivalve bed varied from 0.028 up to 0.086 N m^{-2} and from 0.006 up to 0.016 N m^{-2}, for a mussel and oyster bed respectively. Even at a maximum tidal flow velocity of 1 m s^{-1} (with a bed shear stress of 2.7 N m^{-2} on a bare bed), the bed shear stress inside the mussel and oyster bed is below the critical bed shear stress (see Section 5.4). The bed shear stress inside an oyster bed is lower than the bed shear stress inside a mussel bed due to higher shell length of oysters. A reduction of the density or shell height will not result in erosion due to exceeding of the critical bed shear stress.

Oyster beds cannot survive large consecutive sedimentation rates and it appears that there is a missing process, because there is no negative feedback between a bivalve bed and sedimentation (even at high current rates, low densities and low shell heights). Waves are probably the missing link between a bivalve bed and erosion. Donker (2015) and Drost (2013) measured the hydrodynamic forces, including waves, on a mussel bed in October and November. They

concluded that waves can have a large impact on a mussel bed in this period. This period has (normally) rougher conditions than during the summer. The total bed shear stress induced by waves has a contribution of 60 to 80% of the total bed shear stress (based on a measurement campaign in October 2011 of Drost (2013)). The total bed shear stresses induced by waves are between 0.6 and 2.5 N m^{-2}. The total bed shear stress is the stress forced on the bed, so the total shear stress on the shells and sediments. These total bed shear stresses induced by waves are high enough to erode the sediment between the shells (if these stresses are (for a big part) forced on the sediments). The total bed shear stress (waves and currents) varied between 0.6 and 3 N m^{-2}, and this corresponds with the variation of the bed shear stress induced by currents (on a bare bed) in our model.

According to this study, currents cannot erode the sediment inside a bivalve bed. Waves can presumably penetrate a bivalve bed better than currents; consequently, waves can probably increase the bed shear stress on the sediment inside the bivalve bed more and erode this sediment. Bed shear stresses induced by waves must increase the bed shear stress on the sediment between the shells more in comparison with currents; otherwise this sediment cannot erode, because the largest shear stresses, induced by currents, cannot erode this sediment either. The (precise) influence of waves on the hydrodynamics and sediment dynamics inside a bivalve bed is not known and further research is needed.

Besides, waves have also an influence on the sedimentation patterns around a bivalve bed. Walles et al. (2014) investigated the relationship of natural Pacific oysters and the scale of morphological changes in the intertidal soft sediment environments. The reefs showed an elevated area connected to each reef and this area has a linear relationship with the reef surface area. The elevated areas of the reefs were always located at the lee side of the wave/current direction, corresponding with the results in this study. The net sedimentation in this study occurs at the both (lee) sides due to the bidirectional tidal flow. According to the results in this study, currents can contribute to the net accretion of sediment behind a patch if waves and currents have the same (dominant) direction. If the current and waves are normal to each other, the sedimentation caused by currents and waves can counteract each other, leading to less sedimentation. The influence of waves on the sedimentation and erosion inside and outside the patch can be investigated with a modelling study using a wave model, for example SWAN.

6.1.2 Boundaries

The effect of mussel have been investigated for a variety of conditions, however these conditions were varied for an idealized model. This idealized model gives a first insight into the influence of these conditions on the flow patterns and sedimentation/erosion patterns. Several assumptions have been made, for example the mussel and oyster bed is placed in a subtidal area and the hydrodynamic conditions are harmonic. The field model can be improved by more realistic bathymetry and boundary conditions.

The model predictions are limited to simulations in a flow dominated tidal environments. This corresponds with the natural habitat of mussels and oysters (Troost, 2010), however there are also mussel and oyster beds in the intertidal environment. The model cannot accurately simulate the intertidal environment, because the drying and flooding of grid cells generate numerical problems if the gradient in bed level is quite large (Borsje, 2014). This gradient in bed level is quite large around mussel and oyster beds. A bivalve bed on a intertidal flat can result in less

sedimentation, because the submersion time is reduced and less sediment can settle. However, the drying and flooding of the tidal flat can result in relative high flow velocities and result in erosion.

The hydrodynamic conditions in the model are perfect harmonic; the conditions during flood are identical to the conditions during ebb (including the suspended sediment concentration (SSC). This is an simplifications of reality, because tides are normally asymmetric on intertidal flats such as the Wadden Sea (Van Ledden, 2003). For example, the incoming tide can have higher flow velocities, including higher SSC due to a scour lag, than the outgoing tide. Cohesive sediment can easily kept in suspension, however once cohesive sediment has settled it is difficult to erode. As a consequence, an incoming tide can contain more sediment than the outgoing tide. An asymmetric flow velocity and SSC can result in different accumulation and erosion rates in and around a bivalve bed. For example, the accumulation at the lee side relative to the incoming tide can be higher due to a higher SSC compared to the lee side relative to the outgoing tide.

There is hardly any water elevation during the bidirectional tidal flow velocity and this can be included in a model. The absence of water elevation on the sedimentation and erosion of non-cohesive sediment is assumed to be low, because this type of sediment settles quickly and the SSC is low in the upper part of the water column. This absence of elevation on the sedimentation and erosion of cohesive sediment is also assumed to be reasonably low, because in the flow velocity is only 40 minutes below 0.1 m s^{-1}. The entire sediment fraction in the water column will not settle in this time period (only the sediment in lowest $\pm$ 1.2 m of the water column).

The model results can be more realistic by nesting this model in a larger scale model. The boundaries of the small scale model can be based on the flow conditions in the larger scale model resulting in more realistic boundary conditions of the small scale model. However, it is very hard to nest a small scale model in a larger model, because the nested model is sensitive to the bathymetry and boundary conditions. It is preferred to have one open boundary (and three close boundaries), moreover the open boundary should be in a channel (and should not cross a tidal flat) (Theo van der Kaaij, Personal communication). Such locations are not very common in the Wadden Sea (or other natural habitats of mussels and oysters). It is therefore difficult to make a model for a mussel or oyster bed location in the field.

6.1.3 (Pseudo)faeces

Mussels and oysters produce (pseudo)faeces during the filtration of water and these faeces have different characteristics as the initial sediment, especially the faeces of mussels. The (pseudo)faeces of mussels are heavy and contain high organic material. A part of these faeces settle inside the mussel bed, while the other part can be transported out of the mussel bed or even out of the tidal flat (Oost, 1995). The different characteristics of (pseudo)faeces of bivalves are not included in the model, because the effect of bivalves on the sediment is investigated in first place. Moreover, faeces are heavier than the (normal) sediment and the erosion of faeces is less likely than the erosion of the sediment, because the bed shear stresses inside the bivalve patch do not exceed the critical stresses of the (normal) sediment. The effect of sediment particles with the characteristics of (pseudo)faeces on the sediment dynamics in the bivalve bed is therefore minimal.

The implementation of the characteristics of faeces is more useful if sediment can actually erode from a bivalve bed. Consequently, the influence of several characteristics of (pseudo)faeces on the sediment dynamics can be investigated; examples of characteristics which can be varied are the settling velocity, the erosion rate and the critical bed shear stress of the pseudofeces. It is expected that the (pseudo)faeces of mussels have a large influence on the sedimentation inside the patch in comparison with oysters. These heavy faeces can eventually be crucial for the correct implementation of a mussel in a current and wave model. These faeces can determine if there is a net deposition inside the mussel patch. However, further research is needed to determine the effect of these heavy faeces on the net deposition in an environment with higher hydrodynamic forces.

6.1.4 Cohesive & non-cohesive sediments

The interaction between bivalves and the sediment dynamics has been determined for two types of environments, namely a cohesive and a non-cohesive environment. Each environment has only one sediment fraction. A cohesive environment is more difficult to erode than a non-cohesive environment (as can been seen from Section 5.2.2). An important parameter to distinguish the cohesive behavior is the mud content (fine sediment concentrations). If the fine sediment concentrations are high, the cohesive behavior is more dominant, while otherwise the non-cohesive behavior is more dominant (Van Ledden, 2003).

In this study, the cohesive processes or the non-cohesive processes are (completely) dominant.The cohesive or non-cohesive sediments are also not varied. Moreover, mussels are often located on areas with a high mud content (Oost, 1995) and the activity of mussels can be a cause of the high mud content in these areas (Flemming and Delafontaine, 1994). It would be interesting to investigate the influence of several sediment fraction (cohesive and non-cohesive sediment) on the sedimentation patterns. Moreover, it will be interesting to vary several parameters of the sediment, for example the mud content, the grain sizes and the spatial variation of the mud content (high mud content in and directly around a mussel bed and less mud content a bit further away from the mussel bed).

6.1.5 Patches

Mussel beds can occur in dense (uniform), patterned and isolated clusters, while oysters can occur in dense beds and isolated clusters. This study did research to the influence of a dense uniform mussel or oyster bed on the hydro- and sediment dynamics. The patterned and isolated bed patterns can reduce the sedimentation inside and outside the bivalve bed. According to Van de Koppel et al. (2008) the formation of patterns and clusters is the result of the depletion of food and the erosion due to waves and currents. Clustered and patterned bivalve beds are more resistance to waves and currents than individual bivalves, besides the decreased density of the bivalve bed results in more erosion (Widdows et al., 2002). Older mussel beds and oyster beds provide from erosion (less sedimentation), because older mussels are less mobile and oysters are immobile in comparison with young mussel beds.

The influences of currents on mussel patterns have been investigated by Van Leeuwen et al. (2010) and they found a small decrease in deposition if the bed had transverse stripes relative to the main flow direction. The amount of deposition is still too large for oysters and older mussel beds to survive. It would be interesting to investigate the influence of currents and waves on the sedimentation and erosion in and around a patterned bivalve bed.

This study used the 3D rigid vegetation model to implement mussels and oysters as rigid cylinders in Delft3D, because this model accounts for the reduced bed shear stress on the sediment between the bivalve shells. Another possibility is to model mussels and oysters as very large grains, it is hereby important that the bed shear stress on the sediment between the shells is reduced. In order to determine which model is the most representative measurements are needed to determine the size of the shear stresses on the sediment between the shells.

This model has been developed to represent cylinders with a high porosity ($\pm$ 95%). The model has its limitations regarding low porosities, as is the case for a bivalve bed. The porosity of mussels and oysters is approximately 65%, and this porosity is close to the limitations of this vegetation model, especially in case of oysters due to high drag coefficient and large diameters. Besides, a mussel and oyster bed can be seen as a bed with very large grains and a better approach could be to implement a mussel and oyster bed in a model which can account for these low porosities.

6.1.6 Climbing capacity of mussels

(Young) mussels can climb on top of the sediment and protect hereby the underlying sediment from erosion (Widdows et al., 2002). The climbing capability of (young) mussel beds is not included in the model. However, the model updates the bathymetry (including the mussel bed location) after a predefined time step, so the mussel bed follows the sedimentation and erosion of the bottom (in our case only sedimentation). Besides, the influence of this capability is assumed to be small, because the sedimentation and erosion is determined for a small period (2 days).

6.2 Results

This section presents the discussion of the results of the models and is divided in two parts, namely a section discussing the results of the flume model and a section discussing the result of the field model.

6.2.1 Flume model

The results of the flume model are discussed in this section, for example a disccusion about the influence of the measurements on the results.

6.2.1.1 Measurements

Several flume experiments have been conducted to determine the influence of mussels and oysters on the hydrodynamics. The quality of these flume experiments can be improved from the perspective of a modeling study. For example, the flow velocity and turbulence levels above an oyster bed are measured for relatively few measurement points. The turbulent kinetic energy (TKE) follows no clear pattern and the lack of data points will result in a higher uncertainty about this pattern. Moreover, the flow velocity has not been measured above a flat bottom (De Vries et al., 2012), so these results cannot be compared with the measurements and the model cannot be calibrated with the flow conditions of a flume with a bare bed.

Consequently, more measurements are needed to diminish the uncertainties of the measurements conducted by De Vries et al. (2012). These measurements must be compared with the calibrated results of the model and if necessarily the model must be adapted. However, it not expected that

these measurements deviate a lot with the results of De Vries et al. (2012) and it is expected that the model correspond reasonably well with an oyster bed, because the general flow patterns are described with this data set and this flow pattern is comparable with the flow pattern above a mussel bed.

The simulated bed shear stress inside the bivalve bed cannot be compared with measurements, because there is a lack of knowledge about the size of the shear stresses inside the bivalve bed. Measurements are needed to determine the bed shear stress on the sediment between the shells. Moreover, there is also a lack of measurements around the leading edge of the bivalve bed, over the longitudinal distance of the patch. The flume model can only be calibrated and validated against measurements at one location. The results of the flume study can improve if the model can be compared with the results at several longitudinal locations. Moreover, the models of this study (both flume as well as field model) have its limitations for modeling at a fine scale and the implementations of a bivalve bed. However, the velocity and turbulence profiles and the large scale trends of sediment dynamics inside and outside the bivalve patch can be determined with the presented model and these results can be related with flume and field experiments. In order to reduce the uncertainties of forthcoming measurements and model results it is recommended to combine measurements campaigns (for example field measurements and flume experiments) with modeling studies (Bouma et al., 2007).

From a modeling perspective, it is also important to measure the flow velocity in the entire water column, consequently the average discharge can be determined based on these measurements instead of the using an approximation method to determine the discharge, such as the law of the wall method.

6.2.1.2 Turbulence & variable shell height

A variability of the shell height of the bivalve bed is needed to represent the flow velocity above oyster beds and the TKE above mussel and oyster beds correctly. If the variability of the bed was reduced (smaller difference between the lowest and highest bivalve) the TKE increases (and otherwise). The precise influence of a variable bed on the simulated turbulence levels is unknown. Moreover, the influence of a variable bed on the TKE has not previously been described in other studies (to my knowledge). The results of this model can be circumstantial results, originating form coincidences which have a positive effect on the simulations. However, it is also very likely that these results are a direct effect of the variable bed and that the model reduces the turbulence, because the turbulence is generated at different depths and the flow is partly obstructed by the bivalves. As a consequence, more research needs to be done to this phenomenon, both experiments as modeling.

6.2.2 Field model

Several results of the field model are discussed in this section, for example the sedimentation and erosion inside the mussel and oyster bed, the filtration rate and the possible implementations of mussel and oyster beds.

6.2.2.1 Sedimentation/erosion inside mussel/oyster bed

Mussel are very mobile and can trap a lot of sediment with their climbing capability, especially young mussel beds. These (young) beds can rise 30 – 40 cm in a period of 4 months (Dankers et al., 2004a). This accumulation rates correspond with the sedimentation rates of the mussel

bed in the field model. Older mussel beds are less mobile and their climbing capability is reduced, these older mussel beds are more similar to oyster beds. Moreover, mussel and oyster beds do not rise higher than the mean sea level (Mcgrorty et al., 1993; Walles, 2015). Thence, oyster and older mussel beds must experience erosion to reduce the amount of deposited sediment. In contrast, the simulated bed shear stress inside a mussel and oyster bed are so low that erosion due to currents cannot occur.

The sedimentation rates of an oyster bed do not correspond with the sedimentation rates found in the field (Reise, 1998). The bed shear stress inside a bivalve bed is for a large range of flow velocities substantially lower than the critical bed shear stress and this implies a missing process, namely waves (see Section 6.1.1). Moreover, the shell height can have a significant influence on the bed shear stress (especially for an oyster bed) (see Table C.1). A change in shell height will not lead to a change in the velocity profile above a bivalve bed if the variation between the shell height is constant (see Section 4.5). A shell height reduction has a large effect on the bed shear stress on the sediment between the shells, because the bed shear stress increases significantly if the shell height decreases. This increase in bed shear stress can be essential for a successful implementation of a bivalve bed in a current and wave model.

Besides, the bed shear stresses inside a bivalve patch are underestimated by the model, because these stresses are based on the near-bed flow velocity (Equation B.17). The flow velocity is based on the continuity equation (Equation B.3) and this equation does not take the porosity of the bivalve patch into account (while the momentum equation does take the porosity into account). The flow velocity in the continuity equation is not increased due to a decrease in available space (see Section B.3.3). This flow velocity is the averaged flow velocity for that grid cell (without a decreased cross-section due to a partly blocked flow by bivalves) (Bert Jagers & Jan van Kester, personal communication). However, the bed shear stress will not increase so much that it will affect the results of this study, because these stresses will always be below the critical bed shear stress.

6.2.2.2 Filtration rate

The filtration rate of mussels has a large influence on the amount of deposition of cohesive sediment inside the mussel bed. The filtration rate varies over the time/season, due to variation in food availability and flow velocity (Jorgensen, 1996). The filtration rate is assumed to be constant over time in this study, because the mussel bed is modelled for a small time scale (2 days), the range of particle concentration is small and the flow velocity is larger than the critical velocity most of the tidal cycle (see Section 3.1.2.1). However, a variable filtration rate over time, for example due to less food availability during the night, could have an influence on the sediment dynamics above a mussel bed, because less faeces are produced, consequently less settlement of sediment.

The filtration rate can have a large variation and the influence of the filtration rate on the sedimentation of cohesive sediment is significant. The filtration rate has the largest influence on the sedimentation rate inside a bivalve bed compared to the other bivalve parameters. The filtration rate is included in Delft3D by an increased local settling velocity and is based on measurements of the clearance rate of mussels. The amount of biodeposition inside a mussel bed in a cohesive environment is therefore promising compared to the biodeposition found in field observations on a mudflat (Ten Brinke et al., 1995).

6.2.2.3 Protection of the coastal zone

It has been suggested that mussels and oysters can play a role in the protection of the coastal zone. Mussels and oysters can promote the settlement of sediment at the lee side of their patches and hereby protect the area behind from erosion. Moreover, mussel and oyster beds can decrease the wave action on the coast (Walles et al., 2014; Borsje et al., 2011). On the other hand, mussel and oyster beds can reduce the deposition or even promote erosion due to the increased flow velocities at the left and right side of the patch. Waves can amplify this effect of currents (if the dominant direction is similar as the dominant current direction) or can counteract the effects of currents. It is therefore important to study the effect of a bivalve bed on the sediment dynamics on a certain location, before a bivalve bed is implemented as part of the flood defence. For example, the erosion at the left and right side of a bivalve patch due to higher flow velocities can promote the wave action on the coast at these locations.

Mussels and oysters cannot protect large parts of the coast, because large bivalve patches suffer from food competition. The implementation of mussel and oysters as part of the flood defence can therefore only be locally. Mussels and oyster can for example take over the role of groins or revetments (Borsje et al., 2011). However, more research is needed to investigate the influence of mussels and oysters on the sediment dynamics if these bivalves are exposed on currents and waves.

Conclusion and recommendations

7

7.1 Conclusion

The aim of this study is: *To determine the different influences of mussels and oysters on the hydrodynamics and sediment transport on a patch scale by implementing the phenotypes of these bivalves in the process-based model Delft3D.* The conclusions of this thesis are given by answering the research questions.

How can mussel beds and oyster beds be implemented in the process-based model Delft3D?
A mussel and oyster bed has been implemented in a Delft3D model with the rigid 3D vegetation module. The mussel and oyster bed are presented in this module as rigid cylinders and this module accounts for the resistance force imposed by the bivalves on the flow. Moreover, this module accounts for the impact of the bivalves on the velocity momentum equation, the turbulent kinetic energy equation and the dissipation equation. One essential parameter for the implementation of a bivalve bed in Delft3D is the variability in shell (cylinder) height over the bivalve bed. A variable shell height is needed to simulate the flow velocity above the bivalve patch correctly, especially for oysters. Moreover, variability in shell height decreases the turbulence levels above the canopy of the bivalve bed, and these turbulence levels correspond with the measurements of two flume studies. The turbulence above a variable shell height is reduced, because the flow is partly obstructed by the bivalves and the turbulence is generated at different depths.

Mussels have an increased sediment flux towards the bed due to the production of heavy (pseudo)faeces. The heavy faeces of mussel are implemented in Delft3D by adapting the transport equation; the settling velocity above the bivalve bed is increased with an extra term, the filtration rate. The filtration rate is only imposed for the lowest 10-15 cm of the water column, because mussels can only filter the lowest part of the water column. The model represents a bivalve bed for summer conditions, it is assumed that the hydrodynamic forces imposed by the currents are dominant compared to the forces imposed by waves.

What is the influence of mussels and oysters on the hydrodynamics?
Mussels and oysters partly obstruct the flow and reduce hereby the flow velocities near the bed. The velocity gradient above the canopy of the bivalve bed is steep and the resistance force of the bivalves result in a turbulent kinetic energy peak at the top of the canopy. High turbulence levels results in a more mixed water column. Oyster decrease the flow velocity near and inside the bivalve bed more than mussels. The hydrodynamic model predictions showed good agreement with flume experiments for flow velocity adaptions above a mussel or oyster bed, while the TKE patterns above the bivalve beds correspond reasonably well with these data sets. The flow velocity at $z = 3$ cm from the bed is 0.020 m s^{-1} for a mussel bed and 0.011 m s^{-1} for oyster bed (for a free stream velocity of 0.15 m s^{-1}), while the velocity above a bare bed correspond with 0.08 m s^{-1} at $z = 3$ cm. The peak turbulence levels above a mussel and oyster bed are roughly similar,

$\pm$ 4 $\times$ 10^{-4} m^2 s^{-2} for mussels and $\pm$ 3.5 $\times$ 10^{-4} for oysters (the free stream velocity is hereby 0.15 m s^{-1}).

The main difference between mussels and oysters are the shell height, the variation in shell height and the density of the bivalve bed. The shell height and the variation in shell height is roughly two times larger than the shell height and the variation in shell height of a mussel bed. Besides, the density of an oyster patch is $\pm$ 13% compared to the density of a mussel patch. Thus, an oyster produces substantially more turbulence per individual compared to a mussel; however the turbulence above an oyster and mussel patch is roughly similar.

What is the influence of mussel and oyster beds on sediment dynamics on a tidal flat?
Mussels and oysters have an influence on the sediment dynamics in and around their patch. The roughness of the bivalve bed decreases the near bottom velocity resulting in sedimentation inside the bivalve bed. The sedimentation rates inside a mussel and oyster patch are respectively 4.9 and 3.3 mm after two days in a cohesive environment (or $\pm$ 7.4 and 4.9 cm per month, respectively). The sedimentation rate on a bare bed is 0.5 mm after two days (or 0.8 cm per month), so the amount of sedimentation inside a mussel or oyster bed is substantially. The deposition inside a mussel patch corresponds reasonably well with the sediment deposition in (young) mussel beds, while the simulated accumulation rates in an oyster bed are higher in comparison with the rates found in the field. The forces induced by currents are never high enough to erode the sediment inside the bivalve bed. The maximum bed shear stress induced by currents on the sediment inside a mussel and oyster bed are 0.18 and 0.14 N m^{-2}, respectively. The net biodeposition is approximately 30% of the total deposition inside the mussel bed. This amount of biodeposition showed good agreement with the literature.

Mussels and oysters have also a large effect on the sediment dynamics around their patch. Calmer conditions occur behind the bivalve patch; resulting in sediment deposition on this side. The amount of sedimentation at 50 meters behind a mussel and oyster patch is 1.2 and 1.8 mm in two days in a cohesive environment, respectively. Moreover, the flow velocity at the left and right side of the patch (with respect to the main flow direction) is higher due to flow routing. These increased flow velocities lead to erosion at these sides; oysters have hereby a larger effect on the erosion as a result of the larger resistance force of oysters in contrast to mussels. The erosion is more pronounced in a non-cohesive environment in comparison with a cohesive environment, due to the relatively low critical bed shear stress of non-cohesive sediments. These sedimentation patterns correspond with the patterns found in the field.

This modeling study presents the influence of currents on the hydro- and sediment dynamics above and around a mussel or oyster patch. According to this study, currents cannot erode sediment inside a bivalve bed and it appears that there is a missing process. The missing process is probably waves; waves can presumably penetrate easier in the bivalve bed than current and it is likely that waves can increase the bed shear stress and start the erosion of sediment in a bivalve bed. The shell height is also important factor to determine the sediment transport, because the velocity and turbulence patterns above a bivalve patch with a decreased height are similar to the reference model, while the bed shear stress on the sediment between the shells significantly increases.

7.2 Recommendations

7.2.1 Experiments

The recommendations for the future experiments are:

- More (laboratory) measurements: At this moment there is a lack of longitudinal measurements, including measurements around the leading edge, above a mussel or oyster bed, consequently the flume model (in this study) cannot be calibrated in the streamwise direction and the effect of these bivalves along the flume cannot be described. For example, suitable measurement locations are 1 m and 10 cm before the edge, above the edge and 10 cm, 50 cm 1 m, 2 m and 3 m behind the leading edge. Moreover, the actual bed shear stresses on the sediment between the bivalve shells are unknown. Detailed near-bed measurements (between the shells) are therefore needed to determine the actual bed shear stress on this sediment.
- Determine influence of variable shell height: According to the flume model, a variable shell height has a significant effect on the turbulence levels above a bivalve bed. The precise influence of a variable bed on the simulated turbulence levels is unknown. There is a possibility that the model results are circumstantial, originating from coincidences which have a positive effect on the simulations. This influence can be determined with flume experiments; for example by measuring the flow above a bed with a variable cylinder height and above a bed with a constant cylinder height.

7.2.2 Methodology

- Limitations of the vegetation model: This study used the 3D rigid vegetation model to implement mussels and oysters in Delft3D. This model has been developed to represent cylinders with a high porosity ($\pm$ 95%). The model has its limitations regarding low porosities, as is the case for a bivalve bed. The porosity of mussels and oysters is approximately 65%, and this porosity is close to the limitations of this vegetation model, especially in case of oysters due to high drag coefficient and large diameters. Besides, a mussel and oyster bed can be seen as a bed with very large grains and a better approach could be to implement a mussel and oyster bed in a model which can account for these low porosities.
- Including turbulence effects in equation: Mussels and oysters are presented as cylinders with a variable shell height and the amount of layers near the bed must be sufficient to account for this variability (otherwise the model will interpolate the variable shell height resulting in less good results). In the case of the field model, the layers near the bed have a vertical height of approximately 1 – 1.5 cm. The computational time will be more sufficient if the amount of layers can be reduced without deterioration of the simulated turbulence. A possibility is to account for the effect of the variable shell height in a turbulence equation, consequently, the amount of vertical layers can decrease and the computational will decrease.

7.2.3 Modeling

- Incorporate waves in the model: Waves are presumably the missing process which can start the erosion of the sediment inside the bivalve bed. One of the main recommendations is therefore to determine the effect of waves on the hydro- and sediment dynamics above and around mussel and oyster beds. Mussels and oysters can possibly be implemented in the wave model SWAN with the vegetation module (similar as the implementation of mussels and oysters in Delft3D with the 3D rigid vegetation model) (Dalrymple et al., 1984; Kobayashi et al., 1993;

Mendez and Losada, 2004). This implementation will be more reliable if the wave model can be calibrated with measurements. Integrating flume experiments, field measurements and a modeling study appears to be the best way.

The height of the mussel or oyster shells is an important factor which has an influence on the sediment transport; because a decrease in shell height leads to an increase in bed shear stress. The velocity profile above the bivalve bed does not significantly change for different shell heights (if the variation of the shell heights is constant). The decrease in shell height was not sufficient to increase the bed shear stress more than the critical bed shear stress in a current dominated environment. However, this reduction can be essential in a current and wave environment to erode the sediment inside the bivalve bed.

- Incorporate mussels and oysters in a larger scale model: This study investigated the influence of mussel and oyster bed for an idealized situation. The field model used in this study can be improved by nest mussels and oysters in a larger scale (tidal inlet) model. The hydro- and sediment dynamics will be more realistic and can be compared with the actual sedimentation pattern found in the field. A good method will be to integrate field measurements around a mussel or oyster bed location with the implementation of a mussel and oyster bed in Delft3D (including sediment transport).

Bibliography

Baptist, M. J. (2005). *Modelling floodplain biogeomorphology*. PhD thesis, Delft University of Technology, Delft.

Baptist, M. J., Babovic, V., Rodríguez Uthurburu, J., Keijzer, M., Uittenbogaard, R. E., Mynett, A., and Verwey, A. (2007). On inducing equations for vegetation resistance Sur l ' établissement des équations traduisant la résistance due à la végétation. *Journal of Hydraulic Research*, 45(4):435–450.

Berenbrock, C. and Tranmer, W. (2008). Simulation of Flow , Sediment Transport , and Sediment Mobility of the Lower Coeur d'Alene River , Idaho. Technical report, U.S. Geological Survey Scientific Investigations Report 2008-5093, Reston, Virginia.

Borsje, B. W. (2014). *Marine Dynamics; Short Waves; Part 4-8*. University of Twente, Enschede, 1 edition.

Borsje, B. W., Bouma, T. J., Rabaut, M., Herman, P. M. J., and Hulscher, S. J. M. H. (2014). Formation and erosion of biogeomorphological structures: A model study on the tube-building polychaete Lanice conchilega. *Limnology and Oceanography*, 59(4):1297–1309.

Borsje, B. W., Van Wesenbeeck, B. K., Dekker, F., Paalvast, P., Bouma, T. J., Van Katwijk, M. M., and De Vries, M. B. (2011). How ecological engineering can serve in coastal protection. *Ecological Engineering*, 37(2):113–122.

Bos, A. R. and Van Katwijk, M. M. (2007). Planting density, hydrodynamic exposure and mussel beds affect survival of transplanted intertidal eelgrass. *Marine Ecology Progress Series*, 336:121–129.

Bougrier, S., Geairon, P., Deslous-Paoli, J. M., Bacher, C., and Jonquieres, G. (1995). Allometric relationships and effects of temperature on clearance and oxygen consumption rates of Crassostrea gigas (Thunberg). *Aquaculture*, 134:143–154.

Bouma, T. J., De Vries, M. B., Low, E., Peralta, G., Tánczos, I. C., Van De Koppel, J., and Herman, P. M. J. (2005). Trade-offs related to ecosystem engineering: A case study on stiffness of emerging macrophytes. *Ecology*, 86(8):2187–2199.

Bouma, T. J., van Duren, L. A., Temmerman, S., Claverie, T., Blanco-Garcia, A., Ysebaert, T., and Herman, P. M. J. (2007). Spatial flow and sedimentation patterns within patches of epibenthic structures: Combining field, flume and modelling experiments. *Continental Shelf Research*, 27:1020–1045.

Bradshaw, P. and Huang, G. P. (1995). The Law of the Wall in Turbulent Flow. *Osborn Reynolds Centenary Volume. Proceedings: Mathematical and Physical Sciences*, 451(1941):165–188.

Brinkman, A. G., Bult, T., Dankers, N., Meijboom, A., van Stralen, M. R., and de Vlas, J. (2003). Mosselbanken: Kenmerken, Oppervlaktebepaling en Beoordeling van Stabiliteit. Alterra-rapport 707. Technical report, Alterra, Research Instituut voor de Groene Ruimte, Wageningen.

Brinkman, A. G., Dankers, N., and Van Stralen, M. (2002). An analysis of mussel bed habitats in the Dutch Wadden Sea. *Helgoland Marine Research*, 56:59–75.

Callier, M. D., Weise, A. M., McKindsey, C. W., and Desrosiers, G. (2006). Sedimentation rates in a suspended mussel farm (Great-Entry Lagoon, Canada): Biodeposit production and dispersion. *Marine Ecology Progress Series*, 322(Hargrave 2005):129–141.

Carlsson, M. S., Glud, R. N., and Petersen, J. K. (2010). Degradation of mussel (Mytilus edulis) fecal pellets released from hanging long-lines upon sinking and after settling at the sediment. *Canadian Journal of Fisheries and Aquatic Sciences*, 67:1376–1387.

Carrington, E., Moeser, G. M., Thompson, S. B., Coutts, L. C., and Craig, C. A. (2008). Mussel attachment on rocky shores: The effect of flow on byssus production. *Integrative and Comparative Biology*, 48(6):801–807.

Chamberlain, J., Fernandes, T. F., Read, P., Nickell, T. D., and Davies, I. M. (2001). The impact of biodeposits from suspended mussel (Mytilus edulis) culture on the surrounding surficial sediments. *ICES Journal of Marine Science*, 58(1995):411–416.

Chriss, T. M. and Caldwell, D. R. (1982). Evidence for the Influence of Form Drag on Bottom Boundary Layer Flow. *Journal of Geophysical Research: Oceans*, 87(C6):4148–4154.

Comeau, L. A. (2014). Spring awakening temperature and survival of sediment-covered eastern oysters Crassostrea virginica. *Aquaculture*, 430:188–194.

Dalrymple, R. A., Kirby, J. T., and Hwang, P. A. (1984). Wave Diffraction Due to Areas of Energy Dissipation. *Journal of Waterway, Port, Coastal, and Ocean Engineering*, 110(1):67–79.

Dame, R. F. and Dankers, N. (1988). Uptake and release of materials by a Wadden sea mussel bed. *Journal of Experimental Marine Biology and Ecology*, 118:207–216.

Dankers, N. and Fey-Hofstede, F. (2015). *Een zee van Mosselen. Handboek ecologie, bescherming, beleid en beheer van mosselbanken in de Waddenzee.* Stichting ANEMOON, Lisse.

Dankers, N., Meijboom, A., De Jong, M., Dijkman, E., Cremer, J., and Van der Sluis, S. (2004a). Het ontstaan en verdwijnen van droogvallende mosselbanken in de Nederlandse Waddenzee. Alterra-rapport 921. Technical report, Alterra, Wageningen.

Dankers, N. M. J. A., Dijkman, E. M., De Jong, M. L., De Kort, G., and Meijboom, A. (2004b). De verspreiding en uitbreiding van de Japanse Oester in de Nederlandse Waddenzee. Alterra-rapport 909. Technical report, Alterra, Wageningen.

De Vries, M. B., Borsje, B. W., Bouma, T. J., Dankers, N., and Augustijn, D. C. M. (2012). Bedform formation by contrasting ecosystem engineers: A case study for two reefbuilding bivalve species. *Not published*, pages 1–38.

Deltares (2014). *Delft3D-FLOW, User Manual*. Deltares, Delft, 3.15.34158 edition.

Donker, J. J. A. (2015). *Hydrodynamic processes and the stability of intertidal mussel beds in the Dutch Wadden Sea*. PhD thesis, Utrecht University, Utrecht.

Donker, J. J. A., Van der Vegt, M., and Hoekstra, P. (2013). Wave forcing over an intertidal mussel bed. *Journal of Sea Research*, 82:54–66.

Dowell, M. (2012). Crassostrea gigas; Morphology. Encyclopedia of Life. Date accessed: 2015-04-20 http://eol.org/data_objects/17255753.

Drost, E. (2013). *Hydrodynamics over a patch structure on an intertidal mussel bed*. MSc thesis. Utrecht University, Utrecht.

Dunnington, E. A. (1968). Survival time of oysters after burial at various temperatures. *Proceedings of the National Shellfisheries Association*, 58:101–103.

Duran-Matute, M., Gerkema, T., De Boer, G. J., Nauw, J. J., and Gräwe, U. (2014). Residual circulation and freshwater transport in the Dutch Wadden Sea: A numerical modelling study. *Ocean Science*, 10:611–632.

Dybas, C. and Carrington, E. (2013). Blue mussels 'hang on' along rocky shores: For how long?

Fey, F., Dankers, N., Meijboom, A., De Jong, M., Van Leeuwen, P., Dijkman, E., and Cremer, J. (2006). De ontwikkeling van de Japanse oester in de Nederlandse Waddenzee : Situatie 2006. Technical report, IMARES, Wageningen.

Flemming, B. W. and Delafontaine, M. T. (1994). Biodeposition in a juvenile mussel ed of the east Frisian -wadden Sea (Southern North Sea). *Netherlands journal of aquatic ecology*, 28:289–297.

Folkard, A. M. and Gascoigne, J. C. (2009). Hydrodynamics of discontinuous mussel beds: Laboratory flume simulations. *Journal of Sea Research*, 62(4):250–257.

Gerdes, D. (1983). The pacific oyster Crassostrea gigas; Part I. Feeding behaviour of larvae and adults. *Aquaculture*, 31:195–219.

Giles, H. and Pilditch, C. A. (2004). Effects of diet on sinking rates and erosion thresholds of mussel Perna canaliculus biodeposits. *Marine Ecology Progress Series*, 282:205–219.

Gittenberger, A. (2000). Achtergrond; Onderdeel van Exoten.

Graf, G. and Rosenberg, R. (1997). Bioresuspension and biodeposition: A review. *Journal of Marine Systems*, 11(July 1995):269–278.

Haven, D. S. and Morales-Alamo, R. (1966). Aspects of biodeposition by oysters and other invertebrate filter feeders. *Limnology and Oceanography*, 11:487–498.

Hertweck, G. and Liebezeit, G. (1996). Biogenic and geochemical properties in intertidal biosedimentary deposits related to Mytilus beds. *P.S.Z.N. I: Marine Ecology*, 17:131–144.

Horstman, E., Dohmen-Janssen, M., and Hulscher, S. J. M. H. (2013). Modeling tidel dynamics in a mangrove creek catchment in Delft3D. *Coastal Dynamics*, pages 833–844.

Huisman, B. J. A. and Luiendijk, A. P. (2009). Sand demand of the Eastern Scheldt. Technical report, Deltares, Delft.

Janssen-Stelder, B. (2000). The effect of different hydrodynamic conditions on the morphodynamics of a tidal mudflat in the Dutch Wadden Sea. *Continental Shelf Research*, 20:1461–1478.

Johannesson, B., Larsvik, M., Loo, L., and Samuelsson, H. (2000). Mytilus edulis; Blue mussel.

Jones, C. G., Lawton, J. H., and Shachak, M. (1994). Organisms as ecosystem engineers. *Oikos*, 69:373–386.

Jorgensen, C. B. (1996). Bivalve filter feeding revisited. *Marine Ecology Progress Series*, 142:287–302.

Klausmeier, C. A. and Litchman, E. (2001). Algal games: The vertical distribution of phytoplankton in poorly mixed water columns. *Limnology and Oceanography*, 46(8):1998–2007.

Kobayashi, N., Raichle, A. W., and Asano, T. (1993). Wave attenuation by vegetation. *Journal of Waterway, Port, Coastal, and Ocean Engineering*, 119:30–48.

Le Hir, P., Monbet, Y., and Orvain, F. (2007). Sediment erodability in sediment transport modelling: Can we account for biota effects? *Continental Shelf Research*, 27:1116–1142.

Lee, H. and Swartz, R. (1980). *Biological processes affecting the distribution of pollutants in marine sediments. Part II. Biodeposition and bioturbation.* Ann Arbor Science Publishers, Contaminants and Sediments. Ann Arbor, Michigan, in: baker edition.

Lesser, G. R., Roelvink, J. A., van Kester, J. A. T. M., and Stelling, G. S. (2004). Development and validation of a three-dimensional morphological model. *Coastal Engineering*, 51:883–915.

Mcgrorty, S., Goss-Custard, J. D., and Clarke, R. T. (1993). Mussel Mytilus edulis (Mytilacea) dynamics in relation to environmental gradients and intraspecific interactions. *Netherlands Journal of Aquatic Ecology*, 27:163–171.

Mendez, F. J. and Losada, I. J. (2004). An empirical model to estimate the propagation of random breaking and nonbreaking waves over vegetation fields. *Coastal Engineering*, 51(2):103–118.

Mitchell, I. M. (2006). In situ biodeposition rates of Pacific oysters (Crassostrea gigas) on a marine farm in Southern Tasmania (Australia). *Aquaculture*, 257:194–203.

Mosselwad (2016). Mosselwad. Date accessed: 2016-02-10 http://www.mosselwad.nl/index.htm.

Nehls, G., Witte, S., Buttger, H., Dankers, N., Jansen, J., Millat, G., Herlyn, M., Markert, A., Sand Kristensen, P., Ruth, M., Buschbaum, C., and Wehrmann, A. (2009). Beds of blue mussels and Pacific oysters. Thematic Report No. 11. Quality Status Report 2009. Wadden SeaEcosystem No. 25. Technical Report 25, Wilhemshaven, Germany.

Nepf, H. M. and Vivoni, E. R. (2000). Flow structure in depth limited, vegetated flow. *Journal of Geophysical Research*, 105(C12):28,547–28,557.

Nezu, I. and Rodi, W. (1986). Open-channel flow measurements using a Laser Doppler Anemometer. *Journal Of hydraulic Engineering*, 112(5):335–355.

Nishikawa-Kinomura, K. A. (1978). *Trace Elements in Oyster Biodeposits*. MSc thesis, Oregon State University, Corvallis.

Okamoto, T. and Nezu, I. (2013). Spatial evolution of coherent motions in finite-length vegetation patch flow. *Environmental Fluid Mechanics*, 13(5):417–434.

Oost, A. P. (1995). *Dynamics and sedimentary development of the Dutch Wadden Sea with emphasis on the Frisian inlet*. PhD thesis, Utrecht University, Utrecht.

Paarlberg, A. J., Knaapen, M. A. F., De Vries, M. B., Hulscher, S. J. M. H., and Wang, Z. B. (2005). Biological influences on morphology and bed composition of an intertidal flat. *Estuarine, Coastal and Shelf Science*, 64:577–590.

Partheniades, E. (1965). Erosion and Deposition of Cohesive Soils. *Journal of Hydraulics Division*, 91(1):105–139.

Postma, H. (1981). Exchange of materials between the North Sea and the Wadden Sea. *Marine Geology*, 40:199–213.

Prins, T. C., Smaal, A. C., Pouwer, A. J., and Dankers, N. (1996). Filtration and resuspension of particulate matter and phytoplankton onan intertidal mussel bed in the Oosterschelde estuary (SW Netherlands). *Marine Ecology Progress Series*, 142:121–134.

Reise, K. (1998). Pacific oysters invade mussel beds in the European Wadden Sea. *Senckenbergiana maritima*, 28(4):167–175.

Ribberink, J. S. and Hulscher, S. J. M. H. (2012). *River Dynamics I: Shallow-Water flows*. University of Twente, Enschede, march 2012 edition.

Risk, M. J. and Moffat, J. S. (1977). Sedimentological significance of fecal pellets of Macoma balthica in the Minas Basin, Bay of Fundy. *Journal of Sedimentary Petrology*, 47(4):1425–1436.

Stoesser, T. and Nikora, V. I. (2008). Flow structure over square bars at intermediate submergence: Large Eddy Simulation study of bar spacing effect. *Acta Geophysica*, 56(3):876–893.

Temmerman, S., Bouma, T. J., Govers, G., Wang, Z. B., De Vries, M. B., and Herman, P. M. J. (2005). Impact of vegetation on flow routing and sedimentation patterns: Three-dimensional modeling for a tidal marsh. *Journal of Geophysical Research*, 110(4):1–18.

Ten Brinke, W. B. M., Augustinus, P. G. E. F., and Berger, G. W. (1995). Fine-grained sediment deposition on mussel beds in the Oosterschelde (The Netherlands), determined from echosoundings, radio-isotopes and biodeposition field experiments. *Estuarine, Coastal and Shelf Science*, 40:195–217.

Troost, K. (2010). Causes and effects of a highly successful marine invasion: Case-study of the introduced Pacific oyster Crassostrea gigas in continental NW European estuaries. *Journal of Sea Research*, 64(3):145–165.

Troost, K., Stamhuis, E. J., Van Duren, L. A., and Wolff, W. J. (2009). Feeding current characteristics of three morphologically different bivalve suspension feeders, Crassostrea gigas, Mytilus edulis and Cerastoderma edule, in relation to food competition. *Marine Biology*, 156:355–372.

Tubantia (2016). Oesterriffen in Noordzee. Tubantia Newspaper, 25 March 2016, page 13.

Uittenbogaard, R. E. (2003). Modelling turbulence in vegetated aquatic flows. In *Unpublished Results. Riparian Forest Vegetated Channels*, pages 1–17, Trento, Italy.

Van de Koppel, J. (2012). The study of spatial ecology.

Van de Koppel, J., Gascoigne, J. C., Theraulaz, G., Rietkerk, M., Mooij, W. M., and Herman, P. M. J. (2008). Experimental evidence for spatial self-organization and its emergent effects in mussel bed ecosystems. *Science (New York, N.Y.)*, 322(October):739–742.

Van Duren, L. A., Herman, P. M. J., Sandee, A. J. J., and Heip, C. H. (2006). Effects of mussel filtering activity on boundary layer structure. *Journal of Sea Research*, 55:3–14.

Van Kessel, T. (2015). Opzet en toepassing slibmodel Waddenzee. Technical report, Deltares, Delft.

Van Ledden, M. (2003). *Sand-mud segregation in estuaries and tidal basisn*. PhD thesis, Delft University of Technology, Delft.

Van Leeuwen, B. (2008). *Modeling mussel bed influence on fine sediment dynamics on a Wadden Sea intertidal flat*. MSc thesis, University of Twente, Enschede.

Van Leeuwen, B., Augustijn, D. C. M., Van Wesenbeeck, B. K., Hulscher, S. J. M. H., and De Vries, M. B. (2010). Modeling the influence of a young mussel bed on fine sediment dynamics on an intertidal flat in the Wadden Sea. *Ecological Engineering*, 36:145–153.

Van Loon, A. F. (2005). *Modelling the long-term fine sediment balance in the Western Wadden Sea*. MSc thesis, University of Wageningen, Wageningen.

Van Rijn, L. C. (1993). *Principles of Sediment Transport in Rivers, Estuaries and Coastal Seas*. Aqua Publications, The Netherlands.

Van Rijn, L. C. (2011). *Principles of fluid flow and surface waves in rivers, estuaries, seas and oceans*. Aqua Publications, Blokzijl, The Netherlands, 2011 edition.

Van Rijn, L. C., Roelvink, J. A., and Ter Horst, W. (2001). Sand transport by currents and waves; General approximation formulae. Technical Report Z3054, Delft Hydraulics, Delft, The Netherlands.

Van Rijn, L. C., Walstra, D. J. R., and Van Ormondt, M. (2004). Description of TRANSPOR2004 and Implementation in Delft3D-ONLINE. Technical Report Z3748, Delft Hydraulics, Delft, The Netherlands.

Walles, B. (2015). *The Role of ecosystem engineers in the ecomorphological development of intertidal habtitats*. PhD thesis, Wageningen University, Wageningen.

Walles, B., Salvador de Paiva, J., Van Prooijen, B. C., Ysebaert, T., and Smaal, A. C. (2014). The Ecosystem Engineer Crassostrea gigas Affects Tidal Flat Morphology Beyond the Boundary of Their Reef Structures. *Estuaries and Coasts*, 37(5).

Widdows, J., Brinsley, M. D., Salkeld, P. N., and Elliott, M. (1998). Use of Annular Flumes to Determine the Influence of Current Velocity and Bivalves on Material Flux at the Sediment-Water Interface. *Estuaries*, 21(4):552–559.

Widdows, J., Fieth, P., and Worrall, C. M. (1979). Relationships between seston, available food and feeding activity in the common mussel Mytilus edulis. *Marine Biology*, 50:195–207.

Widdows, J., Lucas, J. S., Brinsley, M. D., Salkeld, P. N., and Staff, F. J. (2002). Investigation of the effects of current velocity on mussel feeding and mussel bed stability using an annular flume. *Helgoland Marine Research*, 56:3–12.

Wright, L. D., Friedrichs, C. T., and Hepworth, D. A. (1997). Effects of benthic biology on bottom boundary layer processes, Dry Tortugas Bank, Florida Keys. *Geo-Marine Letters*, 17:291–298.

Xue, Q. G., Itoh, N., Schey, K. L., Li, Y. L., Cooper, R. K., and La Peyre, J. F. (2007). A new lysozyme from the eastern oyster (Crassostrea virginica) indicates adaptive evolution of i-type lysozymes. *Cellular and Molecular Life Sciences*, 64:82–95.

Zagata, C., Young, C., Sountis, J., and Kuehl, M. (2008). Mytilus edulis. Animal Diversity WEb. Date accessed: 2015-04-20 http://animaldiversity.org/site/accounts/information/Mytilus_edulis.html.

A Analysis of results of laboratory experiments

In this appendix the experimental set-up of the experiments of Van Duren et al. (2006) and De Vries et al. (2012) are presented. Hereafter, the results of both studies are shortly discussed. Finally, the implementation of these studies in Delft3D is presented in Section A.3.

A.1 Experimental set-up

This section introduces the experimental set up of two flume studies. The first flume study is conducted by Van Duren et al. (2006). The hydrodynamics above a mussel bed are investigated in this study. The second study investigates the hydrodynamics above an oyster bed and was conducted by De Vries et al. (2012).

A.1.1 Van Duren

Van Duren et al. (2006) investigated the general structure of the benthic boundary layer over a dense bed of (open and closed) mussels (*Mytilus Edulis*) and the effect of filtration action of mussels on the flow. This study consists of flow velocity, turbulent kinetic energy and Reynolds stresses measurements. The experiments of Van Duren were conducted at the straight section in a large racetrack flume at the NIOO laboratory in Yerseke. The flow is generated at the other side of this straight working section using a conveyor belt system. The straight working section has a length of 10.8 meters, a width of 60 cm and the water depth is maintained at 40 cm. The 2.1 m long test section is at the downstream end of the working section. Measurements were conducted using a carriage with a 3D positioning system, this carriage can be placed anywhere along the length of this working section. Figure A.1 presents a schematic overview of the NIOO flume. A more detailed description of these experiments is presented by Van Duren et al. (2006).

A mussel bed with a distinct leading edge was created in the working section of the flume. This mussel bed was transferred from the Eastern Scheldt to the working section and the mussels covered the complete ground area of the flume over a total length of 3.3 m. The range of the mussel bed height was 49 to 86 mm and the average mussel bed height was 61 mm. The average shell length of these mussels was 38.5 mm (with a standard deviation of 8.3 mm) and the mussel bed had a density of 1800 mussels m^{-2} (Van Duren et al., 2006). Figure A.2 presents the open and closed mussels in the flume. There is a variation in height between every single mussel, moreover some mussels have settled on top of other mussels (Van Duren et al., 2006).

To determine the influence of mussels on the hydrodynamics different flow rates were chosen, namely a low, intermediate and high free stream flow velocities. These rates correspond with free stream velocities over a flat bottom of 45, 100 and 275 mm s^{-1}, respectively and over a mussel bed of 55, 130 and 350 mm s^{-1} (Van Duren et al., 2006). The flow velocity is not measured over the total height of the flume, besides the averaged flow velocity or discharge is not determined.

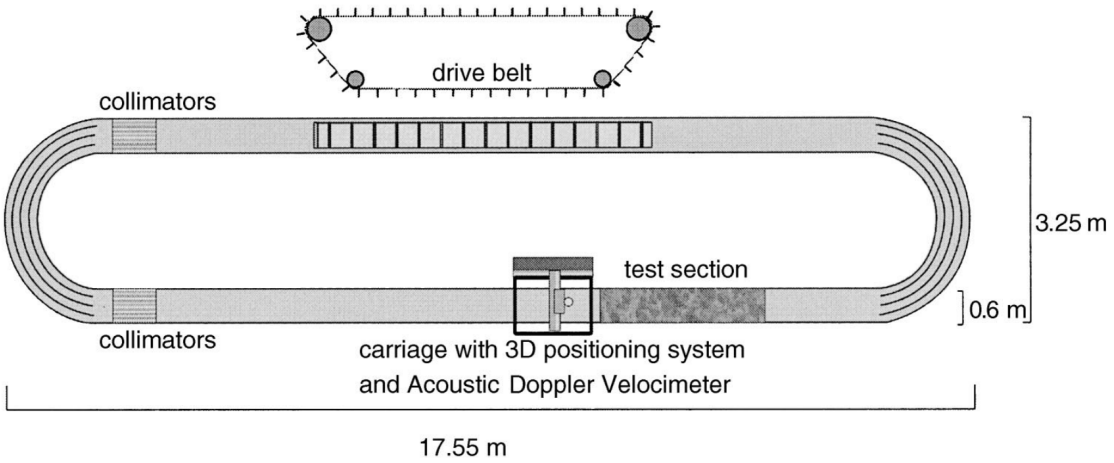

Fig. A.1. Schematic top view of the NIOO racetrack flume. The conveyor belt system (or drive belt), the flow straighteners, the measurement carriage, the straight working section are depicted. (Bouma et al., 2005)

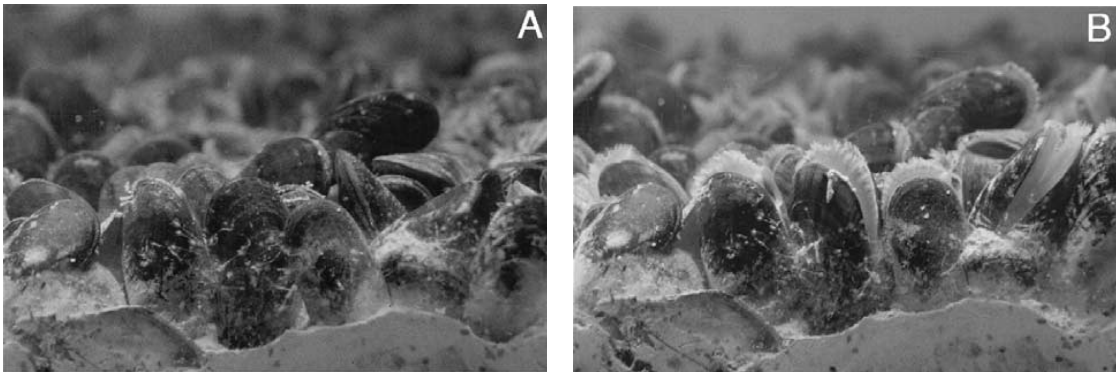

Fig. A.2. (A) Mussels in the flume during the experiments of Van Duren et al. (2006). (A) Inactive mussels (closed), (B) active mussels (open). The distribution of mussels is (very) randomly.

The flow measurements were taken using an Acoustic Doppler Velocimeter (ADV) and this ADV measured in three directions (x, y and z). The ADV operates at a rate of 25 Hz and the measurement volume was 0.25 cm^3. The ADV measure the flow by the scattering of high frequency sound by fine particles in the flow, therefore very fine deep-sea clay sediment was added in the flume. This sediment stays in suspension even at very low flow velocities. The flow was measured at three different locations and at 24 depths at each location (Van Duren et al., 2006).

A.1.2 De Vries

De Vries et al. (2012) investigated the influence of traits of mussels (*Mytilus Edulis*) and oysters (*Crassostrea gigas*) on the hydrodynamics and bedforms. This study consists of velocity and turbulent kinetic energy measurements above a mussel and oyster bed in a laboratory flume and drag measurements of an individual mussel or oyster caused by the flow. The experiments were conducted in a flume channel with a total horizontal distance of 15 m and a width of 0.5 m. The bivalve patch is located 7.6 m downstream and the length of this patch is 3 m. A platform of 15 cm was constructed in the flume in order to place the bivalves in the flume. The current profiles in the x and z directions are measured with a vertically moveable electromagnetic flow meter operating at 10 Hz. The measurement volume of this meter is a few cubic centimetres and this

meter measured only the spatial averaged velocities within this volume. A schematic overview of the flume channel is presented in Figure A.3 (De Vries et al., 2012).

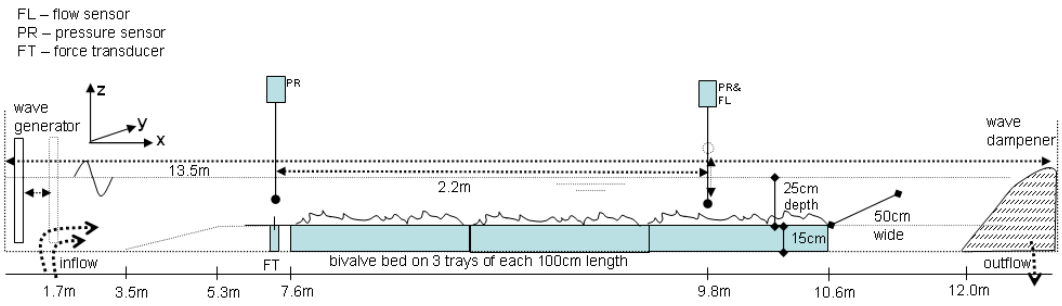

Fig. A.3. Schematic top view of the laboratory flume for the mussel and oyster experiments. The measurement location a indicated with the PR (De Vries et al., 2012).

Blue mussels and Pacific oysters were collected from locations in the Eastern Scheldt and placed on three trays of 0.5 m^2. The living mussels attached to themselves and the bed within 24 hours. The order of the trays was alternated to account for the influence of specific bivalve configuration. The density of the mussel bed was 1400 individuals m^{-2} and the average height of the mussel bed was 60 mm with a standard deviation of 20 mm. The density of the oyster patch was 148 individuals m^{-2} and the average height of the oyster bed was 88 mm with a standard deviation of 25 mm. The characteristics of these mussels and oysters are similar to the characteristics of these bivalves occurring in the field (De Vries et al., 2012).

Flow experiments were conducted at several flow rates, namely between 0.05 and 0.25 m s^1 (at the front of the flume). Currents were generated by a frequency controlled pumping system. The flow was measured at 2, 4, 6, 8 and 11 cm from the top of the bivalve bed. The currents are not measured above the flat bottom of the flume; moreover, the currents are not measured over the total height of the flume. The average flow velocity or discharge is also not determined in this study (De Vries et al., 2012).

An aim of the experiments of De Vries et al. (2012) was to determine the influence of currents (and waves) on the erosion of faeces from a mussel bed. The faeces were mimicked using couscous to investigate the influence of a mussel bed on sediment transport (see Figure A.4). The transport of sediment from an oyster bed was not investigated by De Vries.

Moreover, De Vries et al. (2012) measured also the influence of a single mussel or oyster on the drag force exerted by currents and waves. A force transducer was connected to an intact mussel or oyster shell. Before the drag measurements of a single mussel or oyster, the force transducer was calibrated with several measurements of known weights. The drag measurements were taken at 20 Hz for at least 720 s.

A.2 Results of the flume studies

This section presents the results of the flume studies of Van Duren et al. (2006) and De Vries et al. (2012).

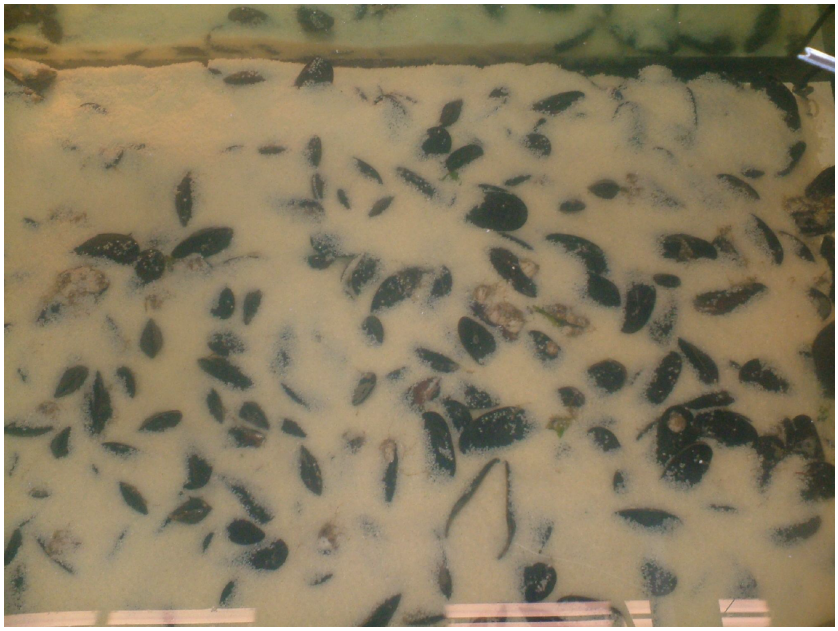

Fig. A.4. Picture of the sediment expirement. The sediment is mimicked with couscous (De Vries et al., 2012).

A.2.1 Van Duren

First of all, the velocity profile above a flat bottom of the NIOO flume will be analysed. The velocity profile is shown in Figure A.5. It can be noted that the flow velocity does not follow a logarithmic profile especially for the intermediate and high flow velocity. The profile has a similar trend as above a mussel bed in this flume (see Figure A.6).

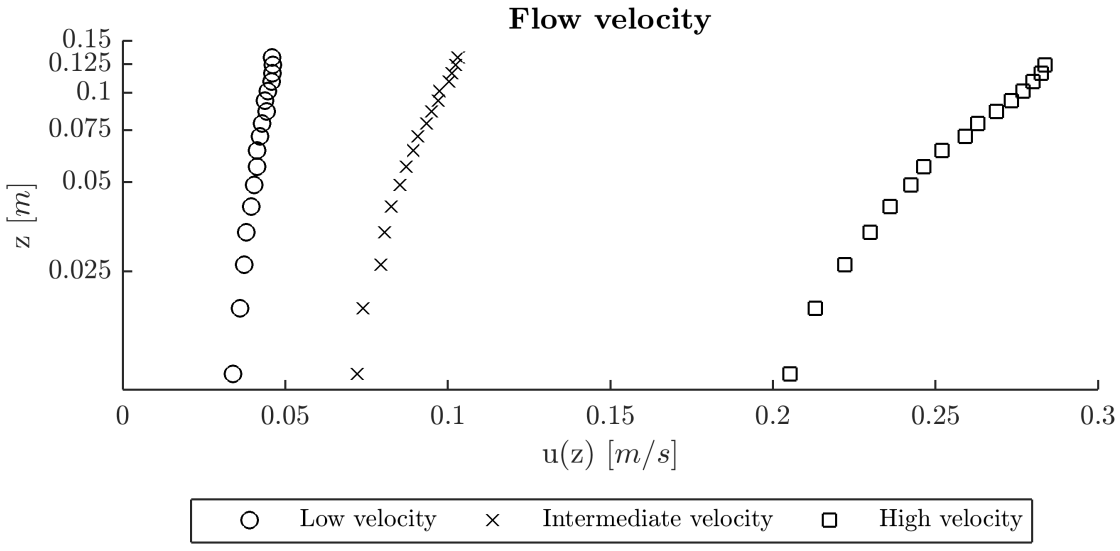

Fig. A.5. The flow velocity above the flat bottom of the NIOO flume (Van Duren et al., 2006).

Figure A.6 presents the measured flow velocity by Van Duren et al. (2006) plotted against a logarithmic z axis and Figures 4.2 and 4.6 presents the flow velocity plotted against linear z axis. There is a small difference between active (open symbols) and inactive mussels (grey symbols). This difference is most visible at the low flow velocity. An ideal boundary layer has a straight line when the velocity is plotted against a logarithmic z axis. The flow over a mussel bed did not fit one straight line, but the flow fits often two straight lines. These two straight lines can be

determined by the clear visible break in the measuring points. Each line has a different velocity gradient and the existence of two velocity gradients indicates that there is an internal boundary layer. An internal boundary layer is common for rough surfaces (such as a mussel bed) (Chriss and Caldwell, 1982). The internal boundary layer is less pronounced at high flow velocities, but this internal layer can still be observed (Van Duren et al., 2006).

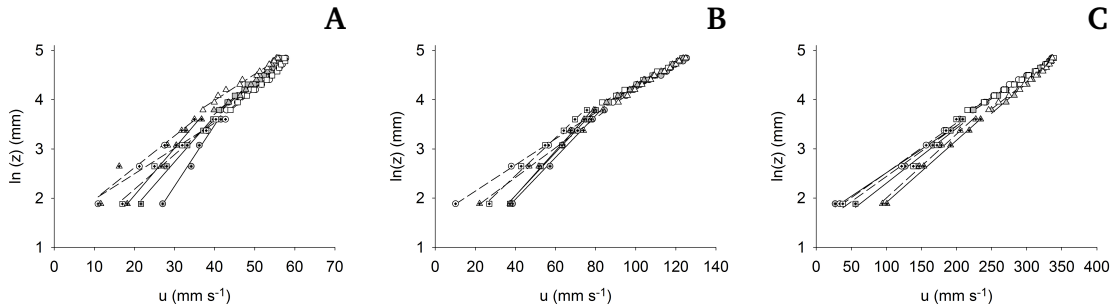

Fig. A.6. The flow velocity over active and inactive mussels at three different flow rates: (A) low velocity, (B) intermediate velocity and (C) high velocity. The grey symbols and solid lines represent the flow velocity above inactive mussels, the open symbols and dashed lines represent the flow velocity above active mussels (Van Duren et al., 2006).

The turbulent kinetic energy (TKE) above a flat bottom, inactive mussels and active mussels is presented in Figure A.7. Mussels increase the turbulence levels near the bed compared to the turbulence levels of a flat bottom (especially for the intermediate and high flow velocity). These higher turbulence levels are the result of higher roughness of a mussel bed. Moreover, the activity of mussels leads to an increased TKE compared to inactive mussels. This increased TKE can be caused by the exhalent (and inhalant) jets. Another explanation for this increased TKE is the higher (physical) roughness of active mussels compared to inactive mussels. Active mussels can have a rougher topography than inactive mussels. Therefore, active mussels can have a higher bed shear stress as a result of the rougher topography and this higher bed shear stress results in higher TKE above the bed (Van Duren et al., 2006).

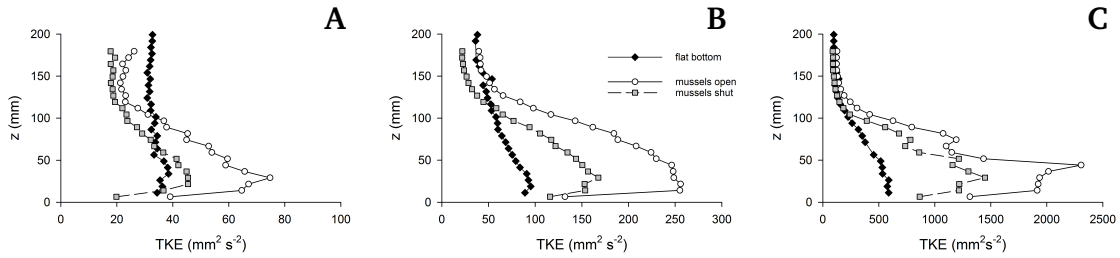

Fig. A.7. The turbulent kinetic energy over a flat bottom, active and inactive mussels at three different flow rates: (A) low velocity, (B) intermediate velocity and (C) high velocity. The presented graphs of the turbulent kinetic energy are average of three replicate experiments (Van Duren et al., 2006).

A mussel bed has also a strong influence on the Reynolds stresses, the Reynolds stress is increased for the low, intermediate and high flow velocities (see Figure A.8). In contrast to the TKE, the Reynolds stresses are not significantly affected by the inhalent and exhalent jets, because the Reynolds stresses above active and inactive mussels are similar. An explanation for this difference is that turbulent eddies created by the jets are uncorrelated and these jets lose their energy in a shorter time scale than the time taken by larger eddies to strain smaller ones (Van Duren et al., 2006).

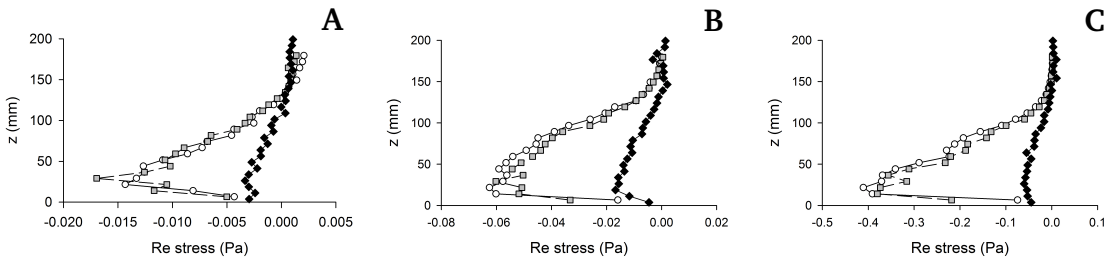

Fig. A.8. The Reynolds stress over a flat bottom, active and inactive mussels at three different flow rates: (A) low velocity, (B) intermediate velocity and (C) high velocity. The presented Reynolds stresses are average of three replicate experiments (Van Duren et al., 2006).

According to Nezu and Rodi (1986), a flow completely is developed if the distribution of Reynolds stresses over the water depth is linear over the water depth. In this case, the Reynolds stresses are not linear distribution over the water depth; therefore, the flow is not completely developed at the measuring point. Consequently, the vertical profiles of velocity, turbulence and Reynolds stress change at different longitudinal locations in the flume. As a result, it can be hard to make conclusions about the velocity and turbulence profiles above a mussel bed at different longitudinal locations.

A.2.2 De Vries

De Vries et al. (2012) measured the form drag forces on mussel and oysters shells. The form drag forces exerted by the currents are larger on oyster shells than on mussel shells. The drag force increases exponentially with the increasing flow velocity. The drag coefficient is a factor 4 larger for oysters than for mussels. The drag coefficient for oysters is 1.84 and the drag coefficient for mussels is 0.42. Figure A.9 presents the drag force for mussels and oysters (De Vries et al., 2012).

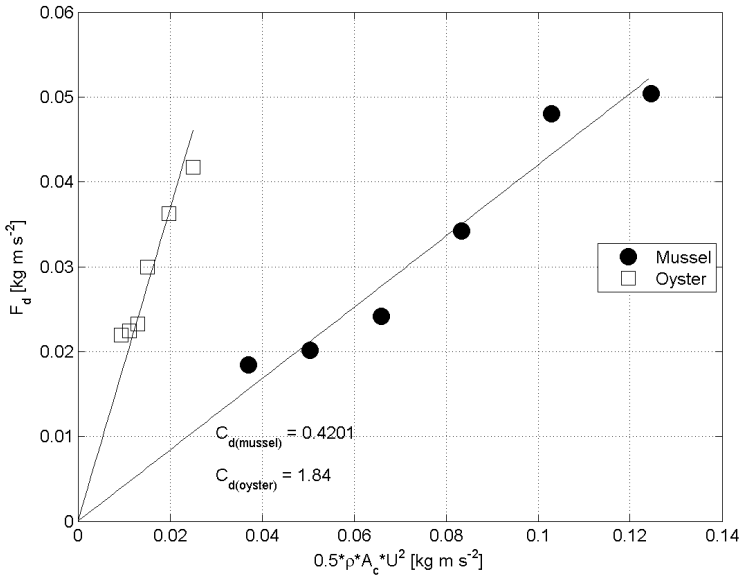

Fig. A.9. The drag force produced by an individual mussel or oyster shell in relation to the curren speed squared and exposed area (De Vries et al., 2012).

Figure A.10 presents the flow velocity above an oyster bed. The velocity gradient above an oyster bed is steep due to the large roughness of the oyster bed. The velocity just above the oyster bed is very low for the different flow velocities. This implies that there is always a low flow velocity inside the oyster bed despite of a high or low flow velocity above the oyster bed. It can be noted that the flow velocity is reduced with more than 50% if the flow velocity at the upper part of the water column is compared with the lower part of the water column (De Vries et al., 2012).

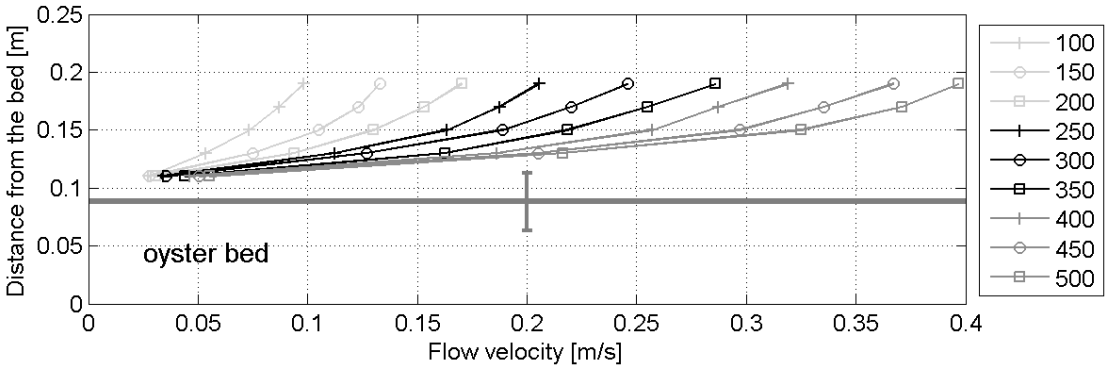

Fig. A.10. The velocity profiles above an oyster patch. The horizontal line indicates the average height of the oyster patch. The bar at 0.2 m/s indicates the standard deviation of the average oyster patch height. The different flow rates are indicated by the number 100-500, these numbers represent the pump rotation frequency (De Vries et al., 2012).

An oyster bed has a large influence on the turbulence levels above the bed (see Figure A.11). The peak turbulence production above an oyster bed is at a distance of 4 cm above the canopy and this turbulence declines steeply around the top of the canopy. A reduction of the turbulence levels in the upper part of the water column is hardly visible (for almost all the flow velocities) in these flume measurements. Moreover, there are relatively few data points measured and there is not clear TKE pattern visible. Therefore, these measurements should be taken with caution.

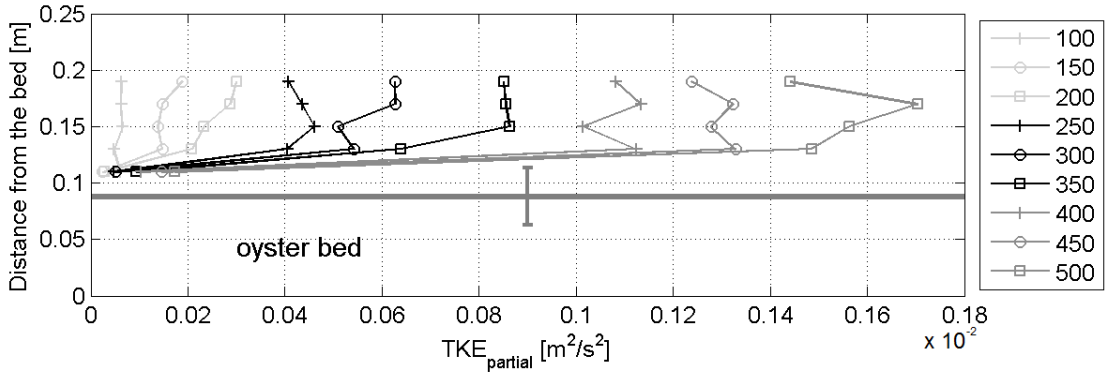

Fig. A.11. The turbulent kinetic energy profiles above an oyster patch. The horizontal line indicates the average height of the oyster patch. The bar at 0.09×10^{-2} m^2 s^{-2} indicates the standard deviation of the average oyster patch height. The different flow rates are indicated by the number 100-500, these numbers represent the pump rotation frequency (De Vries et al., 2012).

A.3 Implementing flume studies in Delft3D

One of the main objectives of this study is to investigate the influence of a mussel or oyster bed on the hydrodynamics. In order to determine the influence of mussels or oysters on the

hydrodynamics a Delft3D model has been setting up. The simulated hydrodynamics above mussels and oysters in Delft3D needs to be calibrated and validated with measured data, so it can be determined if mussels and oysters are successfully implemented in Delft3D. Therefore, the flume studies of Van Duren et al. (2006) and De Vries et al. (2012) are used as calibration and validation data.

The flume set-ups of both flume studies are implemented in Delft3D. As explained in Section 3.2, the model has two open boundaries and two closed boundaries. The two closed boundaries representing the wall of both laboratory flumes. In order to simulate a steady flow in the Delft3D model, the upstream boundary has a constant discharge, while the downstream boundary has a constant water level. The water level in both flume studies was constantly 0.4 m; therefore, the water level in both models has been set at the same level, namely 0.4 m.

The upstream boundary is harder to determine, because both flume studies did not measure the discharge or average flow velocity for the different flow rates. As explained in Section A, Van Duren et al. (2006) and De Vries et al. (2012) measured the flow velocity in a part of the water column. The upstream boundary needs to be calculated using the velocity measurements. The boundary layer of a turbulent shear flow over a rough surface can be determined with the logarithmic law (or 'law of the wall') (Bradshaw and Huang, 1995). The boundary layer is the part of the water column where the flow velocity is not uniform. The following equation is used to determine the average flow velocity in the channel (Van Rijn, 2011):

$$\overline{u} = \frac{u_*}{\kappa}\left[\frac{z_0}{h} - 1 + ln\left(\frac{h}{z_0}\right)\right] \tag{A.1}$$

Where:

$\overline{u}$	$[m/s]$	average flow velocity
u_*	$[m/s]$	shear velocity
κ	[-]	Von Karmann constant (0.4)
z_0	$[m]$	reference level near the bottom where velocity is zero (roughness length)
h	$[m]$	water depth

The discharge can be determined with (Ribberink and Hulscher, 2012):

$$Q = uA \tag{A.2}$$

Where:

Q	$[m^3/s]$	discharge
u	$[m/s]$	flow velocity
A	$[m^2]$	cross section

The shear velocity (friction velocity) can be determined with the law of the wall (Van Rijn, 2011):

$$u(z) = \frac{u_*}{\kappa} ln\left(\frac{z}{z_0}\right) \tag{A.3}$$

Where:

The flow velocity increases logarithmically with the height according to the law of the wall. The roughness length (z_0) indicates the point where the flow velocity is zero. The roughness length

$u(z)$	$[m/s]$	flow velocity at height (z)
z	$[m]$	height above bed

depends on the roughness of the bed, a large bed roughness results in a large roughness length. The roughness length is a measure to determine the roughness of the bed. The roughness length can be translated to the Nikuradse roughness (k_s) and to the Chézy coefficient (C) (with the White-Colebrook equation).

The law of the wall is not valid for surfaces with large items, which increase the roughness to a large extent. For example, the law of the wall is not valid for flow over vegetation or rocky beds (Baptist, 2005; Nepf and Vivoni, 2000). However, the flow above these items follows still a logarithmic trend and for this part of the flume an adapted version of the law of the wall is valid. The adapted version of the law of the wall is (Nepf and Vivoni, 2000):

$$u(z) = \frac{u_*}{\kappa} ln\left(\frac{z-d}{z_0}\right) \tag{A.4}$$

Where:

d	$[m]$	zero-plane displacement

The zero-plane displacement (d) corresponds to the mean level of the momentum absorption. This equation does only describe the flow above the roughness items, such as vegetation and in this case mussels or oysters. This adapted version of the law of the wall is only valid if the flow between the mussels or oysters is small. According to the measurements of Van Duren et al. (2006) and De Vries et al. (2012) the flow between mussels and oysters is very small; consequently Equation A.4 is valid.

A.3.1 Discharge

The discharge is determined using the law of the wall (see Equation A.1). Almost every parameter in this equation is known, except the shear velocity (u_*) and the roughness length (z_0). Firstly, the roughness length is determined by extending the logarithmic trend line towards the point where the velocity is zero. The trend line is extended in Figure A.12 and A.13. In the case of the mussel bed, only the data points in the lower part of the water column are used to determine the trend line (see Figures A.5 and A.6). An overview of the determined roughness lengths for the flat bottom in the NIOO flume, the mussel bed and oyster bed is presented in Table A.1.

Another unknown parameter is the shear velocity, this parameter can be determined with Equation A.4. It is assumed that the zero-plane displacement has the same length as the height of the mussel or oyster bed. Van Duren et al. (2006) determined the shear velocity and roughness length with the same assumption. Finally, the average flow velocity can be determined. The discharge is determined with Equation B.31. An overview of the shear velocity, the average flow velocity and the discharge above the flat bottom in the NIOO flume, the mussel bed and oyster bed is presented in Table A.1.

De Vries et al. (2012) measured the flow velocity for several discharges (pump rotation frequencies). Three flow velocities were chosen to calibrate and validate the model which represents the oyster bed. The three flow rates can be distinguished in a low, intermediate and high flow rates. The low, intermediate and high flow rates coincide with a pump rotation frequency of 150, 350

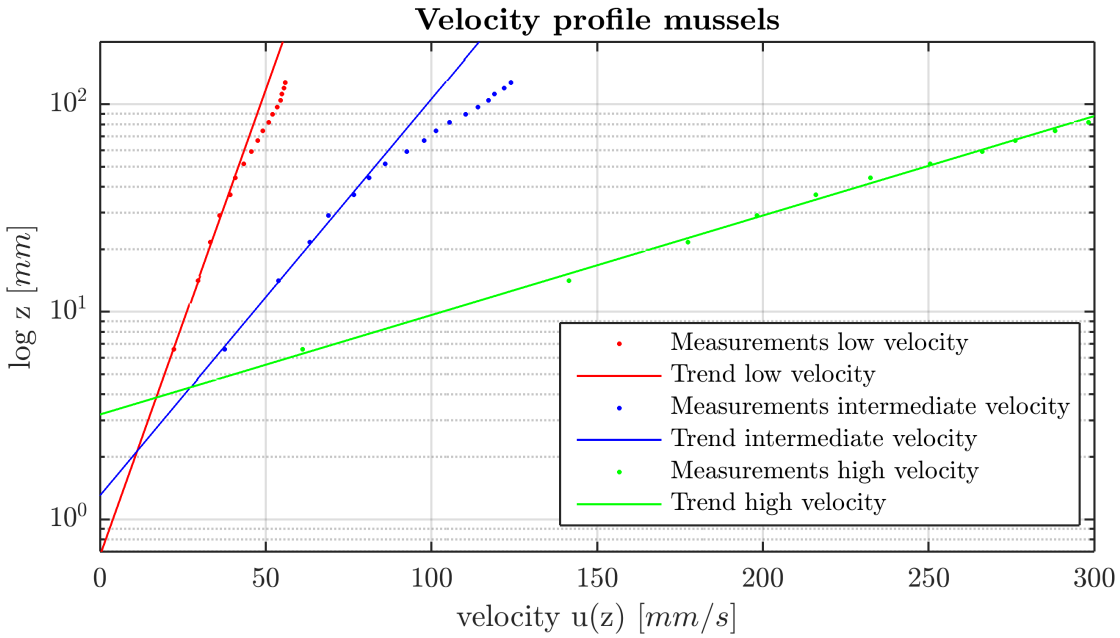

Fig. A.12. The velocity profile above a mussel bed plotted against a logarithmic z-axis. The dots indicates the measurement points and the lines indicates the trend lines for the lowest 6 measurements (Van Duren et al., 2006).

Tab. A.1. An overview of the determined roughness lengt (z_0), shear velocity (u_*), average flow velocity ($\overline{u}$) and discharge (Q).

		Van Duren						De Vries		
		Flat bottom			Mussel bed			Oyster bed		
		L	M	H	L	M	H	L	M	H
z_0	$[mm]$	0.02	0.011	0.06	0.67	1.30	3.20	13.14	14.45	15.17
u_*	$[mm\ s^{-1}]$	2.2	5.7	14.9	3.9	9.1	36.3	26.9	60.3	88.5
$\overline{u}$	$[m\ s^{-1}]$	0.047	0.104	0.291	0.051	0.106	0.34	0.107	0.226	0.321
Q	$[m^3\ s^{-1}]$	0.011	0.024	0.064	0.011	0.025	0.066	0.009	0.018	0.026

and 500, respectively. The low and medium flow rates above an oyster bed correspond roughly with the medium and high flow rates above a mussel bed (if the average flow velocity above a mussel and oyster bed is compared).

The average flow velocity above the flat bottom and above the mussel bed is different as a result of the changed velocity profile due to the higher roughness of the mussel bed and the smaller cross sectional area above the mussel bed compared to the flat bottom. The cross sectional area is smaller as a result of the presence of the mussels which increase bed height. There is a (large) difference between the calculated discharge between the flume of Van Duren et al. (2006) and De Vries et al. (2012). This difference can be explained by the smaller flume of De Vries et al. (2012) and the smaller water depth above the bivalves (See Figure 3.2).

The calculated discharge above a flat bottom corresponds well with the calculated discharge above a mussel bed. The roughness length over a flat bottom is not constant for the three different flow rates. This is remarkable, because the roughness height will normally be constant for a variable flow velocity. This inconstant roughness length is also noticeable over a mussel bed in the NIOO flume. The fact that the flow velocity does not follow a logarithmic profile and that the roughness lengths are not constant for a variable flow rate does not disqualify the results

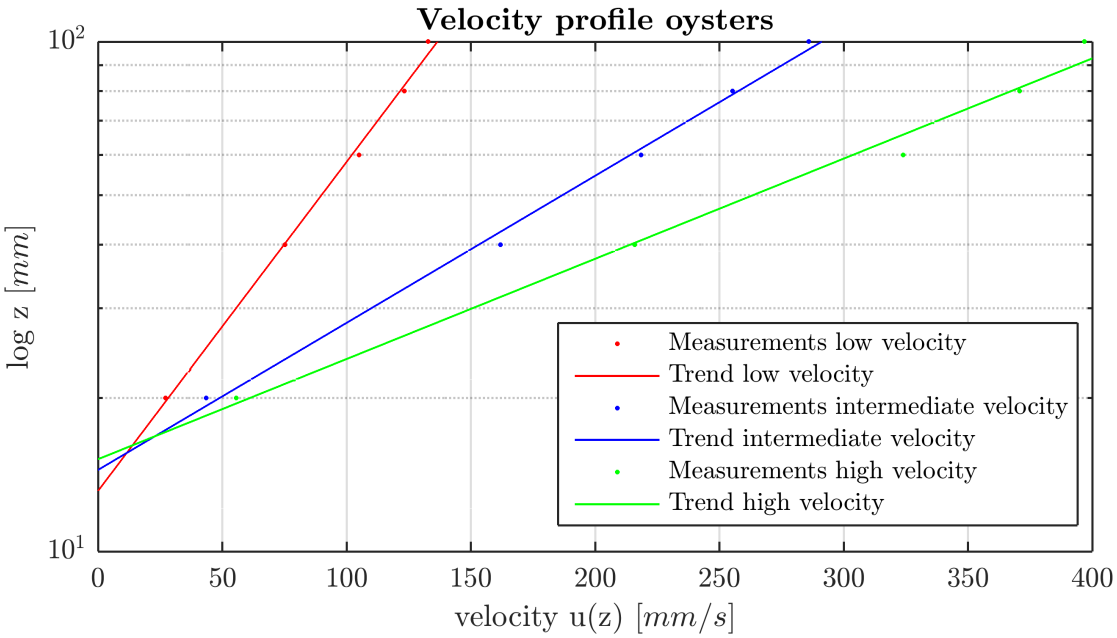

Fig. A.13. The velocity profile above an oyster bed plotted against a logarithmic z-axis. The dots indicates the measurement points and the lines indicates the trend lines for these measurements (De Vries et al., 2012).

of Van Duren et al. (2006) a priori. However, the assumptions of 'law of the wall' are not valid for these measurements (Van Leeuwen, 2008). The calculated discharge must be taken with caution. The simulated results of the vertical velocity profile above a mussel and oyster shows a good agreement with the measurements of Van Duren et al. (2006) and De Vries et al. (2012). Consequently, it can be concluded that the calculated discharge is quite correct.

The roughness lengths in the measurement of De Vries et al. (2012) are more constant for the different flow rates. The roughness length of oysters is significant larger than the roughness length of mussels and this can be explained by the rougher shells of oysters, the larger shells and the larger variation in bivalve bed height. The calculated roughness length of oyster corresponds with the study of Troost et al. (2009).

A.3.2 Bivalve characteristics in the flume studies

Several assumptions have been made to implement a bivalve bed in Delft3D with the 3D vegetation model, for example bivalves can be represented with upright cylinders and these cylinders are evenly distributed over a patch. Moreover, only the upper part of a bivalve bed has influence on the hydrodynamics, therefore only the upper part of bivalves will be represented with cylinders. There are several important parameters in the 3D vegetation model, namely the height, the diameter, the density and the drag coefficient. The definition of density is the amount of bivalves per square meter.

The height, density and drag coefficient can be determined using the studies of Van Duren et al. (2006) and De Vries et al. (2012). The diameters of mussels and oysters are determined using other experiments of De Vries and own observations. According to these experiments, the diameter can be described width the length of the bivalves. The average diameter corresponds reasonably with 50% of the average length of the bivalve, both for mussels as for oysters. Consequently, the diameters of a mussel and oyster are approximately 2 and 5 cm, respectively.

In case of the oyster bed, the height had an average height of 8.8 cm and the standard deviation was 2.5 cm. The density of the oyster bed was 148 oysters m^{-2}. All most all these oysters stand upright and they are not on top of each other. Oyster have also an upright orientation in the field (own observation in Eastern Scheldt). In case of the mussel bed, the average mussel bed height was 61 mm and the range of the mussel bed height is between 4.9 and 8.6 cm. The density of the mussel bed was 1800 mussels m^{-2}; however, the mussels in this bed do not stand all upright and the distribution is very randomly, because some mussels are located close to the sand bed while other mussels are located higher in the water column (on top of each other) (see Figure A.2 and 3.1). Consequently not all of these mussels have influence on the hydrodynamics and the appropriate density must be determined.

First the total volume of mussels in the mussel bed is determined assuming that a mussel can be represented with a cylinder. The volume of a mussel can be determined with:

$$V = \pi r^2 l \tag{A.5}$$

Where:

V	$[m^3]$	volume
r	$[m]$	radius
l	$[m]$	length

The volume of a mussel with an average height of 3.85 cm is $0.0385 \times 0.0096^2 \times \pi = 1.121 \times 10^{-5}$. The total volume of mussels (in the experiment of Van Duren et al. (2006)) is $1800 \times 1.121 \times 10^{-5} = 0.0202$ m^3 m^{-2}. The total volume of one square meter mussel bed width an average height of 6.1 cm is $1 \times 1 \times 0.061 = 0.061$ m^3 m^{-2}. Consequently, 33% of the total volume of the mussel bed is mussels. Taking this consistency into account, the top layer has 1136 mussels per square meter.

De Vries et al. (2012) determined the drag coefficient for mussels and oysters using a force transducer. The drag coefficient of mussels is 0.42, while the drag coefficient of oysters is 1.84. The drag coefficient of mussels has been changed during the calibration of the model (representing the experiments of Van Duren et al. (2006)). The 3D vegetation model represents a mussel bed the best with a drag coefficient of 0.6, therefore this drag coefficient is used to represent mussels. The drag coefficient of oysters is unaltered.

An overview of the implemented characteristics of the mussel and oyster patch is presented in Table 3.1.

A.3.3 Measurements above a mussel bed by De Vries

De Vries et al. (2012) measured also the flow velocity and turbulent kinetic energy above a mussel bed. As explained in Section A.1.2, one of the aims of the experiments with mussels was to determine the erosion of faeces from a mussel bed. In case of mussels, all the measurements were conducted above a mussel bed with large amounts of mimicked sediments. These results of this study were investigated with a model.

It can be determined from Figure A.14 that the mimicked sediments have a large effect on the roughness of the mussel bed. The roughness of the mussel bed has decreased significantly and

the roughness length (z_0) of this mussel bed with large amounts of sediment is 0.2 mm. This roughness does not coincide with the roughness length of mussels. The roughness length of mussels is in the order of 3 mm Van Duren et al. (2006); Troost et al. (2009). Thence, the measurements of De Vries et al. (2012) above a mussel bed are not used to calibrate and validate the model.

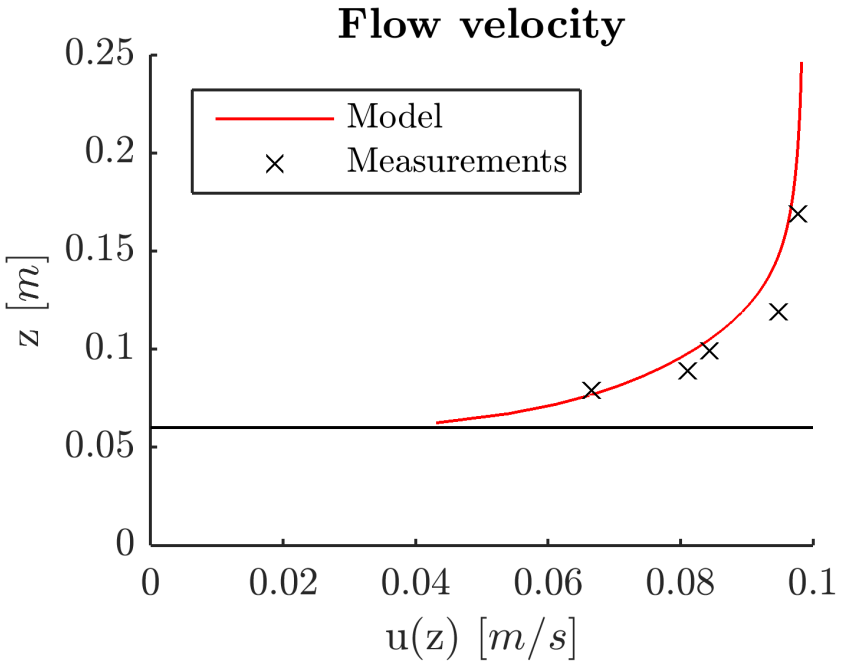

Fig. A.14. The velocity profile above a mussel bed. The horizontal black line indicates the average height of the mussel patch (De Vries et al., 2012).

A.3.4 Wave measurements of De Vries

De Vries et al. (2012) conducted also measurements of the effect of waves on the hydrodynamics above a mussel and oyster patch. The results of this measurements are not usably for this research due to problems with the wave dampener and the roughness of the mussel bed (due to large amounts of mimicked sediments). The results of the influence of waves on the flow above a mussel and oyster bed are therefore not included in this study.

Delft3D-FLOW

B

The influence of mussels and oysters on the hydro- and sediment dynamics is determined using the numerical shallow water model Delft3D-FLOW. Delft3D-FLOW can solve the shallow water equation in two (depht-averaged) or three dimensions (Lesser et al., 2004). In this study, the 3D shallow water equations are used and these equations are presented here. Hereafter, the 3D rigid vegetation model, which is used to implement a bivalve bed, is presented. Finally, the sediment transport equations are described in Section B.3.

B.1 Hydrodynamic

the model in this study uses Delft3D-FLOW to solve the unsteady shallow water equatoin in three dimensions. The system of equations consists of the horizontal momentum equations, the continuity equation, the transport equation and a turbulence closure model. Vertical acceleration are assumed to be small compared to the gravitational acceleration; consequently, the vertical momentum equation is reduced to zero. The equations are solved by applying vertical sigma layers. The amount of layers are constant over the horizontal computational area and for each layer a set of coupled conservations equations are solved. The horizontal momentum equations are (Lesser et al., 2004):

$$\frac{\partial u}{\partial t} + u\frac{\partial u}{\partial x} + v\frac{\partial u}{\partial y} + \frac{\omega}{H}\frac{\partial u}{\partial \sigma} = -\frac{1}{\rho_w}P_u + F_u + \frac{1}{H^2}\frac{\partial}{\partial \sigma}\left(\nu\frac{\partial u}{\partial \sigma}\right) \tag{B.1}$$

$$\frac{\partial v}{\partial t} + u\frac{\partial v}{\partial x} + v\frac{\partial v}{\partial y} + \frac{\omega}{H}\frac{\partial v}{\partial \sigma} = -\frac{1}{\rho_w}P_v + F_v + \frac{1}{H^2}\frac{\partial}{\partial \sigma}\left(\nu\frac{\partial v}{\partial \sigma}\right) \tag{B.2}$$

Where:

u, v, w	$[m\ s^{-1}]$	velocity components in the x, y and z direction, respectively
ω	$[s^{-1}]$	vertical velocity component in sigma coordinate system
H	$[m]$	total water depth
ρ_w	$[kg\ m^{-3}]$	water density
P	$[N\ m^{-2}$ or $kg\ m^{-1}\ s^{-2}]$	pressure gradient
F	$[m\ s^{-2}]$	horizontal Reynold's stresses
ν	$[m^2\ s^{-1}]$	kinematic viscosity

The continuity equations is given by (Lesser et al., 2004):

$$\frac{\partial \omega}{\partial \sigma} = -\frac{\partial \zeta}{\partial t} - \frac{\partial Hu}{\partial x} - \frac{\partial Hv}{\partial y} \tag{B.3}$$

Where:

ζ	$[m]$	water surface elevation above reference level

The vertical eddy viscosity is calculated with the $k-\epsilon$ turbulence closure model. The turbulent energy (k) and the dissipation (ϵ) are produced by production terms represent shear stresses at

the bed, surface and in the flow. (Lesser et al., 2004). The turbulence closure model is extended by Uittenbogaard (2003) to include the influence of cylindrical structures on drag and turbulence (see Section B.2).

B.2 Vegetation model

The vertical velocity profile above a bivalve bed deviates from the general assumed logarithmic profile due to the roughness of the bivalve bed. It is assumed that the vertical velocity profile above a bivalve bed has the same trend as the vertical velocity profile above a vegetated bed (Carrington et al., 2008). According to Baptist et al. (2007) four distinct zones can be identified in the vertical velocity profile above a vegetated bed (see also Figure B.1), namely:

1. The flow velocity is highly influenced by the bed. The vertical velocity profile has a logarithmic pattern in this zone.
2. The second zone is far enough from the bed and far enough from the top of the vegetation, consequently the flow velocity is mostly influenced by the vegetation. A uniform vertical velocity profile is observed.
3. The third zone is near the top of the vegetation and the flow velocity transforms from a uniform velocity profile towards a logarithmic profile.
4. The last zone is the area above the vegetation and the velocity profile is logarithmic.

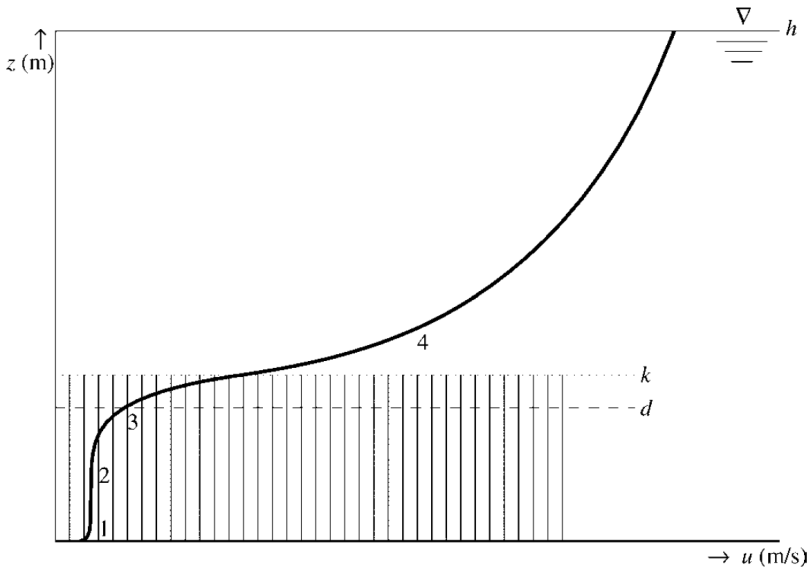

Fig. B.1. The vertical flow velocity profile, including four zones which can be identified for a flow through and above submerged vegetation. h = waterdepth, k = vegetation height, d = zero-plane displacement. Cross-sections of oyster reefs (Baptist et al., 2007).

Vegetation effects (or in this case bivalve effects) can be taken into account in different ways in 3D and 2DH models of Delft3D. The influence of vegetation on hydro- and sediment dynamics can be simulated in a depth averaged (2DH) mode with two different representations, namely a direct method (DPM) and a indirect approximation.

The direct method (or DPM method) takes into account the additional momentum generated by the friction force induced by the vegetation. However, changes in vertical vegetation geometry and changes to vertical fluxes in the momentum equation are not taken into account. The

indirect approximation is based on an artificial Chézy roughness value (Baptist et al., 2007). A disadvantage of a depth averaged model is the disability of calculating changes in the vertical fluxes of the momentum equation (Horstman et al., 2013). The influence of vegetation on the flow velocity, turbulence and Reynolds's stresses in the vertical direction cannot be determined. Moreover, the calibration of the model showed that the influence of a variable bivalve shell height on the turbulence levels was significant (see Figure C.7). This variability in height cannot be included in one of the depth-averaged models. The 3D rigid vegetation model does not have these limitations, as a consequence this model is used to implement a bivalve bed in Delft3D-FLOW. The 3D rigid vegetation model has been validated against laboratory flume experiments by Uittenbogaard (2003). Besides, this model has been calibrated and validated succesfully for salt-marsh vegetation (Temmerman et al., 2005; Bouma et al., 2007).

The roughness of mussels and oysters are implemented in Delft3D with the '(Rigid) 3D vegetation model', because this model takes into account the effect of bivalves on the hydrodynamics. The (rigid) 3D vegetation model is developed by Uittenbogaard (2003), and it represents the flow through and over a porous medium. The vegetation is presented as rigid vertical cylinders and the main input parameter for this model is the plant geometry, such as the density, diameter, height and drag coefficient. The 3D vegetation model takes into account the effect of cylinders on the flow velocity (see Figure B.2).

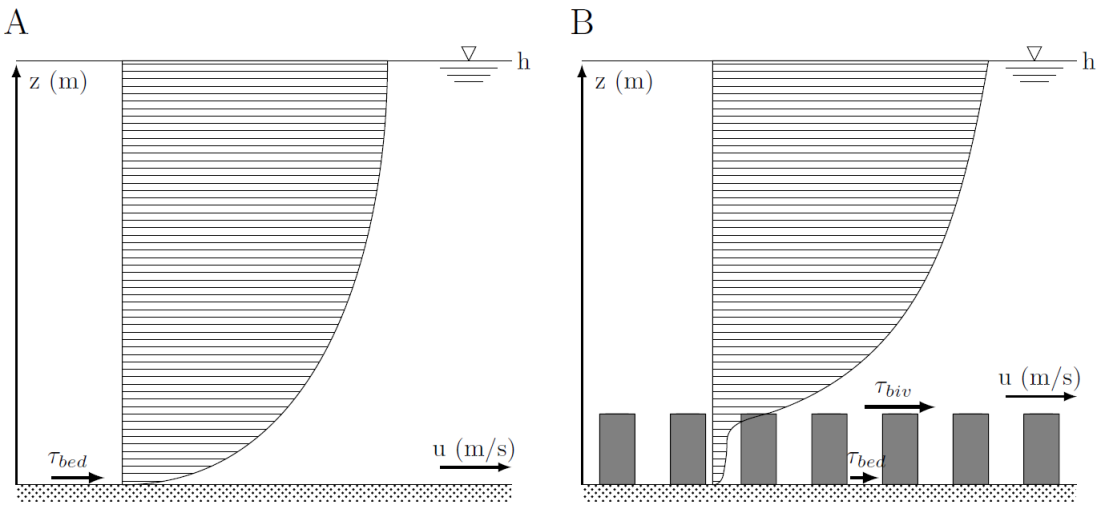

Fig. B.2. (A) Schematic overview of the vertical velocity profile above a flat bottom, including the bed shear stress on the flat bottom. (B) Schematic overview of the vertical velocity profile above a bed with cylinders, including the bed shear stress on the shells and on the sediments on the bottom.

Moreover, to include the effects of the rigid cylinders on the k-ϵ turbulence closure, several processes are included in the rigid 3D vegetation model (Baptist et al., 2007):

- The decrease of the available cross-section for the vertical exchange of momentum, turbulence kinetic energy (TKE) and turbulent dissipation.
- The drag force exerted by the plants.
- The additional turbulence production term due to the cylinders.
- The additional turbulence dissipation term due to the cylinders.

Consequently, a bivalve bed has a significant influence on the turbulence in the water column. There is a turbulence peak around the top of the bivalves and this turbulence will die out towards the bed and towards the water surface. The roughness of mussels and oysters is higher compared

to the roughness of the surrounding bed. If this larger roughness is implemented in Delft3D by increasing the roughness height (k_s), the shear stress on the sediment will also increase (compared to the surrounding bed). However, this is not the case for mussels and oysters. The larger roughness of these bivalves does not result in a larger shear stress on the sediment, because a part of the shear stress is absorbed by the shells of these bivalves, while the other part is absorbed by the bottom. This phenomenon is included in the (rigid) 3D vegetation model, because it includes the reduced flow velocity inside the bivalve bed. In contrast, if a bivalve bed is implemented in a model by increasing the roughness height of the bottom, the model will not include the effect of the bivalves on the bed shear stress (and the hydrodynamics). In this case, the model estimates too high stresses on the sediment between the bivalves and an unrealistic scenario is simulated. A schematic overview of the influence of bivalves on the vertical velocity profile and the bed shear stress is presented in Figure B.2. Hence, the vegetation model combines a large roughness exerted on the flow with a limited force exerted on the sediment in between the plants. A technical description of the sediment transport equations including the equations for the bed shear stress is presented in Appendix B.3.

The effect of vegetation is included in the momentum equation (Uittenbogaard, 2003):

$$\rho_w \frac{\partial u(z)}{\partial t} + \frac{\partial p}{\partial x} = \frac{\rho_w}{1 - A_p(z)} \frac{\partial}{\partial z} \left\{ (1 - A_p(z))(\nu + \nu_T(z)) \frac{\partial u(z)}{\partial z} \right\} - \frac{F_r(z)}{1 - A_p(z)} \tag{B.4}$$

$$A_p(z) = \frac{1}{4} \pi D_{cyl}(z)^2 n(z) \tag{B.5}$$

Where:

$\frac{\partial p}{\partial x}$	$[kg\ m^{-2}\ s^{-2}]$	horizontal pressure gradient
A_p	[-]	solidity of the vegetation measured on a horizontal cross section at vertical level z
ν_T	$[m^2\ s^{-1}]$	eddy viscosity
F_r	$[N\ m^{-3}]$	resistance force
D_{cyl}	$[m]$	diameter of the cylindrical structure
n	$[m^{-2}]$	number of cylinders per unit area

$$F_r(z) = \frac{1}{2} \rho_w C_D a(z) \mid u(z) \mid u(z) \tag{B.6}$$

$$a(z) = d(z) n(z) \tag{B.7}$$

Where:

C_D	[-]	drag coefficient

The influence of the cylinders on the turbulence is included by extra source term of turbulent kinetic energy (Temmerman et al., 2005).

$$\left(\frac{\partial k}{\partial t} \right)_{cylinders} = \frac{1}{1 - A_p(z)} \frac{\partial}{\partial z} \left\{ (1 - A_p(z))(\nu + \nu_T / \sigma_k) \frac{\partial k}{\partial z} \right\} + T(z) \tag{B.8}$$

$$T(z) = F_r(z) u(z) / \rho_w \tag{B.9}$$

Where:

k	$[m^2\ s^{-2}]$	turbulent kinetic energy
T	$[m^2\ s^{-2}]$	work spent by the fluid

The influence of the cylinders on the turbulence is also included by extra source term of turbulent energy dissipation (Temmerman et al., 2005).

$$\left(\frac{\partial \epsilon}{\partial t}\right)_{cylinders} = \frac{1}{1 - A_p(z)} \frac{\partial}{\partial z} \left\{ (1 - A_p(z))(\nu + \nu_T / \sigma_\epsilon) \frac{\partial \epsilon}{\partial z} \right\} + T(z) \tau_\epsilon^{-1} \tag{B.10}$$

Where:

ϵ	$[m^2\ s^{-3}]$	turbulent energy dissipation
τ_ϵ		minimum of τ_{free} or $\tau_{cylinders}$

$$\tau_{free} = \frac{1}{c_{2\epsilon}} \left(\frac{k}{\epsilon}\right) \tag{B.11}$$

$$\tau_{cylinders} = \frac{1}{c_{2\epsilon}\sqrt{c_\mu}} \left(\frac{L^2}{T}\right)^{1/3} \tag{B.12}$$

$$L(z) = C_l \left\{ \frac{1 - A_p(z)}{n(z)} \right\}^{1/2} \tag{B.13}$$

Where:

$c_{2\epsilon}$	[-]	coefficient [= 1.96]
c_μ	[-]	coefficient [= 0.09]
C_l	[-]	coefficient reducing the geometrical length scale to the typical volume averaged turbulence length [= 0.5] scale

B.3 Transport equations

The hydrodynamics are calculated with the equations in Section B.1 and B.2. Hereafter, the sediment dynamics can be computed. The sediment dynamics are computed for two types of environments, namely a cohesive and a non-cohesive environment. The computations in a cohesive and a non-cohesive environment are different. Section B.3.1 presents the sediment equations for a cohesive environment, while Section B.3.2 present the equations for a non-cohesive environment.

B.3.1 Cohesive sediment

Cohesive sediments are fine sediments (grain size $<$ 0.063 mm) and these sediments behave different than 'normal' non-cohesive sediments (sands). Cohesive sediments are generally referred to as mud. Electromagnetic forces are important in a cohesive environment, these forces can bind sediment together (creating large flocs). Moreover, these forces can increase the resistance of the sediment at the bottom to erosion.

There are large differences in the settling velocity of cohesive sediments due to the binding capability of the sediment (flocculation). The larger flocs have a higher settling velocity and deposit therefore quicker to the sea bed. The flocs can be destructed due to turbulent shear

stresses. The implementation of cohesive sediments is simplified in this study, the formation of flocs is ignored. Consequently, the settling velocity of cohesive sediment is constant.

Three dimensional transport of suspended sediment is calculated by solving the three dimensional advection-diffusion equation for suspended sediment (Deltares, 2014):

$$\frac{\partial c}{\partial t}+\frac{\partial uc}{\partial x}+\frac{\partial uc}{\partial y}+\frac{\partial (w-(w_s+fr)c}{\partial z}=\frac{\partial}{\partial x}\left(\epsilon_{s,x}\frac{\partial c}{\partial x}\right)+\frac{\partial}{\partial y}\left(\epsilon_{s,y}\frac{\partial c}{\partial y}\right)+\frac{\partial}{\partial z}\left(\epsilon_{s,z}\frac{\partial c}{\partial z}\right)=E-D \tag{B.14}$$

Where:

c	$[kg\ m^{-3}]$	mass concentration of sediment fraction
$\epsilon_{s,x}$, $\epsilon_{s,y}$ and $\epsilon_{s,z}$	$[m^2\ s^{-1}]$	eddy diffusivities of sediment fraction
w_s	$[m\ s^{-1}]$	(hindered) sediment settling velocity of sediment fraction

The fluxes between the water phase and the bed are calculated with the Partheniades-Krone formulations (Partheniades, 1965).

$$E=M\ S(\tau_{cw},\tau_{cr,e}) \qquad S(\tau_{cw},\tau_{cr,e})=\begin{cases}\left(\frac{\tau_{cw}}{\tau_{cr,e}}-1\right), & \text{when } \tau_{cw}>\tau_{cr,e}\\ 0, & \text{when } \tau_{cw}\leq\tau_{cr,e}\end{cases} \tag{B.15}$$

$$D=w_s\ c_b\ S(\tau_{cw},\tau_{cr,d}) \qquad S(\tau_{cw},\tau_{cr,d})=\begin{cases}\left(1-\frac{\tau_{cw}}{\tau_{cr,d}}\right), & \text{when } \tau_{cw}<\tau_{cr,d}\\ 0, & \text{when } \tau_{cw}\geq\tau_{cr,d}\end{cases} \tag{B.16}$$

Where:

E	$[kg\ m^{-2}\ s^{-1}]$	erosion flux
M	$[kg\ m^{-2}\ s^{-1}]$	erosion rate
$S(\tau_{cw},\tau_{cr,e})$	[-]	erosion step function
D	$[kg\ m^{-2}\ s^{-1}]$	deposition flux
c_b	$[kg\ m^{-3}]$	sediment concentration in the near bottom computational layer
$S(\tau_{cw},\tau_{cr,d})$	[-]	deposition step function
τ_{cw}	$[N\ m^{-2}]$	bed shear stress due to currents and waves
$\tau_{cr,e}$	$[N\ m^{-2}]$	critical bed shear stress for erosion
$\tau_{cr,d}$	$[N\ m^{-2}]$	critical bed shear stress for deposition

Waves are neglected in this study, consequently, the bed shears stress is only based on the currents. The bed shear stress (τ_b) is related to the current just above the bed (Deltares, 2014):

$$\tau_{b,3D}=\frac{g\rho_w|\vec{u_b}|\vec{u_b}}{C_{3D}^2} \tag{B.17}$$

The first grid point above the bed is assumed to be situated in the logarithmic boundary layer and the shear velocity is determined with:

$$\vec{u_b}=\frac{\vec{u_*}}{\kappa}ln\left(1+\frac{\Delta z_b}{2z_0}\right) \tag{B.18}$$

Where:

The bed shear stress is defined as:

u_b	$[m\ s^{-1}]$	horizontal flow velocity in the first layer above the bed
C^2_{3D}	$[m^{1/2}\ s^{-1}]$	Chézy roughness
u_*	$[m\ s^{-1}]$	shear velocity
Δz_b	$[m]$	distance to the computational grid point closest to the bed
z_0	$[m]$	roughness height

$$\tau_{b,c} = \rho_w |u_*| u_* \tag{B.19}$$

B.3.2 Non-cohesive sediment

The influence of a mussel and oyster bed is also determined in a sand dominated environment. The sediment dynamics are differently calculated in s sand dominated environment. In this study the method of Van Rijn et al. (2004) is used to calculate the sediment transport. They distinguish sediment transport in bedload transport and suspended load transport. The exchange of sediment with the bed is governed by the boundary condition:

$$-w_s c - \epsilon_z \frac{\partial c}{\partial z} = D - E \tag{B.20}$$

The bed load transport in direction x is determined with (Van Rijn et al., 2004):

$$S_{b,x} = 0.006 \rho_s w_s d M^{0.5} M_e^{0.7} \tag{B.21}$$

Where:

S_b	$[kg\ m^{-1}\ s^{-1}]$	bedload transport
ρ_s	$[kg\ m^{-3}]$	density of sediment
d	$[m]$	median sediment diameter
M	[-]	sediment mobility number due to waves and currents
M_e	[-]	excess sediment mobility number

The sediment mobility number (M) and the excess sediment mobility number (M_e) are defined as:

$$M = \frac{v_{eff}^2}{(\rho_s/\rho_w - 1) g d} \tag{B.22}$$

$$M_e = \frac{(v_{eff} - v_{cr})^2}{(\rho_s/\rho_w - 1) g d} \tag{B.23}$$

$$v_{eff} = \sqrt{v_R^2 + U_{on}^2} \tag{B.24}$$

Where:

v_{eff}	$[m\ s^{-1}]$	effective velocity due to currents and waves
v_{cr}	$[m\ s^{-1}]$	critical depth averaged velocity for initiation of motion
v_R	$[m\ s^{-1}]$	magnitude of an equivalent depth-averaged velocity computed from the velocity in the bottom computational layer, assuming a logarithmic velocity profile
U_{on}	$[m\ s^{-1}]$	near-bed orbital velocity

Waves are neglected in this study, consequently, U_{on} is zero. The suspended sediment concentration is calculated with the advection-diffusion equation (Equation B.14). Suspended sediment includes all the transport above a certain reference (the reference height) Van Rijn et al. (2001).

$$c_a = 0.015 \rho_s \frac{d T_a^{1.5}}{a D_*^{0.3}} \tag{B.25}$$

Where:

c_a	$[kg\ m^{-3}]$	mass concentration at reference height
T_a	[-]	non-dimensional bed shear stress
a	[m]	reference height
D_*	[-]	non-dimensional particle diameter

$$T_a = \frac{u_c \tau_{b,c} - \tau_{cr}}{\tau_{cr}} \tag{B.26}$$

$$a = 0.01 H \tag{B.27}$$

Where:

u_c	[-]	efficiency factor
$\tau_{b,c}$	$[N\ m^{-2}]$	bed shear stress due to currents

The bed shear stress is calculated with Equation B.17. The suspended load transport is determined with:

$$S_{s,x} = \int_a^H \left(uc - \epsilon_{s,z} \frac{\partial c}{\partial x} \right) dz \tag{B.28}$$

$$S_{s,y} = \int_a^H \left(vc - \epsilon_{s,z} \frac{\partial c}{\partial y} \right) dz \tag{B.29}$$

Where:

S_s	$[kg\ m^{-1}\ s^{-1}]$	suspended load transport

The total sediment transport is based on the bedload transport and the suspended load transport:

$$(1 - \epsilon_p) \frac{\partial z_b}{\partial t} + \frac{\partial (S_{b,x} + S_{s,x})}{\partial x} + \frac{\partial (S_{b,y} + S_{s,y})}{\partial y} = 0 \tag{B.30}$$

Where:

ϵ_p	[-]	bed porosity [= 0.4]

B.3.3 Flow velocity and bed shear stress

The flow velocity in a grid cell is determined with the continuity equation (Equation B.3). The discharge in one grid cell can be determined with Equation B.31.

$$Q = u\ A \tag{B.31}$$

Where:

The flow velocity is the averaged flow velocity in the grid cell over the time step (the calculated time step in Delft3D). However, the continuity equation does not take into account a decreased

Q	$[m^3\ s^{-1}]$	discharge
u	$[m\ s^{-1}]$	flow velocity
A	$[m^2]$	cross-section

cross section due to the blockade of the flume by the shells (cylinders). In case of a vegetated bed, the blockade of the flume by the vegetation is low (± 5%). However, in case of a bivalve bed, the blockade of the flume by the shells is significan (± 30%) and taken this blockade into account can result in higher flow velocities and bed shear stresses inside the bivalve bed. The flow velocity should take into account the decreased flow area with:

$$\begin{aligned} u_{por} &= \tfrac{u}{P} \\ A_{por} &= \tfrac{A}{P} \\ Q &= u_{por}\ A_{por} \end{aligned} \tag{B.32}$$

Where:

u_{por}	$[m\ s^{-1}]$	flow velocity accounted for the decreased area due to blockade
A_{por}	$[m^3\ s^{-1}]$	cross-section accounted for the decreased area due to blockade
P	[-]	porosity

The flow velocity is increased, because it takes into account the decrease in the cross-section.

B.3.4 Model and boundaries

The flow needs time and space to adapt at the boundaries and model conditions. The model dimensions must therefore be large enough to prevent an effect of the boundaries on the hydro- and sediment dynamics. The sediment must also adapt between the boundaries and the hydrodynamics. The boundaries must be far enough away from the area of interest in order te prevent the influences of the boundaries on the model results.

The most dominant parameter in the determination of the model dimensions is the settling velocity of the cohesive sediment. Cohesive sediment is very light and can be travel large distances due to this small settling velocity. Cohesive sediment needs the largest length scales to adapt between the boundaries and model conditions. The settling velocity of cohesive sediment is 0.5 mm s^{-1}, the water depth while the water depth in the reference model is 1.5 m. The maximum water depth that has been tested is 2 m. The maximum flow velocity in the reference model is 0.5 m s^{-1}. The flow is assumed to be adjusted to the model if the sediment can settle half of the water depth. A maximum depth of 2 m is used

Thence, the flow is adjusted after:

$$\frac{1}{0.5 \times 10^{-}3} * 0.5 = 1000\ m \tag{B.33}$$

The length of the model must be at least 2000 m (1000 m for each bidirection direction), excluding the length in the area of interest. The total length in of the model is 2200 m. The flow velocity normal to the tidal flow is approximately zero. Hence, the width of the model does not need a length scale of at least 2000 m. A width of 300 m is sufficient to simulate the effect of a mussel or oyster bed on the hydro and sediment dynamics.

C Sensitivity analysis & other results

This appendix presents the sensitivity analysis of the bivalve characteristics on the hydrodynamics (in the flume model) and the influence of bivalve and environment characteristics on the hydro and sediment dynamics (in the field model). Besides, some detailed results area presented in this Appendix.

C.1 Flume model

This section presents the sensitivity analysis of the flume model, the influence of a random shell height on the results and the turbulent kinetic energy (TKE) in the streamwise direction.

C.1.1 Random shell height

The variation of the bivalve bed height is determined randomly. It is possible that this random function has a positive or negative influence on the model results. Both models have simulated with several different random bed height in order to determine the influence of this random function on the model results. The influence of several random function on the flow velocity and TKE is presented in Figure C.1. Different random bed heights have hardly any effect on the flow velocity profile above the mussel bed, while they have an effect on the TKE above the mussel bed. Different random heights can increase and decrease the TKE peak with $\pm$ 14%, and the random function has an effect on the TKE. However, the simulations of both models are not very dependent on this random variability and the variations of these model results are within the range of acceptance taking into account other uncertainties and assumptions, such as the composition of (pseudo)faeces and the effect of the model on a larger scale.

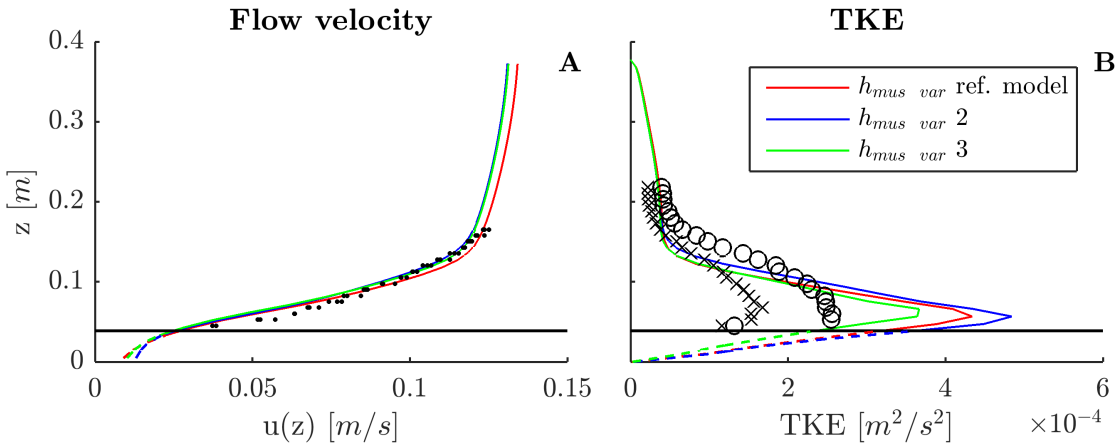

Fig. C.1. Velocity profile (A) and TKE (B) above a mussel patch at intermediate flow velocity for different random distributions of the bed height (red, blue and green line). The measurements conducted by Van Duren et al. (2006) are indicated with black marks. Two TKE levels were measured, namely the turbulence levels above active mussels (black circles) and above inactive mussels (black crosses). The black horizontal line indicates the average mussel height.

C.1.2 Longitudinal TKE

The velocity profiles and TKE are not developed at the measurement location (a lengthwise distance of 11.1 m). This development is especially visible in Figure C.2, because the TKE is still increasing above the mussel patch. According to Figure C.2, the peak turbulence occurs just above the canopy of the bivalve bed and this peak is increasing in the longitudinal direction. This corresponds with the measurements of Okamoto and Nezu (2013), because they concluded that the Reynolds stresses peak occurs at the top of the canopy and this peak is also increasing in the lengthwise direction. In contrast to the flow velocity, there is a difference between the TKE above a mussel patch with a constant height and above a mussel patch with a variable height (for the lengthwise direction). Firstly, the TKE is a lot larger above a constant bed height. Moreover, the effect of a variable mussel bed height is clearly visible in Figure C.2 B, because the TKE does not develop linearly like the TKE does above a constant bed height.

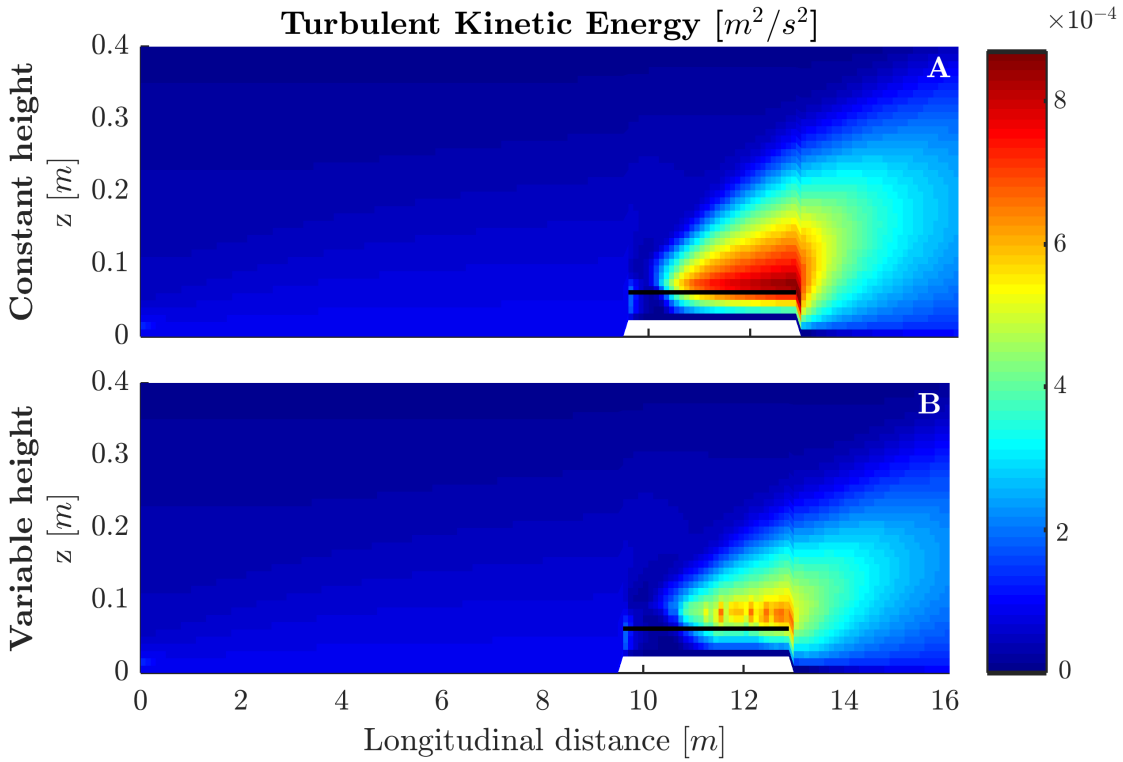

Fig. C.2. TKE along the flume above a mussel patch with a constant height (A) and a variable height (B) (for intermediate velocity). The TKE is averaged over the width of the flume. The measurement location of Van Duren et al. (2006) is at 11.1 m. The black horizontal line indicates the average mussel height.

C.1.3 Close-up

Figure C.3 presents a close up of Figure 4.9, because the measurements and model simulations of the flow velocity and turbulence levels above an oyster patch with a variation within the cell is hardly visible in Figure 4.9.

C.1.4 Sensitivity analysis of flume model

The implementation of a mussel and oyster bed is depended on several parameters, such as the density, the diameter, the shell height and the drag coefficient (see Appendix B.2). Most of these parameters are depended on the characteristics of the bivalve bed. For example, the density and

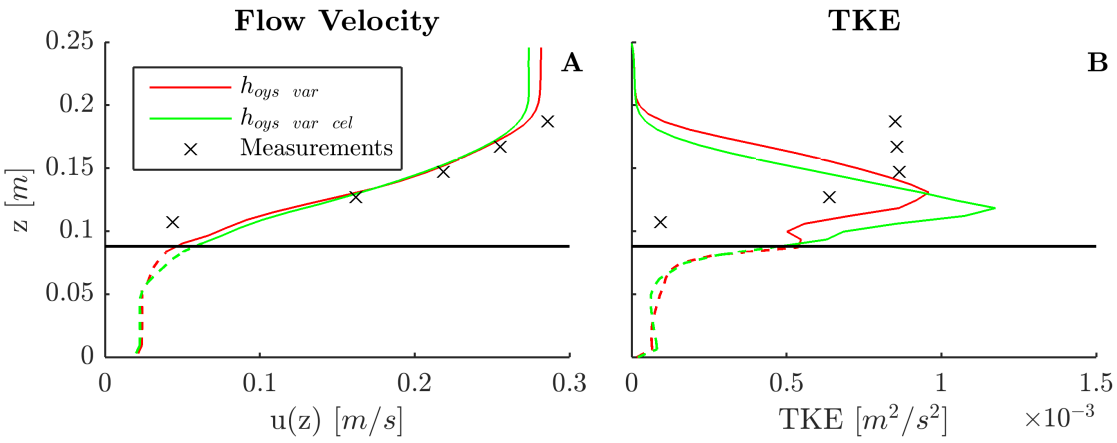

Fig. C.3. Velocity profile (A) and TKE (B) above an oyster patch at intermediate flow velocity. The results of this figure are similar to the results of Figure 4.9, only without the simulations of $h_{oys\ var\ grid}$. The measurements conducted by De Vries et al. (2012) and are indicated with black crosses. The black horizontal line indicates the average oyster height.

shell height is depended on the age of a bivalve bed, the hydrodynamic forces and the availability of food. The influences of several parameters are investigated in this section.

C.1.4.1 Density, diameter and drag coefficient

The density, the diameter and the drag coefficient are increased and decreased with 20% (relative to the reference model settings, see Table 3.1) to determine the influence of each parameter on the flow velocity and turbulence pattern above the bed. The influence of the density, diameter and drag coefficient on the flow velocity and turbulent kinetic energy (TKE) is identical according to Figure C.4, C.5 and C.6. An increase or decrease of these parameters has hardly any influence on the flow velocity above a bivalve bed. In contrast, an increase of these parameters has results in an increase of the turbulence at the top of the canopy, while a decrease of these parameters results in a decrease of the turbulence at the top of the canopy. The three parameters have a similar influence on the turbulence, because these parameters are all proportionate relative to the resistance force (Equation B.6). The increase of the density, diameter or drag coefficient with 20% will result in the same resistance force on the flow.

C.1.4.2 Shell height

The shell height of each shell is also increased and decreased with 20% relative to the reference model settings (Table 3.1). The lower shells have a less absolute increase (in cm) relative to the higher shells, consequently an increase of the shell height with 20% results also in an increase of the variation between the highest and lowest shells with 20% (and otherwise). The influence of the shell height on the flow velocity and turbulence levels above a bivalve bed is significant (see Figure C.7). A decrease of the shell height results in higher near bed velocities and higher turbulence levels at the top of the canopy. The near bed velocities are lower if the shell height is increased with 20%.

The turbulence levels are reduced if the shell height is increased, because the variation of the shell height is increased. The opposite effect is visible if the shell height is decreased; the turbulence at the top of the canopy is strongly increased in this case. A larger shell height will block a larger part of the generated flow; moreover the production of turbulence at the top of each shell has a

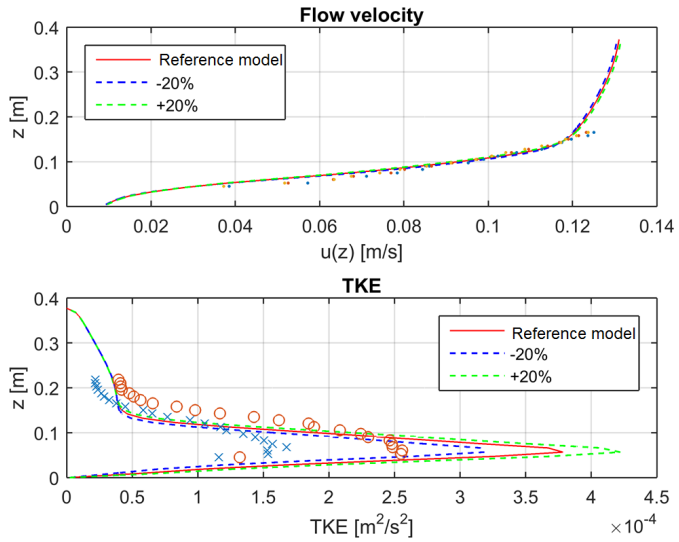

Fig. C.4. Velocity profile (upper) and TKE (lower) above a mussel patch at intermediate flow velocity, whereby the density of the bivalve patch is varied. The measurements conducted by Van Duren et al. (2006) are indicated with black the dots, crosses and circles. Two TKE levels were measured, namely the turbulence levels above active mussels (circles) and above inactive mussels (crosses). The reference model indicates the model with a variable bed height per grid cell (Figure 4.2)

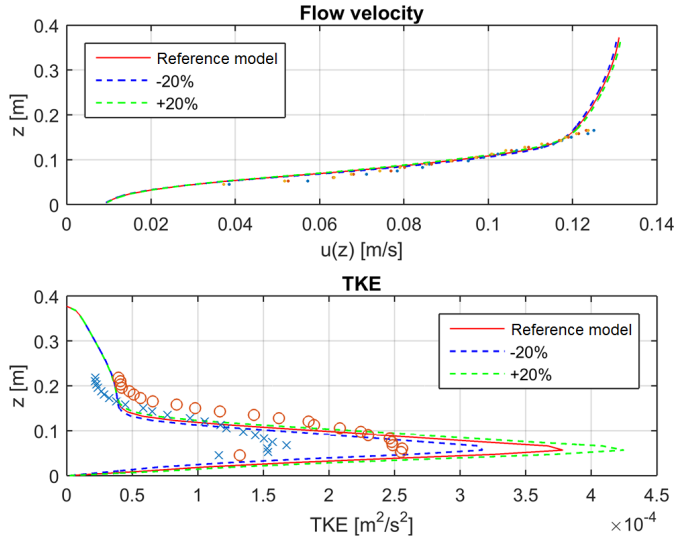

Fig. C.5. Velocity profile (upper) and TKE (lower) above a mussel patch at intermediate flow velocity, whereby the bivalve diameter is varied. The measurements conducted by Van Duren et al. (2006) are indicated with black the dots, crosses and circles. Two TKE levels were measured, namely the turbulence levels above active mussels (circles) and above inactive mussels (crosses). The reference model indicates the model with a variable bed height per grid cell (Figure 4.2)

larger variation and will be more spread out over the water column. The variation of the shell height in the reference model corresponds with the measurements of the flume studies.

The variation has a large influence on the height has a significant influence on the turbulence levels, moreover the increase or decrease of this variation will affect the correspondence of the simulated flow velocity with the measurements negatively.

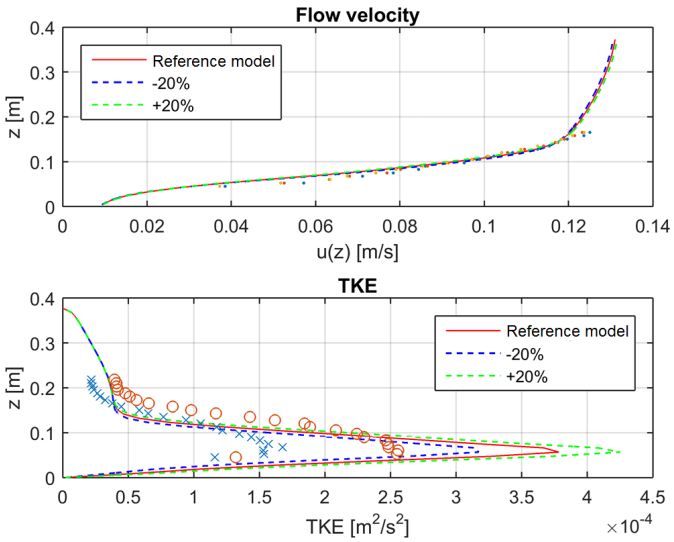

Fig. C.6. Velocity profile (upper) and TKE (lower) above a mussel patch at intermediate flow velocity, whereby the drag coefficient is varied. The measurements conducted by Van Duren et al. (2006) are indicated with black the dots, crosses and circles. Two TKE levels were measured, namely the turbulence levels above active mussels (circles) and above inactive mussels (crosses). The reference model indicates the model with a variable bed height per grid cell (Figure 4.2)

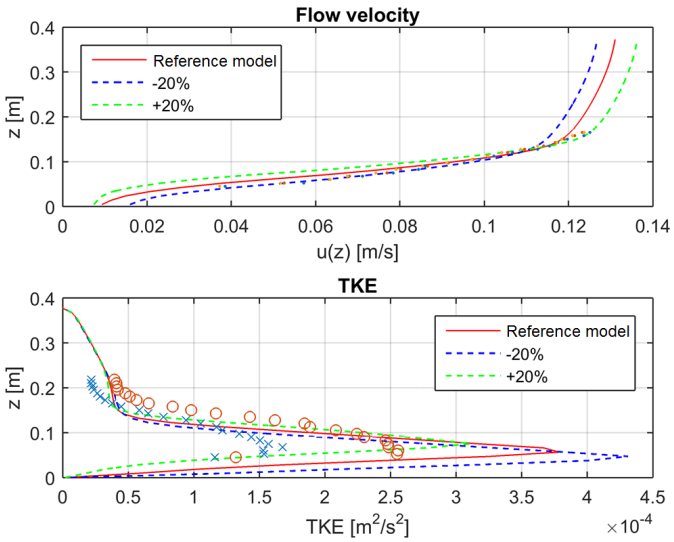

Fig. C.7. Velocity profile (upper) and TKE (lower) above a mussel patch at intermediate flow velocity, whereby the shell height is increased/decreased. The measurements conducted by Van Duren et al. (2006) are indicated with black the dots, crosses and circles. Two TKE levels were measured, namely the turbulence levels above active mussels (circles) and above inactive mussels (crosses). The reference model indicates the model with a variable bed height per grid cell (Figure 4.2)

C.2 Field model

The effects of mussels and oysters on the flow velocities, bed shear stress and sediment dynamics are presented in Section 5. However, these effects are determined for a pre-defined set of parameters. These set of parameters are based on several studies, such as Brinkman et al. (2002) and Van Ledden (2003). In this section the sensitivity of the model to these parameters is presented. The parameters can be divided in parameters that are influenced by the environment, in this case the flow velocity, and parameters that are influenced by the bivalve bed, such as

the height of the bed, the density, the height of the shells and the filtration rate. The influence of these parameters on the bed shear stress and cumulative sedimentation in the center of the bivalve patch is also presented in Table C.1 and C.2.

Tab. C.1. The bed shear stress (N m^{-2}) in the center of the model (center of the bivalve bed). The height of the bivalve shells indicate the reduction of this height relative to the average shell height.

	Bare bed	Mussels	Oysters
Reference	0.69	0.060	0.012
Velocity			
u = 0.3 m/s	0.32	0.028	0.006
u = 0.4 m/s	0.47	0.041	0.008
u = 0.6 m/s	1	0.086	0.016
Height base			
0 m	-	0.051	0.008
0.4 m	-	0.070	0.012
Height bivalves shells			
-25%	-	0.075	0.020
-50%	-	0.086	0.078
-75%	-	0.110	0.125
Density			
-25%	-	0.079	0.046
-50%	-	0.109	0.077
-75%	-	0.178	0.135

C.2.1 Flow velocity

The effects of a mussel and oyster bed on the hydrodynamics and sediment dynamics is determined for a maximum tidal flow velocity of 0.5 m s^{-1}. According to Brinkman et al. (2002), mussel beds are present at a large scale of flow velocities, namely between 0.3 and 1 m s^{-1}. The flow velocities at several mussel beds is also investigated with the PACE model (Duran-Matute et al., 2014; Van Kessel, 2015). Most mussel beds occur at maximum flow velocities of 0.2 - 0.4 m s^{-1} (measured for in the period January 2009). The flow velocity will therefore be varied between 0.3 and 0.6 m s^{-1} to determine the effect of velocity on the hydro- and sediment dynamics. Moreover, the influence of an extreme flow velocity has also been tested (maximum tidal flow velocity = 1 m s^{-1}).

Figure C.8 presents the bed shear stress for three different flow velocities, namely 0.4, 0.5 (the reference situation) and 0.6 m s^{-1} (note the scale difference between Figure C.8 A, B and C). This variation in flow velocities have an influence on the stresses exceeds on the bottom. The bed shear stress at a bare bottom varied from 0.47 up to 1 N m^{-2} for a variation in flow velocities of 0.4 and 0.6 m s^{-1}. There is hardly any cohesive sediment transport at flow velocities of 0.4 m s^{-1} or lower, because the bed shear stress does not exceed the critical bed shear stress. The sediment transport of non-cohesive sediment is also very low at 0.3 m s^{-1}, consequently the results of a flow velocity of 0.3 m s^{-1} are not presented here.

The bed shear stress inside the mussel or oyster patch is low for all three flow velocities. The bivalves slow down the flow and the bed shear stress decreases significantly. The maximum bed shear stress inside the center mussel and oyster bed for a flow velocity of 0.6 m s^{-1} are 0.09 and

Tab. C.2. The cumulative sedimentation/erosion (m) in the center of the model (center of the bivalve bed). The height of the bivalve shells indicate the reduction of this height relative to the average shell height. This height reduction of 25, 50 and 75% correspond with a height reduction of 1, 2 and 3 cm in case of mussels and a height reduction of 2.2, 4.4 and 6.6 cm in case of oysters.

	Bare bed		Mussels		Oysters	
$\times 10^{-3}$	Cohesive	Non-cohesive	Cohesive	Non-cohesive	Cohesive	Non-cohesive
Reference	0.5	-0.1	4.91	3.58	3.28	2.66
Velocity						
u = 0.3 m/s	1.58	-0.0017	1.88	0.0006	1.28	0.0005
u = 0.4 m/s	1.95	-0.019	2.42	0.3	1.64	0.202
u = 0.6 m/s	-3.28	-0.45	10.4	17.8	6.92	13.5
Height base						
0 m	-	-	4.97	4.37	3.32	3.27
0.4 m	-	-	4.85	2.82	3.23	1.93
Height bivalves						
-25%	-	-	4.93	3.91	3.29	2.77
-50%	-	-	4.96	4.83	3.3	3.19
-75%	-	-	4.98	9.43	3.37	4.47
Density						
-25%	-	-	4.92	3.72	3.29	2.76
-50%	-	-	4.94	3.93	3.31	2.98
-75%	-	-	4.97	4.52	3.35	3.35
Filtration						
0 mm/s	-	-	3.35	3.57	-	-
0.5 mm /s	-	-	6.4	3.6	-	-

0.02 N m^{-2}, respectively. An extreme flow velocity of 1 m s^{-1} does also not result in erosion inside the mussel or oyster bed, because the bed shear stress do not exceed the critical bed shear stress. The bed shear stress on a bare bottom is 2.73 N m^{-2}, while the bed shear stress inside the mussel and oyster bed are 0.23 and 0.04 N m^{-2}, respectively, for this extreme flow velocity. The bed shear stress never exceeds the critical bed shear stress and according to this model currents cannot erode sediment inside a bivalve bed.

The amount of sedimentation inside the mussel or oyster patch differs with the flow velocity. The highest sedimentation rates occur at the highest flow velocities, because high flow velocities transport a lot of sediment and increase the sediment concentration in the water column. A part of these sediments flows over the bivalve bed and these sediments settle in the bivalve bed due to the decreased flow velocities near the bed. Higher flow velocities lead to higher sediment availability above the bivalve bed (and higher sedimentation rates inside the bed). Once sediments have settled inside the bivalve bed, the sediments are trapped due to the small bed shear stresses. Low flow velocities lead to the opposite effect. The lowest sedimentation rates occur at the lowest flow velocities.

The bed shear stress has a similar pattern for all three flow velocities and the main difference is the magnitude of the bed shear stress. This similar stress pattern results also in similar cumulative sedimentation/erosion patterns for cohesive and non-cohesive sediments (see Figure C.9 and C.10). Thence, the flow velocity does not affect the sedimentation/patterns. The differences in

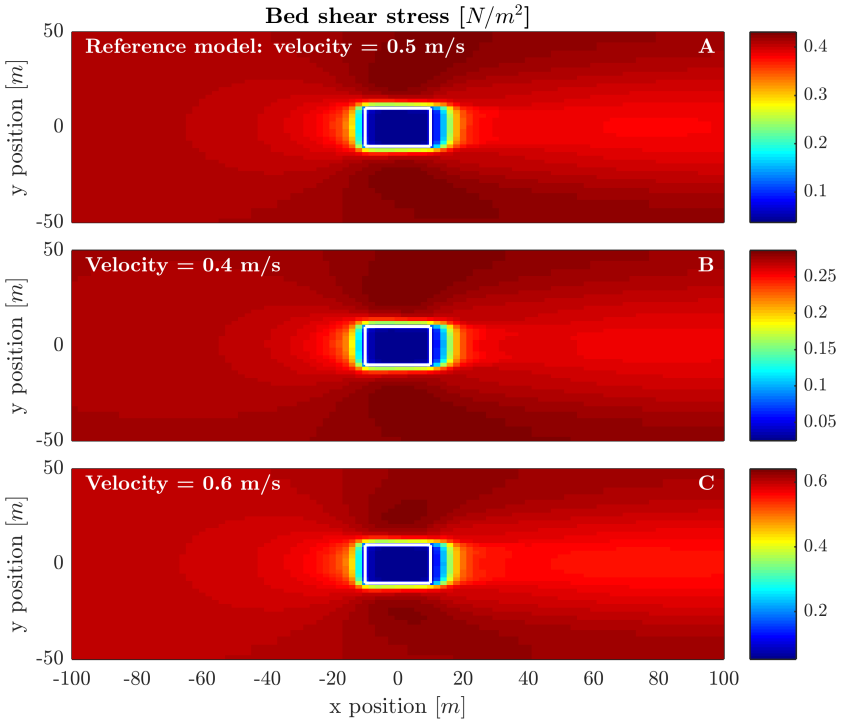

Fig. C.8. The bed shear stress inside and around a mussel bed for different flow velocities. (A) the reference model with a maximum flow velocity of 0.5 m s^{-1}, (B) and (C) model with a maximum flow velocity of 0.4 and 0.6 m s^{-1}, respectively. The white framed box indicates the location of the bivalve bed. Note the difference in colour scale between (A), (B) and (C).

accumulation patterns between mussel and oyster beds can also be distinguished with different flow velocities.

C.2.2 Base height of bivalves

A mussel and oyster bed is elevated relative to the surrounding area and these elevated areas can have heights from several centimeters to even 1 meter. The height of the bivalve bed without the shells is 20 cm in the reference model (this height is called base height, see Figure 3.2. The base height is varied from 0 cm till 40 cm to determine the influence of the base height on the hydro- and sediment dynamics.

A variation in the base height does not significantly change the flow velocities inside the bivalve patch (Figure C.11). In contrast, an increased base height does increase the flow routing, because the cross section above the bivalve bed decreases. This increase of height cause more erosion at the LR sides of the bivalve patch, while there is a calmer condition at the lee side of the patch resulting in more sedimentation behind the patch. More sediment is eroded directly at the lee side of the patch (for a non-cohesive environment) of the patch with the lower base height and these dynamics can be accounted for the increased flow velocities above the patch as a consequence the bed shear stress behind the patch increases (more) (see Figure C.12).

The sedimentation rates inside the bivalve bed are higher and lower for a base height of 0 and 40 cm, respectively. These higher and lower rates are hardly visible in a cohesive environment (due to the high sediment concentrations in the whole water column). The rates are significant higher and lower in a non-cohesive environment and can partly be ascribed to the suspended

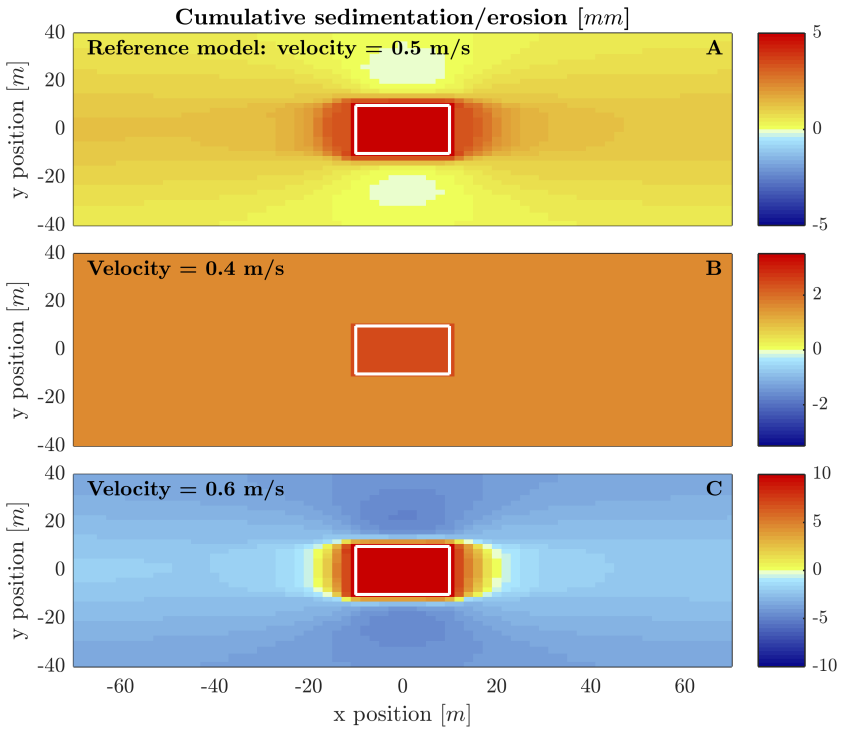

Fig. C.9. The cumulative sedimentation/erosion inside and above a mussel bed after two days in a cohesive environment. (A) the reference model with a maximum flow velocity of 0.5 m s^{-1}, (B) and (C) model with a maximum flow velocity of 0.4 and 0.6 m s^{-1}, respectively. The white framed box indicates the location of the bivalve bed. Note the difference in colour scale between (A), (B) and (C).

sediment concentration in the water column. The highest SSC occurs near the bottom in the non-cohesive environment (Figure 5.1). The maximum SSC at 20 and 40 cm is 0.023 and 0.007 kg m^{-3}, respectively (for a bare bottom). The sediment concentration at 40 cm is significant lower than at 20 cm, as a consequence less sediment is transported of the bivalve patch, so less sediment can settle in the patch.

C.2.3 Height bivalve shells & Density

The height of the bivalve shells and the density of the bivalve bed are important parameters that determine the roughness of the bed. Moreover, these parameters have an influence on the bed shear stress which is imposed on the sediment inside the bivalve patch. The porosity of the patch increases if the density decreases, as a consequence the resistance force of the bivalve patch decreases as well (see Section B.2). The influence of an decrease in density, diameter and drag coefficient on the flow velocity and turbulence is similar, consequently the influence of these parameters has only be tested by changing one of these parameters (see Section C.1). The cross sectional area above the patch increases if the height of the bivalve shells decreases. The roughness of the bivalve bed decreases if the height of the bivalve shells or the density decreases. The height of the bed is reduced with 25, 50 and 75% of the average bivalve height.

The increase in porosity and cross sectional area and a decrease in roughness result in less flow routing (comparing Figure C.17A with Figure C.17 (B and C). A larger part of the water flows over the bivalve bed and the flow velocity increases (see Figure C.15 and C.16). The flow velocity increases more in the lower and middle part of the water column in the case of a reduction of the shell height compared to a reduction of the density; however, the flow velocity inside the

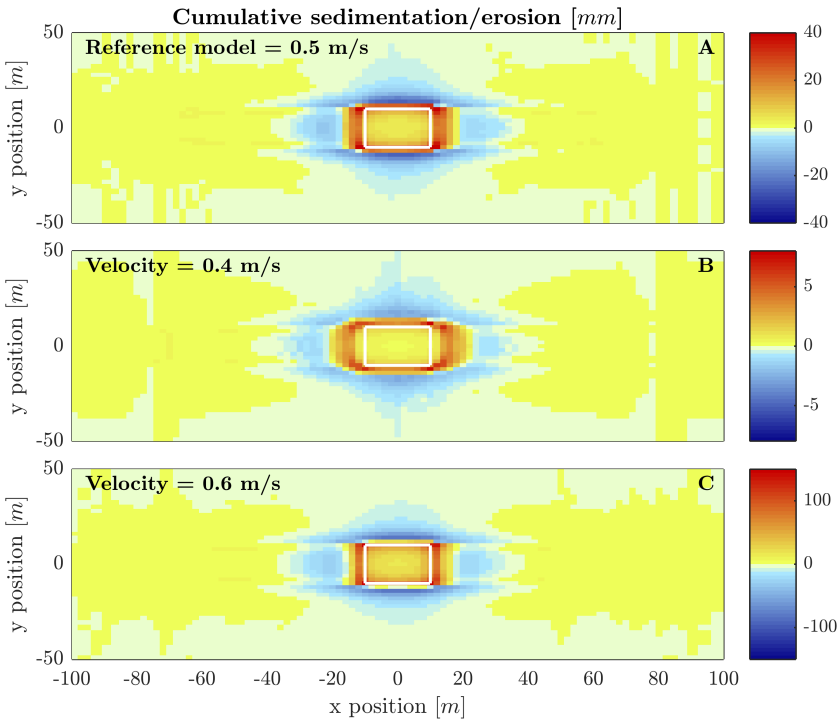

Fig. C.10. The cumulative sedimentation/erosion inside and above a mussel bed after two days in a non-cohesive environment. (A) the reference model with a maximum flow velocity of 0.5 m s^{-1}, (B) and (C) model with a maximum flow velocity of 0.4 and 0.6 m s^{-1}, respectively. The white framed box indicates the location of the bivalve bed. Note the difference in colour scale between (A), (B) and (C).

bivalve bed is higher if the density is reduced (Figure C.16). Consequently, a reduction in density results in a higher bed shear stress than a reduction in the shell height, namely 0.11 and 0.086 N m^{-2}, respectively. Thence, shell height reduction leads to less flow routing in comparison with a density reduction, so the sediment accumulation behind the bivalve bed is less if you compare accumulation rates behind both patches (Figure C.18 and C.19).

C.2.4 Filtration rate

Mussels and oysters filter the water column for food and they produce hereby (pseudo)faeces. As explained in Section 2.3.1.2, there is a difference between the (pseudo)faeces of mussel and oysters. The faeces of mussels are heavy and they settle in and around the mussel bed, while the faeces of oysters are light and they are transported in the water column (they do not (or hardly) settle in and around the oyster patch). So, mussels increase the sediment flux towards the bed due to their activity and this extra flux of sediment is implemented in Delft3D with the filtration rate. The filtration rate is an increased settling velocity in the lowest layers of the water column above the mussel bed. The influence of the filtration rate is determined in this section.

The filtration rate is estimated based on the measurements of Widdows et al. (1979) and the hydrodynamic conditions in the model (see Section 3.1.2.1). Several assumptions have been made to estimate the filtration rate, namely: the filtration rate is 1.5 l h^{-1} ind^{-1}, the filtration rate is constant and the water is partly re-filtered by mussels. However, it is difficult to estimate a representative filtration rate, because the filtration rate is depended on many things, for example the SSC in the water column. The filtration rate will therefore be varied to determine the influence

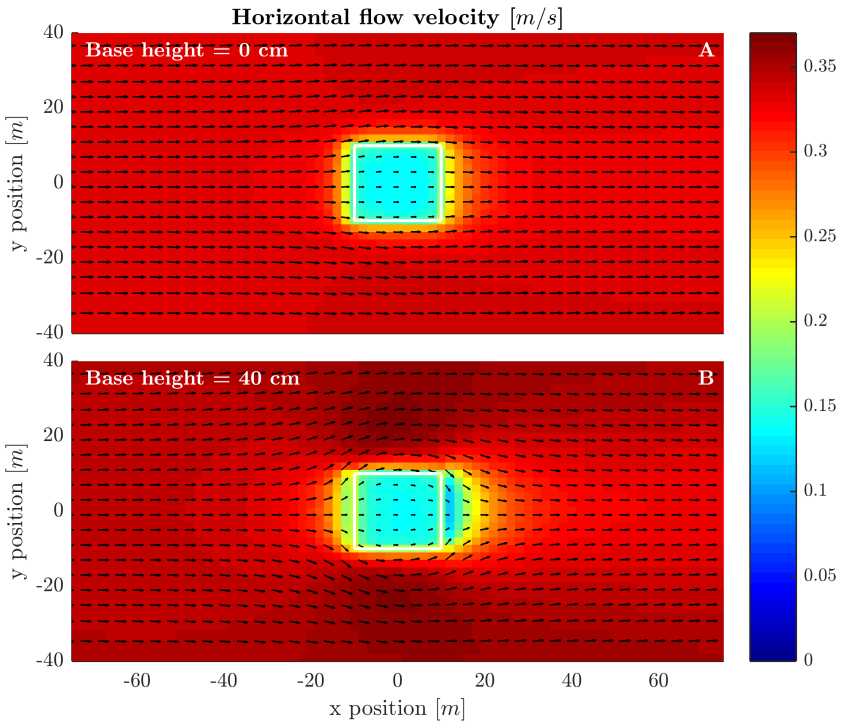

Fig. C.11. The interaction between a mussel patch and the environment for different base heights. Top view of the horizontal flow velocity (m s^{-1}) at the height of z = 4.5 cm from the bivalve bed. (A) a mussel patch with a base height of 0 cm (at sea bottom), (B) a mussel patch with a base height of 40 cm. The arrows indicate the velocity vectors (u and v) strength and angle. The cross-patch velocity component (v) is multiplied by a factor of 5 for visualization purpose. The white framed box indicates the location of the bivalve bed.

of this rate on the accumulation of sediment. The filtration rate has been varied from 0 up to 0.5 mm s^{-1}.

Figures C.20 and C.21, present the cumulative sedimentation and erosion after two days for a mussel bed with a filtration rate of 0 and 0.5 mm s^{-1}. The sedimentation rates in the center of the mussel bed are 3.3×10^{-3} and 6.4×10^{-3} for a filtration rate of 0 and 0.5 mm s^{-1}, respectively, for a cohesive environment. The sedimentation around the mussel bed is slightly decreased if a filtration rate of 0.5 mm s^{-1} is applied. More sediment is accumulated inside the mussel bed; thence, less sediment is available at the lee side of the patch to accumulate. The filtration rate has barely influence on the accumulation of sediment in a non-cohesive environment, because the filtration rate is small compared to the settling velocity of non-cohesive sand (23.5 mm s^{-1}).

C.2.5 Bed shear stress & shell height

The bed shear stress induced by currents never exceeds the critical bed shear stress of the cohesive and non-cohesive sediments (according to the model). It is interesting to determine for which bivalve shell height the bed shear stress exceeds the critical bed shear stress based on the model results. It is assumed that there is an exponential relation between the bed shear stress on top of the canopy and the bed shear stress on the bivalve bed, however more research is needed to determine this relation. The bed shear stress on top of the canopy is assumed to be equal to the bed shear stress at the bare bed. Figure C.22 presents the relation between the bed shear stresses and the shell height. The shell height must decrease substantially for a bed shear stress similar to the critical bed shear stress. The mussel and oyster shell height should be 0.75 and 1.5 cm,

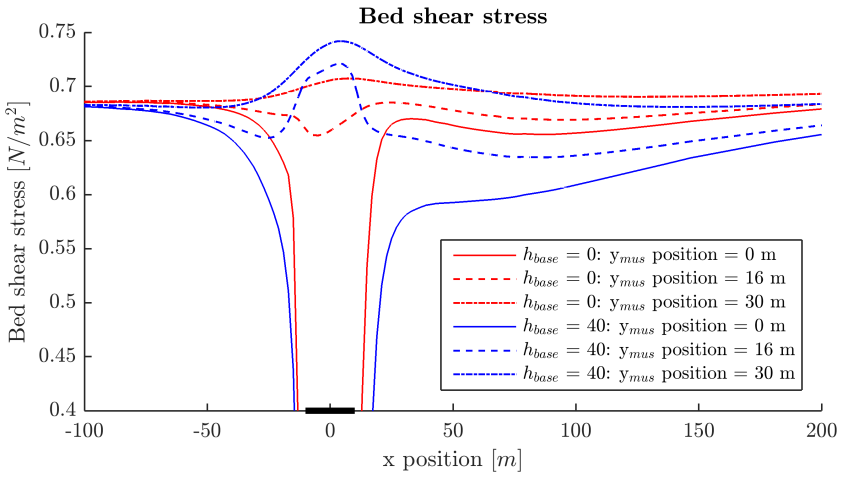

Fig. C.12. A side view of the bed shear stress around a mussel bed (for different base heights). (A) a mussel patch with a base height of 0 cm (at sea bottom), (B) a mussel patch with a base height of 40 cm. A side view of the bed shear stress around a mussel bed in the center of the patch (y = 0 m), at the gully (y = 16 m) and at the right side of the patch (y = 30 m). The white framed box indicates the location of the bivalve bed.

respectively, according to the model results. These height do not correspond with the heights found in the field (De Vries et al., 2012; Walles, 2015) and this is an indication of an missing process (see Section 6).

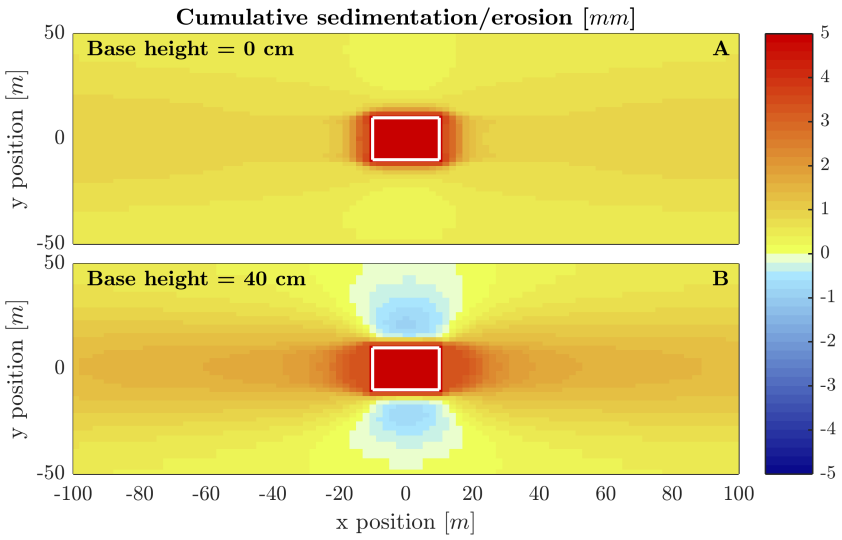

Fig. C.13. The cumulative sedimentation/erosion inside and around a bivalve bed for a cohesive environment. (A) a mussel patch with a base height of 0 cm (at sea bottom), (B) a mussel patch with a base height of 40 cm. The white framed box indicates the location of the bivalve bed.

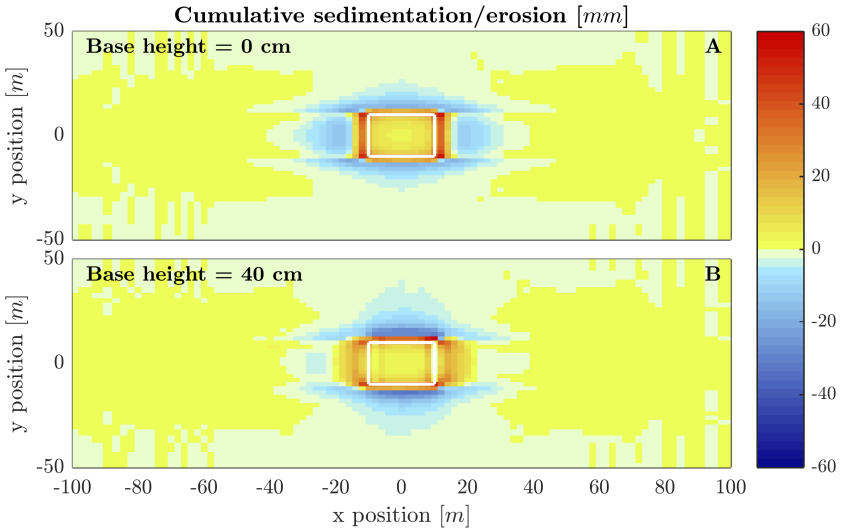

Fig. C.14. The cumulative sedimentation/erosion inside and around a bivalve bed for a non-cohesive environment. (A) a mussel patch with a base height of 0 cm (at sea bottom), (B) a mussel patch with a base height of 40 cm. The white framed box indicates the location of the bivalve bed.

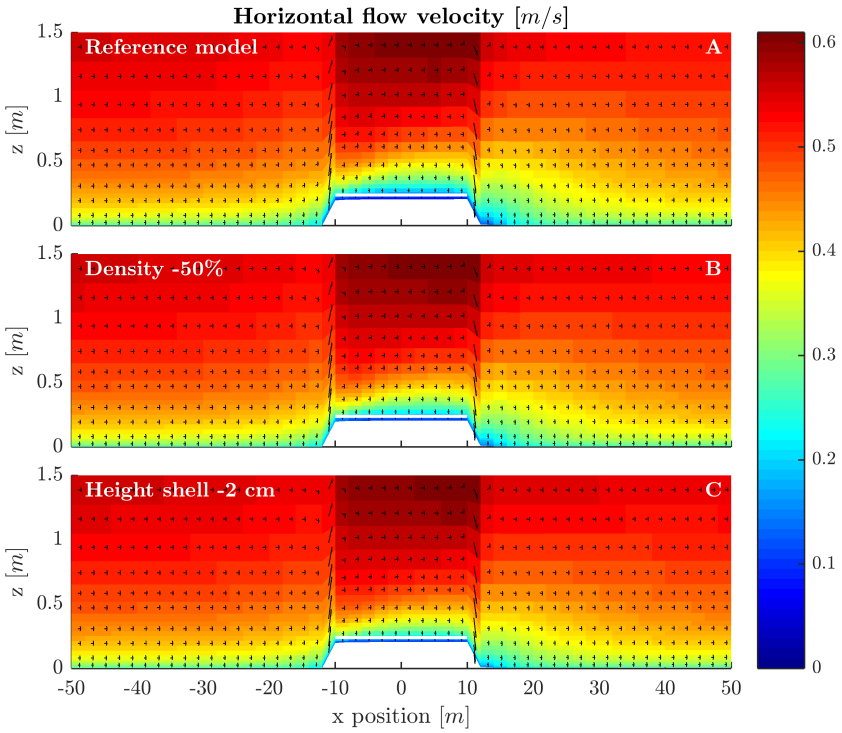

Fig. C.15. The interaction of a mussel of 20 by 20 m and the environment. Side view of the horizontal flow velocity (m s^{-1}) in the center of the patch (y = 0 m). (A) the reference model, (B) decrease of the density with 50% and (C) decrease of the height of the shell with 2 cm (50%). The white framed box indicates the location of the bivalve bed.

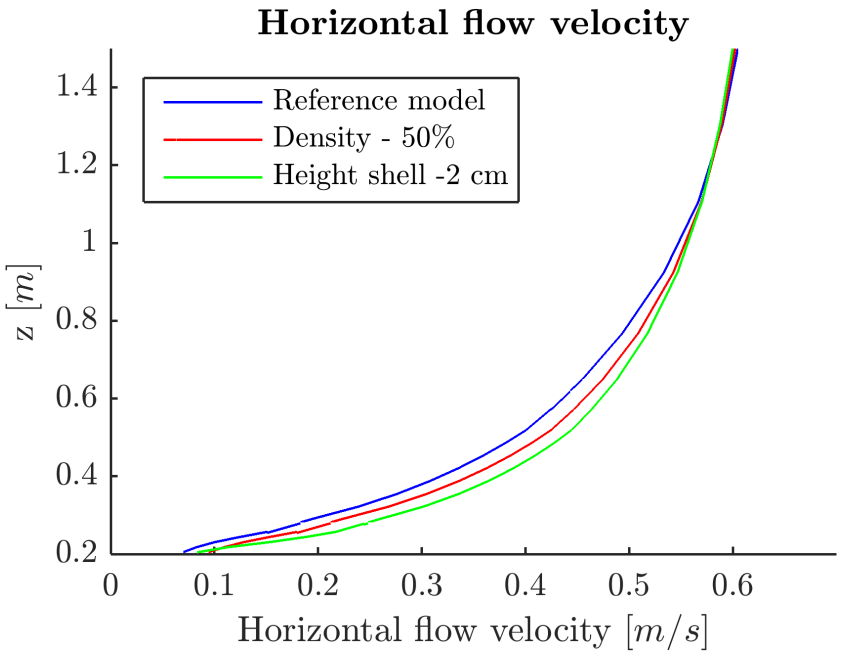

Fig. C.16. The horizontal flow velocity (m s^{-1}) in the center of the patch (x = 0 m and y = 0 m). The location of the base height of the mussel is at z = 0.2 m.

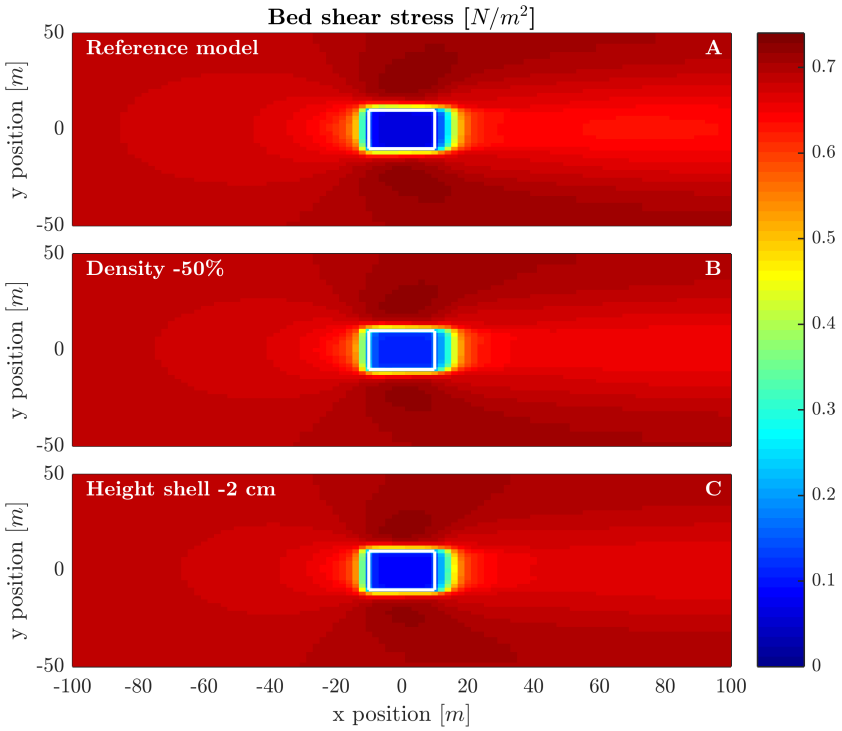

Fig. C.17. A side view of the bed shear stress around a mussel bed. (A) the reference model, (B) decrease of the density with 50% and (C) decrease of the height of the shell with 2 cm (50%). The white framed box indicates the location of the bivalve bed.

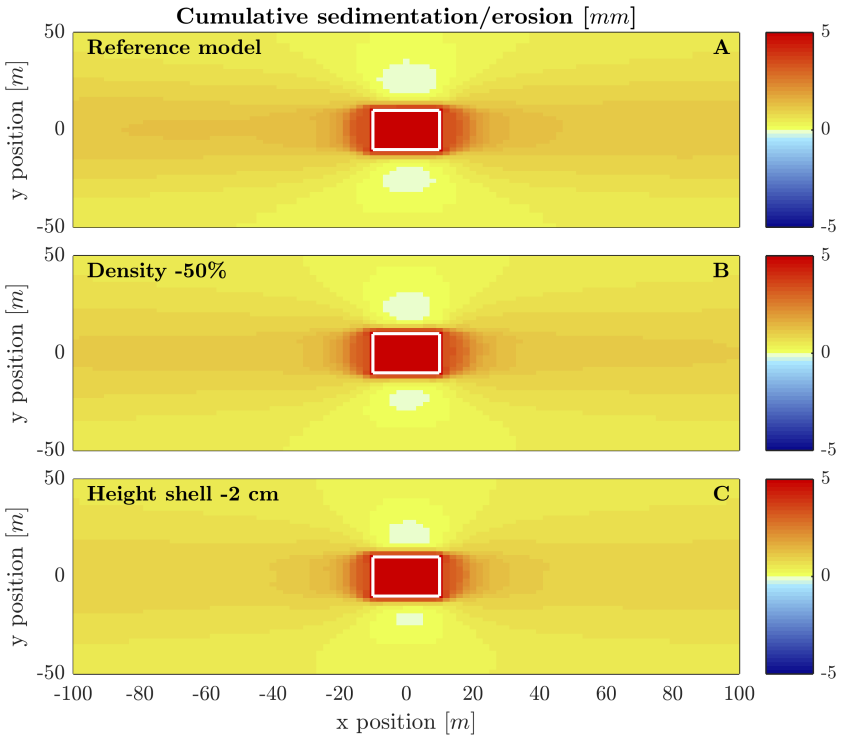

Fig. C.18. The cumulative sedimentation/erosion inside and around a bivalve bed for a cohesive environment. (A) the reference model, (B) decrease of the density with 50% and (C) decrease of the height of the shell with 2 cm (50%). The white framed box indicates the location of the bivalve bed.

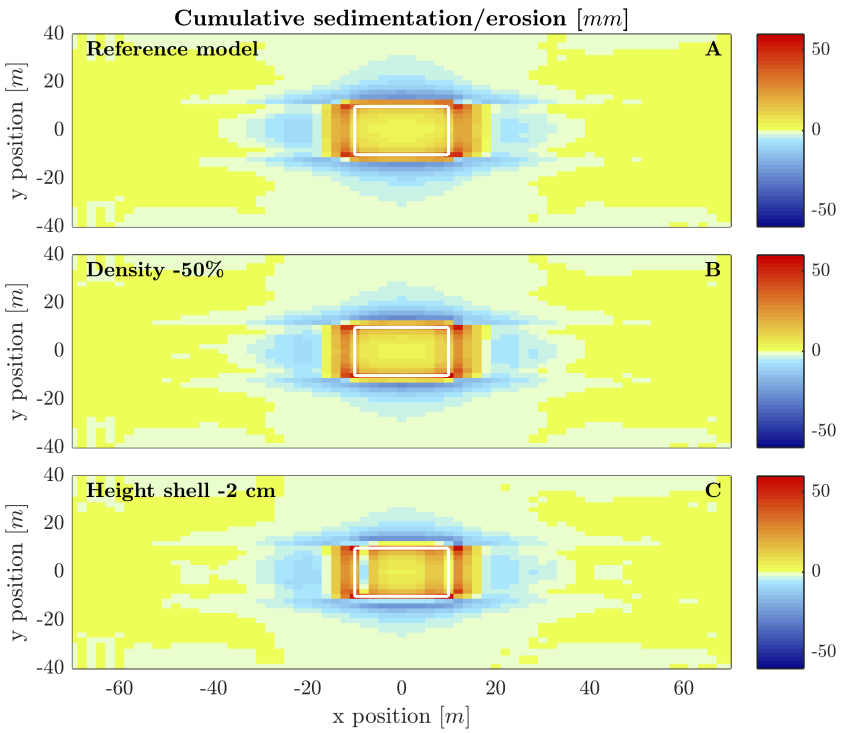

Fig. C.19. The cumulative sedimentation/erosion inside and around a bivalve bed for a non-cohesive environment. (A) the reference model, (B) decrease of the density with 50% and (C) decrease of the height of the shell with 2 cm (50%). The white framed box indicates the location of the bivalve bed.

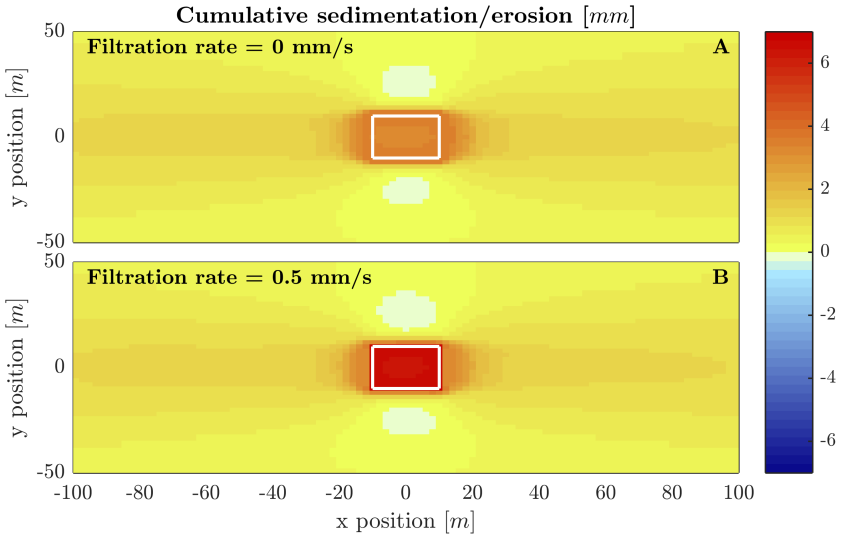

Fig. C.20. The cumulative sedimentation/erosion inside and around a mussel bed for a cohesive environment. (A) a mussel bed with a filtration rate of 0 mm/s (B) a mussel bed with a filtration rate of 0.5 mm/s. The white framed box indicates the location of the bivalve bed.

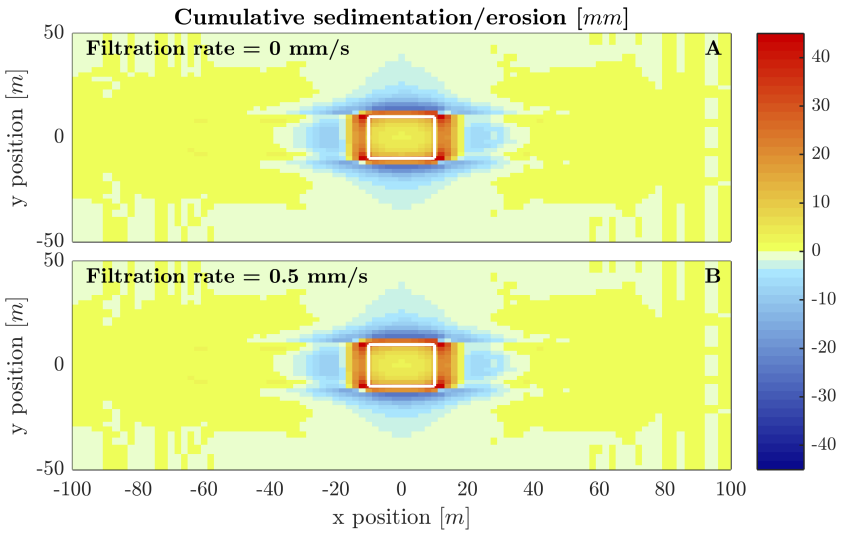

Fig. C.21. The cumulative sedimentation/erosion inside and around a bivalve bed for a non-cohesive environment. (A) a mussel bed with a filtration rate of 0 mm/s (B) a mussel bed with a filtration rate of 0.5 mm/s. The white framed box indicates the location of the bivalve bed.

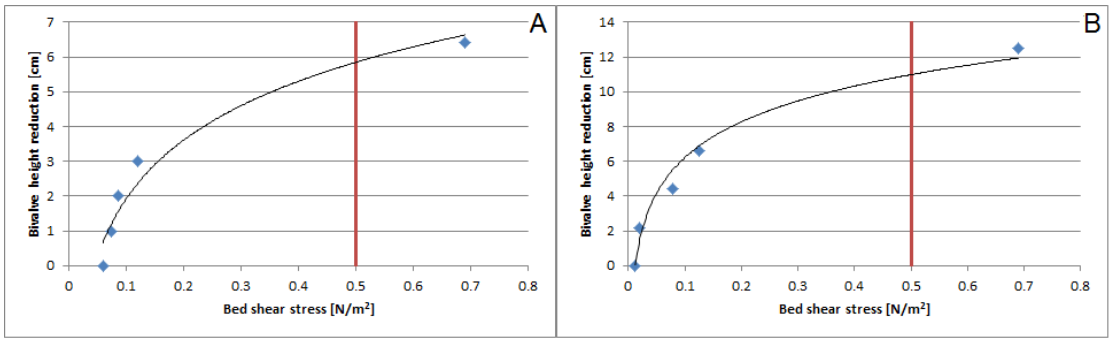

Fig. C.22. The relation between the bed shear stress and the shell height for a mussel bed (A) and an oyster bed (B). The dots indicates the results of the model, the red line indicates the critical bed shear stress for cohesive sediments and the black line is a logarithmic trendline between the dots.